RAPID NON-DESTRUCTIVE ESTIMATION OF PINUS TAEDA L. PHYSICAL, MORPHOLOGICAL AND CHEMICAL PROPERTIES USING NEAR INFRARED SPECTROSCOPY

by

PAUL DAVID JONES, JR

(Under the Direction of Laurence R. Schimleck)

ABSTRACT

Sixty percent of the nation's timber products are produced from trees grown in the Southern United States, with plantation grown *Pinus taeda* L. (loblolly pine) being the major fiber source. Density, microfibril angle, stiffness, tracheid coarseness, specific surface, wall thickness, perimeter, and radial and tangential diameter from 120 radial strips of *Pinus taeda* L. (loblolly pine) trees grown on 14 sites in 3 physiographic regions of Georgia (USA) were measured by SilviScan. NIR spectra were also collected in 10 mm increments from the radial longitudinal surface of each strip and split into calibration (9 sites, 729 spectra) and prediction sets (6 sites, 225 spectra). NIR spectra were correlated using untreated and mathematically treated (first and second derivative and multiplicative scatter correction) with tracheid properties to develop calibrations for the estimation of these properties. Strong correlations were obtained for properties related to density, the strongest R^2 being 0.83 (density), 0.90 (MFA), 0.93 (stiffness), 0.80 (coarseness), 0.78 (specific surface) and 0.84 (wall thickness). The addition of a small number of cores from the prediction set (one core per new site) to the calibration set improved the accuracy of predictions and, importantly, minimized the differences obtained with the various math treatments. Also, seventeen *P. taeda* radial strips, representing seven different sites were selected and NIR spectra were obtained from the radial longitudinal face of each strip. The spectra were obtained in 12.5 mm sections from predetermined positions that represented juvenile wood (close to pith), transition wood (zone between juvenile and mature wood) and mature wood (close to bark). For these sections, cellulose, hemicellulose, lignin (acid soluble and insoluble), arabinan, galactan, glucan, mannan, and xylan contents were determined by standard analytical chemistry methods. Calibrations were developed for each chemical constituent using the NIR spectra, wood chemistry data and partial least squares (PLS) regression. Relationships were variable with the best results being obtained for cellulose, glucan, xylan, mannan and lignin. Prediction errors were high and may be a consequence of the relatively small number of samples available for NIR analysis and the diverse origins of the samples in the test set.

INDEX WORDS: air-dry density, microfibril angle, near infrared spectroscopy, *Pinus taeda*, SilviScan, stiffness, morphological, tracheid, cellulose, lignin, hemicellulose

RAPID NON-DESTRUCTIVE ESTIMATION OF PINUS TAEDA L. PHYSICAL, MORPHOLOGICAL AND CHEMICAL PROPERTIES USING NEAR INFRARED SPECTROSCOPY

by

PAUL DAVID JONES, JR

BS, Clemson University, 2000

MSF, Stephen F. Austin State University, 2002

A Dissertation Submitted to the Graduate Faculty of The University of Georgia in Partial Fulfillment of the Requirements for the Degree

DOCTOR OF PHILOSOPHY

ATHENS, GEORGIA

2006

RAPID NON-DESTRUCTIVE ESTIMATION OF PINUS TAEDA L. PHYSICAL, MORPHOLOGICAL AND CHEMICAL PROPERTIES USING NEAR INFRARED SPECTROSCOPY

by

PAUL DAVID JONES, JR

Major Professor:	Laurence R. Schimleck
Committee:	Richard F. Daniels Jeffrey F. D. Dean Tharuvai N. Sriram Robert O. Teskey

Electronic Version Approved:

Maureen Grasso
Dean of the Graduate School
The University of Georgia
May 2006

DEDICATION

This dissertation is dedicated to my wife Alicia, who has stood by me in the trials and tribulations of completing the research contained in this document and the research published elsewhere, I love you.

ACKNOWLEDGEMENTS

I would like to thank my parents for their support and encouragement. I also want to thank the UGA Wood Quality Consortium for *P. taeda* sample collection and the Georgia TIP^3 program for funding the SilviScan analysis of the samples. Drs. Laurie Schimleck and Dick Daniels for their guidance, patience, and friendship.

TABLE OF CONTENTS

Page

Chapter 1

INTRODUCTION

Sixty percent of the nation's timber products are produced from trees grown in the Southern United States, with plantation grown *Pinus taeda* L. (loblolly pine) being the major fiber source (Wear and Greis 2002). The South will continue to be a major timber producer in both national and international markets with the area of plantation forests expected to increase in the Southern United States by 67% between 1995 and 2040 to an area of approximately 54 million acres (Wear and Greis 2002). The area of natural timberland is actually expected to decrease, increasing pressure to maximize the volume and quality of wood obtained from the plantation resource of the future.

The deployment of genetically improved planting stock coupled with intensive silvicultural management has greatly improved the growth and yields of *P. taeda*. Li et al. (1999) report that *P. taeda* trees grown from seeds obtained from first-generation seed orchards have produced 7-12% more volume per acre at harvest than trees grown from wild seed, while for second-generation seed orchards it is estimated that gains in volume will be 13-21%. It is expected that the inclusion of quality traits such as stem straightness and wood quality in *P. taeda* breeding programs will greatly increase genetic gains and the value of the trees (Li et al. 1999). Wood properties that could be used for selection include, but are not limited to density, microfibril angle, stiffness, tracheid morphological characteristics, cellulose, hemicellulose, and lignin content. The importance of these fundamental wood properties is supported by how they influence product properties, for example trees with high density and low microfibril angle are desirable for providing stiff and strong structural lumber, while trees with high density, cellulose and low lignin are required for high yields of pulp. Traditional methods of measuring wood properties such as microfibril angle, stiffness, and chemical composition, are slow and expensive, hindering the number of trees that can be analyzed for tree improvement programs and therefore impeding potential gains.

A rapid method to measure wood properties (physical, chemical, and morphological) that may be considered important to breeding programs is required. Near infrared spectroscopy has the potential to measure large populations of samples, whether they be whole-tree chips or increment cores, with minimal or no sample preparation, and in a non-destructive manner. Traditionally trees have been destructively sampled to determine their wood properties, and while destructive sampling may give a better measure of the whole-tree, the tree is no longer available for breeding purposes. Using increment cores taken from standing trees allows for the non-destructive estimation of wood properties.

Several studies (Birkett and Gambino 1988; Garbutt et al. 1992; Michell 1995; Raymond and Schimleck 2002; Schimleck et al. 1997; Wright et al. 1990) have used near infrared spectroscopy to estimate the chemical composition of wood on a whole-tree basis. Generally these studies used milled wood from a composite whole-tree sample or milled increment cores, they did not use intact wood as planned in this study. Only recently have studies began to use near infrared spectra collected from intact wood to estimate chemical composition. For example, Kelley et al. (2004) estimated the chemical composition of three *P. taeda* trees grown in Arkansas (USA) using near infrared spectra collected from the surface of static bending samples while Poke and Raymond (2006) also estimated chemical composition of intact wood using near infrared spectra collected from intact *Eucalyptus globulus* Labill. (Tasmanian blue gum) pith-to-bark strips. An advantage of working with solid wood is that it eliminates milling samples prior to near infrared analysis (Poke and Raymond 2006).

Studies have shown that near infrared spectroscopy can also be used to estimate the physical-mechanical properties of wood, including density and stiffness, for a range of species (Gindl et al. 2001; Hoffmeyer and Pedersen 1995; Schimleck et al. 2001b; Schimleck et al. 2002; Thumm and Meder 2001; Thygesen 1994; Via et al. 2005a). Studies based on near infrared spectra collected from radial wooden strips cut from selected *P. radiata* increment cores have shown promising results for air-dry density, microfibril angle, stiffness (determined using SilviScan-2 diffractometric data and measured density), and several tracheid morphological characteristics (Schimleck and Evans 2002b; 2002a; 2003; 2004). The calibrations performed well when applied to a separate test set of two cores that were from the same population. However, these studies were based on a small sample set with limited variation and it is unknown if it will be possible to obtain strong calibrations using samples from multiple sites or, assuming strong calibrations can be obtained, if the calibrations will perform well when applied to samples from new (or different) sites. The use of large diverse sets in agricultural applications indicates that calibrations based on highly variable populations can give strong statistics and are more robust (Berzaghi et al. 2002).

In this dissertation the estimation of a range of *P. taeda* wood properties by near infrared spectroscopy will be examined. Near infrared spectroscopy will also be used to estimate three selected physical properties (density, microfibril angle, and stiffness) of plantation grown *P. taeda* in Georgia. Near infrared spectroscopy will be used to estimate selected tracheid properties (coarseness, specific surface, perimeter, radial and tangential diameter, and wall thickness) of plantation grown *P. taeda*. Finally near infrared spectroscopy will be used to estimate selected chemical properties (cellulose, lignin, arabinan, galactan, glucan, mannan, and xylan) of *P. taeda* grown in Georgia. With all wood properties the goals are to examine if calibrations can be obtained using samples from a range of sites representative of the Piedmont, Upper and Lower Coastal Plains, and if these calibrations are directly applicable to samples from new sites not originally included in the calibrations.

Literature Cited

Berzaghi, A.J.P., Flinn, P.C., Dardenne, P., Lagerholm, M., Shenk, J.S., Westerhaus, M.O. and Cowe, I.A., 2002, Comparison of linear and non-linear near infrared calibration methods using large forage databases, Near Infrared Spectroscopy: Proceedings of the 10th International Conference, NIR Publication, 107-111.

Birkett, M.D. and Gambino, M.J.T., 1988. Potential applications for near-infrared spectroscopy in the pulping industry. Pap. S. Afr., November/December: 34-38.

Garbutt, D.C.F., Donkin, M.J. and Meyer, J.H., 1992. Near-infrared reflectance analysis of cellulose and lignin in wood. Pap. S. Afr., April: 45-48.

Gindl, W., Teischinger, A., Schwanninger, M. and Hinterstoisser, B., 2001. The relationship between near infrared spectra of radial wood surfaces and wood mechanical properties. J Near Infrared Spectrosc., 9(4): 255-261.

Hoffmeyer, P. and Pedersen, J.G., 1995. Evaluation of Density and Strength of Norway Spruce Wood by Near-Infrared Reflectance Spectroscopy. Holz Roh Werkst., 53(3): 165-170.

Kelley, S.S., Rials, T.G., Snell, R., Groom, L.H. and Sluiter, A., 2004. Use of near infrared spectroscopy to measure the chemical and mechanical properties of solid wood. Wood. Sci. Technol., 38(4): 257-276.

Li, B., McKeand, S. and Weir, R., 1999. Tree improvement and sustainable forestry - impact of two cycles of loblolly pine breeding in the U.S.A. Forest Genetics, 6(4): 229-234.

Michell, A.J., 1995. Pulpwood quality estimation by near-infrared spectroscopic measurements on eucalypt woods. Appita J., 48(6): 425-428.

Poke, F.S., Wright, J.K. and Raymond, C.A., 2004. Predicting Extractives and Lignin Contents in *Eucalyptus globulus* Using Near Infrared Reflectance Analysis. J. Wood Chem. Technol., 24(1): 55-67.

Poke, F.S. and Raymond, C.A., 2006. Predicting extractives, lignin and cellulose contents using near infrared spectroscopy on solid wood in *Eucalyptus globulus*. J. Wood Chem. Technol., (In Press).

Raymond, C.A. and Schimleck, L.R., 2002. Development of near infrared reflectance analysis calibrations for estimating genetic parameters for cellulose content in *Eucalyptus globulus*. Can. J. For. Res., 32(1): 170-176.

Schimleck, L.R., Wright, P.J., Michell, A.J. and Wallis, A.F.A., 1997. Near-infrared spectra and chemical compositions of *E. globulus* and *E. nitens* plantation woods. Appita J., 50(1): 40-46.

Schimleck, L.R., Evans, R. and Ilic, J., 2001. Estimation of *Eucalyptus delegatensis* wood properties by near infrared spectroscopy. Can. J. For. Res., 31(10): 1671-1675.

Schimleck, L.R. and Evans, R., 2002a. Estimation of microfibril angle of increment cores by near infrared spectroscopy. IAWA J., 23(3): 225-234.

Schimleck, L.R. and Evans, R., 2002b. Estimation of wood stiffness of increment cores by near infrared spectroscopy: The development and application of calibrations based on selected cores. IAWA J., 23(3): 217-224.

Schimleck, L.R., Evans, R. and Matheson, A.C., 2002. Estimation of *Pinus radiata* D. Don clear wood properties by near-infrared spectroscopy. J. Wood Sci., 48(2): 132-137.

Schimleck, L.R. and Evans, R., 2003. Estimation of air-dry density of increment cores by near infrared spectroscopy. Appita J., 56(4): 312-317.

Schimleck, L.R. and Evans, R., 2004. Estimation of *Pinus radiata* D. Don tracheid morphological characteristics by near infrared spectroscopy. Holzforschung, 58(1): 66-73.

Thumm, A. and Meder, R., 2001. Stiffness prediction of radiata pine clearwood test pieces using near infrared spectroscopy. J. Near Infrared Spectrosc., 9(2): 117-122.

Thygesen, L.G., 1994. Determination of dry matter content and basic density of Norway spruce by near-infrared reflectance and transmission spectroscopy. J. Near Infrared Sectrosc., 2: 127-135.

Via, B.K., So, C.L., Shupe, T.F., Eckhardt, L.G., Stine, M. and Groom, L.H., 2005. Prediction of wood mechanical and chemical properties in the presence and absence of blue stain using two near infrared instruments. J. Near Infrared Spec., 13(4): 201-212.

Wear, D.N. and Greis, J.G., 2002. Southern forest resource assessment, General technical report SRS ; 53. Asheville, NC : Southern Research Station.

Wright, J.A., Birkett, M.D. and Gambino, M.J.T., 1990. Prediction of Pulp Yield and Cellulose Content from Wood Samples Using near-Infrared Reflectance Spectroscopy. Tappi J., 73(8): 164-166.

Chapter 2

LITERATURE REVIEW

Wood Properties

Wood can be characterized by its chemical composition, morphological properties, and its overall physical properties. The chemical composition of wood can be divided into four distinct chemical groups, cellulose, hemicellulose, lignin, and extractives. Important morphological properties include: coarseness, cell perimeter, radial and tangential cell diameter, specific surface, tracheid length, and cell wall thickness. Important physical wood properties include density, microfibril angle, stiffness, and strength, which are dependent upon chemical composition and morphological properties. This study is primarily concerned with, cellulose, monosaccharide content, lignin, coarseness, cell perimeter, radial and tangential cell diameter, specific surface, and cell wall thickness, and the estimation of these properties using near infrared spectroscopy.

Chemical Composition

Cellulose

Approximately 40-50% of wood is comprised of cellulose (Panshin and De Zeeuw 1980; Pereira et al. 2003; Sjöström 1993). Cellulose forms the skeletal structure of cell walls and plays an important role in determining their strength. Cellulose is a homo-polymer comprised of glucose; the overall degree of polymerization is about 10,000 glucose molecules (Panshin and De Zeeuw 1980; Pereira et al. 2003). Products made of wood are highly dependent on the amount of cellulose and its arrangement. It is an important determinant of the yield of chemical pulp from wood and the overall strength of wood products.

The cellulose content of wood may be determined by several different destructive, labor intensive methods including the peroxyacetic acid method described by Garbutt (1989), a nitric-acetic method developed by Pereira (1988), a dioxane-acetylacetone-hydrochloric acid method described by Seifert (1960), which is considered by many the standard method for measurement, and the use of high performance anion-exchange chromatography as described by Wright and Wallis (1996) and later by Pronto (1998). A summary of the above methods and other methods can be found in Wallis et al. (1997), who also provide a comparison of the purity of the cellulose obtained.

Hemicellulose

The percentage of hemicellulose in wood varies from 15-35% (Panshin and De Zeeuw 1980; Pereira et al. 2003; Sjöström 1993). Hemicellulose is compromised of two primary groups of sugars, hexoses (6-carbon sugars including galactan, glucan and mannan) and pentoses (5-carbon sugars including arabinan and xylan) (Alén 2000; Panshin and De Zeeuw 1980; Pereira et al. 2003; Sjöström 1993). These monosaccharides combine to form relatively short-branched chains (≈ 700 sugar units). In softwoods, hemicellulose is primarily comprised of galactoglucomannans that are composed of varying amounts of galactose, glucose, and mannan (Alén 2000; Pereira et al. 2003; Sjöström 1993). Hardwood hemicellulose is primarily composed of glucuronoxylan, a combination of glucose and xylan (Alén 2000; Pereira et al. 2003; Sjöström 1993). Other common hemicelluloses include arabinoglucuronoxylan, and arabinogalactan in softwoods and glucomannan in hardwoods (Alén 2000; Pereira et al. 2003;

Sjöström 1993). The function of hemicellulose includes sheathing cellulose microfibril bundles, hydrogen bonding with lignin, and linking lignin and cellulose (Bowyer et al. 2002).

Hemicellulose is often measured by chromatography, either in the form that it is found in the wood or as the monosaccharides that combine to make hemicelluloses (Sjöström 1993). Hemicelluloses can also be estimated along with cellulose content by using high performance anion exchange chromatography as was described by Wright and Wallis (1996), or by methods described by Pronto (1998).

Lignin

Lignin compromises approximately 15-35% of wood (Panshin and De Zeeuw 1980; Pereira et al. 2003; Sjöström 1993). As a highly heterogeneous substance, investigations still persist into its properties *in situ* cell wall structure (Pereira et al. 2003). Lignin is formed by the polymerization of phenylpropane units, including *p*-hydroxyphenyl, guaiacyl, and syringyl (Pereira et al. 2003). Hardwoods primarily have lignin comprised of guaiacyl-syringyl lignin, while softwood lignin is composed of guaiacyl-lignin. In cell walls, lignin is known to act as a bonding agent with hemicellulose; lignin also acts as a bulking element that fills in fine cavities, reducing the effect moisture has on dimensional changes (Panshin and De Zeeuw 1980; Pereira et al. 2003). The amount of lignin found between, and particularly within, cell walls is dictated by the growing season. In the spring, earlywood is formed, which is characterized by large cell diameters and lower amounts of lignin (25 to 30% lignin), while in the later part of the growing season, latewood is formed and has been described as having smaller cell wall diameters (in the radial direction), thicker cell walls and higher lignin content (Panshin and De Zeeuw 1980).

Typically, lignin content is determined using 72% sulfuric acid. The carbohydrate fraction is dissolved leaving the insoluble lignin, referred to as Klason lignin (Sjöström 1993). A small portion of the lignin is dissolved and is referred to as acid-soluble lignin. Acid-soluble lignin can be detected using ultraviolet spectroscopy to measure the absorbance at 206 or 280 nm and comparing the measured absorption with that of samples of known concentration. Lignin can also be measured using the acetyl bromide method. The method forms acetyl derivatives and a bromine replacement of an OH group allowing the lignin to dissolve in acetic acid, the assayed lignin is then measured by ultraviolet spectroscopy. This method is much faster and easier to perform than other methods and there is no need to correct for acid soluble lignin (Hatfield and Fukushima 2005; Johnson et al. 1961).

Physical properties

Density

Density of wood can be defined as mass per unit volume. When reporting density the moisture content of the wood at the time of measurement must be known. A common measure of density is basic density. Basic density is defined as oven-dry mass divided by volume at green condition or above the fiber saturation point. Other than basic density the moisture content of the wood must be reported (i.e. air-dry density at 10% moisture content). As previously discussed, cellulose, hemicellulose, and lignin comprise the majority of the cell wall, and variation in the ratio of the three components, extractive content and void volume determines wood density (Panshin and De Zeeuw 1980; Saranpää 2003). The overall density of the wood minus the air that it contains is approximately 1.5 g cm^{-3}, and is approximately the same regardless of species (Panshin and De Zeeuw 1980). Pulp yield, pulp quality, and the strength and stiffness of wood are all well correlated with density, particularly in softwoods (Saranpää 2003).

Density has been traditionally measured in two different ways. The first method is based on Archimedes' principle. The green volume (for basic density or a density using the volume above fiber saturation point) is measured by water displacement. The volume can also be estimated by taking dimensional measurements and calculating the volume. The mass of the sample is then measured at the appropriate moisture content and density is calculated. For basic density or any density involving the oven-dry mass the sample must be dried at 105° C until the mass becomes constant (Panshin and De Zeeuw 1980; Saranpää 2003). Unfortunately, once the sample has been oven dried, the green volume can not be completely recovered (Megraw 1985; Panshin and De Zeeuw 1980; Saranpää 2003; Stamm 1964).

Alternately, the second method uses X-ray densitometry to determine density (Echols 1970; Polge 1978; Saranpää 2003). X-ray densitometry, employs X-rays from a radioactive source or an X-ray generator that are focused through the wood sample and are detected by a digital radiation sensor or used to expose a film. Depending on the density of the wood substance the amount of radiation that reaches the film or the sensor varies (Echols 1970; Megraw 1985; Polge 1978). This method is both fast and non-destructive.

Microfibril angle

The cell wall of an individual wood cell has two distinct sections, the primary wall and the secondary cell wall. The primary wall is created at the differentiation stage of cell development and is comprised of microfibrils of cellulose loosely arranged and interwoven (Panshin and De Zeeuw 1980). The secondary cell wall comprises the majority of the cell wall and has three distinct layers, designated S1, S2, and S3. The S1 layer is approximately 0.1 to 0.2 μm thick, the S2 layer, is the thickest layer at approximately 0.6 μm, and the S3 layer is approximately 0.1 to 0.2 μm thick. Each layer consists of a dense structure of microfibrils arranged parallel to each other. Microfibril angle can be defined as the orientation of microfibrils relative to the central axis of the wood cell (Butterfield 2003; Panshin and De Zeeuw

1980). Microfibril angle varies between layers, the S1 layer has microfibril angles that vary from 50 to 70º, the S2 has microfibril angles that vary from 10 to 30º, and the S3 layer has microfibril angles that vary from 60 to 90º. For practical purposes the S2 layer is the most important in determining the properties of the cell wall as it is the thickest, and is most frequently measured (Panshin and De Zeeuw 1980). Figure 2.1 illustrates all 3 layers and the relationship of the microfibrils to the cell orientation.

Approximately 80% of the strength of wood can be explained by microfibril angle, Cave (1968) described the relationship of increasing wood stiffness with a decrease in microfibril angle (Booker et al. 1997; Butterfield 2003). Several methods have been developed, to measure microfibril angle. Polarized light microscopy use polarized light to examine the different orientation of the microfibrils. This is done by orienting the fiber parallel to the vertical crosshair in an ocular lens, then rotating the stage until the central part of the fiber is darkest. The difference between the initial angle and the final angle is the microfibril angle (Cousins 1972; Preston 1952). Iodine staining uses the formation of iodine crystals along the microfibrils to determine their angle (Bailey and Vestal 1937). Inducing checks in wood fibers using ultrasonics and measuring the angle of the checks has also been used (Huang 1995). The angle of crossfield-pit apertures has also be widely used to determine microfibril angle (Pillow et al. 1953). All of the methods described only measure the microfibril angle of individual fibers. X-ray diffraction has been widely used, but only average microfibril angles can be measured (Cave 1966; Evans 1999). The above methods are all time consuming or cost prohibitive for use in large scale studies.

Stiffness

The elastic behavior of wood is often referred to as the modulus of elasticity or stiffness. Wood stiffness can be defined as the strain (deformation of a material body under the action of applied forces) induced on a piece of wood for which the wood will return to its original dimensions (Panshin and De Zeeuw 1980; Zink-Sharp 2003). Proportionally, stiffness is the amount of stress to strain. The larger the measured stiffness the less likely a piece of wood is to deform under a given load.

Stiffness can be measured in two different ways. Physically breaking a sample in a static bending testing machine is one method to determine stiffness, this method is outlined in ASTM D 143 (2000). Acoustics can also be used to determine wood stiffness, because the speed at which sound travels along a wood sample is proportional to its stiffness (Huang et al. 2003; Kumar 2004). Both methods have draw backs, breaking the sample is destructive, while the acoustic methods require a calibration to be created.

Morphological properties

Coarseness

Fiber coarseness, or the oven-dry mass of material per the unit length of the fiber is an important property for pulp and papermaking because it helps to determine the number of fibers present for bonding and their ability to bond (McKenzie 1994; Muneri and Raymond 2001). To measure coarseness a wood sample must be delignified (macerated), the fibers are separated in water by mechanical agitation, then the length of the fibers is measured by examining their length under a microscope or with an automated fiber length detector (Kajaani), finally the fibers are oven-dried and an oven-dry weight is taken (Muneri and Raymond 2001). The process is time consuming and tedious.

Specific surface

The specific surface of wood tracheids can be calculated by dividing the perimeter of the fiber by the coarseness of the fiber (Evans 1994). Specific surface is the surface area available for bonding when making products such as paper and fiber board (Risén et al. 2004). For the determination of specific surface, coarseness must first be measured, leading to time constraints previously mentioned.

Wall thickness

Wall thickness refers to the thickness of the secondary cell wall of a wood fiber or tracheid. Wall thickness is an important determinant of wood density because the substance that the cell wall is made from has a constant density; the thicker the cell wall, the higher the density and therefore the higher the pulp yield (Saranpää 2003).

Cell wall thickness can be measured by several different methods. Traditionally cell wall thickness has been measured by microscopy, thin sections are cut from the cross-sectional surface of a wood sample using a microtome and placed on slides, the thicknesses of the walls are then measured using a slide or optical lens mounted micrometer. Another method is the use of an analyzer such as the Kajaani FiberLab fiber dimension analyzer (Metso Automation Atlanta, GA) which uses optical sensors to measure fiber properties.

Perimeter, radial and tangential diameters

Perimeter is simply the outside perimeter of the cell wall. Cell wall perimeter is important as it is used to calculate more important morphological properties such as specific surface, and wall thickness by SilviScan (Evans 1994). Perimeter can also be measured by microscopy or image analysis.

The calculation for perimeter requires two other measurements that characterize wood structure; these measurements are radial and tangential diameter. Radial diameter is the measure of the cell diameter along the radial axis, while tangential diameter is measured along the tangential axis. Primarily the two separate measurements are made because the dimensions of wood cells differ in the two dimensions. These measurements are generally performed by the same methods as described for perimeter.

SilviScan Analysis

SilviScan is based on 3 different measurement techniques, X-ray densitometry (density), X-ray diffraction (microfibril angle), and image analysis (coarseness, specific surface, wall thickness, perimeter, radial and tangential diameter) (Evans 1994; 1997; 1999; Evans et al. 1999). SilviScan was developed in the early 1990's by the Cooperative Research Centre for Harwood Fibre and Paper Science (Australia) to measure properties considered, at the time, to be important to the Australian pulp and paper industry, hence the focus on tracheid morphological characteristics. SilviScan has been widely used to understand the effects of silviculture, the environment, and genetic selection on wood formation (Downes et al. 1993; 2002; Downes and Turvey 1993; Kibblewhite et al. 1998; Wimmer et al. 2002a; 2002b; 2002c).

SilviScan measures the wood properties of radial strips 2mm tangentially by 7mm longitudinally by the radial diameter of the tree the sample is taken from. Measurement of density and microfibril angle is performed by passing X-rays through the radial face of the sample. The sample is placed on a stage that steps the sample past a X-ray beam in a given increment. The stage also rotates the sample so that the X-ray beam only passes through the wood parallel to growth ring boundaries (Evans 1997; 1999; Evans et al. 1999). For morphological properties such as radial and tangential diameter, image analysis is performed on the cross-sectional surface (polished) by scanning the surface with a video microscope and analyzing the image with software that recognizes the cell walls (Evans 1994). Density is measured in 50 μm increments along the entire length of the sample, microfibril angle can be measured at a resolutions ranging from 0.2 mm to 10 mm, and the morphological properties are also measured at 50 μm increments. SilviScan measures a wide range of properties but it can not measure tracheid length or the chemical composition of wood.

Near Infrared Spectroscopy

Near infrared spectroscopy is a method that has been frequently used for measuring the chemical, physical, and even morphological properties of a sample. There are some clear advantages of near infrared spectroscopy over other analytical methods. In most cases near infrared spectroscopy is faster, requires little or no sample preparation, has the ability to measure multiple properties with a single operation (providing a calibration exists), and near infrared spectroscopy is non-destructive so that the sample can be used for other procedures if desired (Marten et al. 1989). There are disadvantages to using near infrared spectroscopy, near infrared spectra are difficult to interpret owing to the presence of overlapping overtones, the multivariate statistical approaches are considered by many to be "black box" techniques, a calibration can only be as good as the laboratory data that is used to create the calibration, and the applicability of calibrations to new populations is often uncertain.

Despite its advantages, near infrared spectroscopy has only recently been widely used in analytical studies. The near infrared region of the electromagnetic spectrum was originally dismissed as not containing any useful information (Barton 2002). Modern near infrared spectroscopy truly started with Karl Norris in the early 1960's at the United States Department of Agriculture (Barton 2002; Norris and Butler 1961). Who first used near infrared spectroscopy to estimate components of cereal grains in agricultural products. When instrumentation advanced enough that the mid infrared spectrum was separated from the near infrared spectrum, it was realized that the fundamental frequencies present in mid infrared caused overtones and combinations of overtones to occur in the near infrared region. While these overtone regions are less precise than the mid infrared in terms of their fundamental origins, enough information is present for use in statistical applications (Barton 2002). Near infrared spectroscopy was originally used to perform compositional analysis of agricultural commodities such as animal forage, corn, cotton, grains, and silage, but has found increased usage in other industries and research disciplines (Barton 2002).

The electromagnetic spectrum ranges from 10^{-6} nm (Gamma rays) to 100 Mm (radio waves), between that range X-rays, ultraviolet, visible light, near infrared, mid infrared, far infrared, and microwaves occur. A typical near infrared spectrometer scans over the range of 800 to 2500 nm. There are five methods used to collect near infrared spectroscopy (transmittance, specular reflectance, transflectance (fiber optic probes), diffuse reflectance, and interactance), with the two primary methods being diffuse reflectance and transmission. Figure 2.2 illustrates the difference between the two methods. Transmission is primarily used for liquids, while reflectance is reserved primarily for solid materials (Barton 2002; Roberts et al. 2004).

When exposed to near infrared energy, molecular vibrations (stretching and bending of molecules) occur in a sample, when the near infrared energy matches the natural vibration of a molecular bond within a molecule it absorbs the energy. Different molecular structures interact with different wavelengths, hence samples having different chemical composition and physical properties produce different near infrared spectra. The intensities of the interaction with the near infrared energy depend on the change of the dipole moment of the bonds during vibration hence O-H, C-H, N-H, S-H, are all strong absorbers of near infrared energy (Raymond and Schimleck 2002). The spectral variation can be used to create calibrations for predicting properties of the sample that may or may not be directly related to the chemical composition (Marten et al. 1989).

Instruments used in near infrared spectroscopy have improved from those used in the 1960's when filter instruments could only measure a small number of selected wavelengths. Techniques for isolating the near infrared spectral range from light sources have improved, exposing the samples only to a limited range of the electromagnetic spectrum. The detectors used only detect a limited range of the electromagnetic spectrum. For the instrument (FOSS NIRSystems 5000) used in this study, lead sulfide detectors collected spectra ranging from 1100 nm to 2500 nm, silicon detectors used in other FOSS NIRSystems instruments can collect spectra in the range of 400 nm to 1100 nm.

Once spectra have been collected from a set of samples, they can be analyzed in several ways. 1. Principal component analysis can be used to group samples. 2. Provided laboratory data for a given property has been measured a calibration can be developed using the data and the spectra. Simple regression, multiple regression, and multivariate analysis techniques can be used to create the calibrations. 3. Provided a calibration has been created to estimate a given property, the spectra can be used for estimation purposes. With the multivariate techniques, unwanted variation from effects of particle size, moisture content etc can mask the variation in the spectra central to the development of successful calibrations, therefore math treatments are used to remove the noise in the spectra.

There are several commonly used math treatments, they include, but are not limited to: multiplicative scatter correction, first derivative, and second derivative. In each case the resulting data has a decreased amount of noise from shifts in the spectra that do not relate to the desired information contained in the spectra (Næs et al. 2002). Figure 2.3 illustrates the raw spectra (a), and the effects that multiplicative scatter correction (a), the first derivative (b), and the second derivative math treatments have on the spectra (c).

Once a math treatment has been performed to the data it can be analyzed by two different forms of multivariate analysis, by multiple regression, or by simple regression. The later two methods are used less often because more complete analysis can be performed using the multivariate techniques (Næs et al. 2002). The two forms primarily used for multivariate analysis are principal component analysis and partial least square regression. Principal component analysis is a method of data reduction, which uses the matrix of the original data to create new variables that are linear combinations of the original variables that have been weighted with vectors and are orthogonal to each other. The first new variable captures as much of the variability from the original data as possible, with each additional variable accounting for as much of the remaining variability as possible (Næs et al. 2002). By examining the vectors in pair combinations, groupings in the data can be examined to determine relationships between samples. Partial least squares regression is similar to principal component analysis in that the data is reduced using principal components, but the difference is that the components are obtained by maximizing the covariance between the independent variables (spectra) and the dependent variable (constituent), this causes the resulting components to be more directly related to the variability in the dependent variable (Næs et al. 2002).

Wood and fiber analysis

Wood chemistry

Near infrared spectroscopy coupled with multivariate analysis technique allows for the measurement of chemical composition of wood and the resulting pulp yield, with little or no sample preparation and without destroying the sample when it is measured. Much research has been performed in creating calibrations to predict cellulose, hemicellulose, and lignin in wood and wood pulp (Olsson et al. 1995; Poke and Raymond 2006; Poke et al. 2004; Raymond et al. 2001; Schimleck and Michell 1998). The clear advantages over previously mentioned methods of chemical analysis are the ability to obtain a wide range of chemical information with one simple test and avoidance of using hazardous chemicals.

Near infrared spectroscopy has been used to measure chemical composition in a wide range of species, including *Betula papyrifera* Marsh., *Eucalyptus* spp., *Fagus* spp., *Larix* spp., *Liquidambar styraciflua* L., and *Pinus* spp. (Axrup et al. 2000; Garbutt et al. 1992; Raymond and Schimleck 2002; Schimleck et al. 2000; Schimleck et al. 1997; Schultz and Burns 1990; Wright et al. 1990). Several studies (Birkett and Gambino 1988; Garbutt et al. 1992; Michell 1995; Poke et al. 2004; Raymond and Schimleck 2002; Schimleck et al. 1997; Wright et al. 1990) have used near infrared spectroscopy to estimate the chemical composition of wood but these studies did not use intact wood, rather they used milled wood generally representing a composite whole-tree sample or milled increment cores. Recent studies have explored the possibility of measuring chemical composition using solid wood. Kelley et al. (2004) estimated the chemical composition of three *Pinus taeda* L. trees grown in Arkansas (USA) using a reduced spectral range (650 nm-1150 nm) and near infrared spectra collected from the surface of static bending samples. Poke and Raymond (2006) estimated lignin and cellulose of intact radial strips using near infrared spectra collected in 20 mm increments from the transverse surface of *Eucalyptus globulus* Labill. (Tasmanian blue gum) pith-to-bark strips. An advantage of working with solid wood is that it eliminates milling samples prior to near infrared spectroscopy analysis (Poke and Raymond 2006).

In other recent studies Yeh et al. (2004; 2005) and Sykes et al. (2005) have used transmittance near infrared spectroscopy to estimate the lignin and α-cellulose content of wood wafers sliced from the tangential surface of increment cores. The utilization of thin wafers removed from the transverse face allows the analysis of within ring variation of wood properties at much higher spatial resolution than is presently possible using near infrared reflectance spectra collected from the radial face. However, sample preparation is still time consuming relative to near infrared reflectance spectroscopy with intact wood strips.

Physical properties

While measuring density (X-ray densitometer) and microfibril angle (X-ray diffraction) are essentially non-destructive, traditional methods of measuring these properties plus those for modulus of elasticity and modulus of rupture are destructive. Studies have shown that near infrared spectroscopy can be used to estimate the physical-mechanical properties of wood, including density and stiffness (Gindl et al. 2001; Hoffmeyer and Pedersen 1995; Schimleck et al. 1999; Thumm and Meder 2001; Thygesen 1994). Recently, it has been shown that reasonable calibrations can be created for green *P. taeda* samples for air-dry density, microfibril angle and stiffness (Schimleck et al. 2003b). The use of online scanning of green lumber in a sawmill to determine the properties of the sawn lumber has been investigated (Meder et al. 2003). Several recent near infrared spectroscopic studies (Schimleck and Evans 2002b; 2002a; 2003; Schimleck et al. 2003b) have used data provided by SilviScan for calibration purposes.

Strong relationships between SilviScan measured wood properties and near infrared-estimates for a range of wood properties including density (R^2=0.93), microfibril angle (R^2=0.77), and stiffness (R^2=0.90) were obtained for *Eucalyptus delegatensis* R. T. Baker (alpine ash) and *P. radiata* samples (Schimleck et al. 2001b; Schimleck et al. 2002). Studies based on radial wooden strips cut from selected *P. radiata* increment cores have shown promising results for air-dry density, microfibril angle, stiffness (determined using SilviScan-2 diffractometric data and measured density) (Schimleck and Evans 2002b; 2002a; 2003). The use of broad based calibrations has been examined to a limited extent using many different species (Schimleck et al. 2001a).

Morphological properties

It has been demonstrated that fundamental tracheid morphological characteristics such as coarseness and wall thickness (Schimleck and Evans 2004) and length (Hauksson et al. 2001; Schimleck et al. 2004a; Via et al. 2005b) can be determined by near infrared spectroscopy. Such properties are important in determining pulp fiber quality and paper performance but their consideration in tree breeding programs has been limited owing to the difficulties of routine measurement.

The study of Schimleck and Evans (2004) with *P. radiata* utilized data provided by the SilviScan instruments to develop calibrations for tracheid coarseness, perimeter, radial diameter, tangential diameter and wall thickness were based on a relatively small sample set (8 cores, 119 spectra). Coefficients of determination (R^2) ranged from 0.65 for tracheid radial diameter to 0.91 for coarseness. The calibrations, apart from tracheid perimeter and tracheid radial diameter, performed well when applied to a separate test set of two cores that were from the same population as the calibration samples. However, it is unknown if strong calibrations for these morphological traits can be obtained using *P. radiata* samples from a larger and more diverse set or if the calibrations can be successfully applied to sites not included in the calibration.

Objectives

The objectives of this study are:

(*i*) To create wood property calibrations (air-dry density, MFA, stiffness, coarseness, specific surface, wall thickness, perimeter, and radial and tangential diameter) using samples drawn from a wide variety of sites chosen to represent the three physiographic regions in Georgia where *P. taeda* is grown;

(*ii*) To examine the performance of the wood property calibrations when applied to samples from sites not included in the calibration;

(*iii*) To investigate methods for improving the applicability of wood property calibrations to samples from sites not initially included in the calibration set;

(*iv*) Develop calibrations for wood chemical components including cellulose, hemicellulose, lignin (including acid insoluble, soluble and total) and individual monosaccharides (arabinan, galactan, glucan, mannan and xylan) using NIR spectra obtained in 12.5 mm sections from the radial - longitudinal surface of *P. taeda* radial wooden strips; and

(v) Evaluate these calibrations by estimating the wood chemical composition of sections of radial wooden strips in a separate test set based on NIR spectra obtained from the radial-longitudinal surface of each strip.

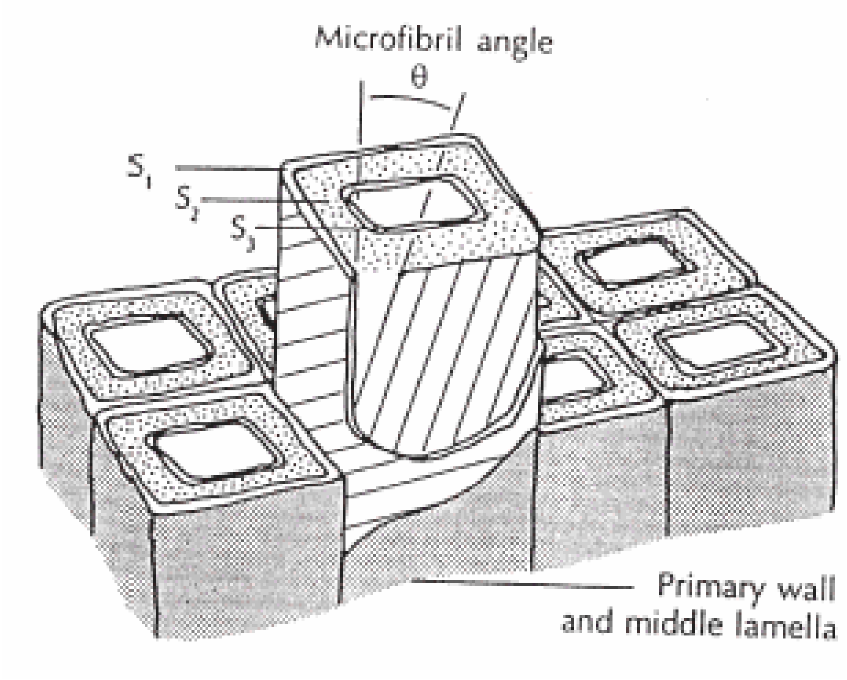

Fig. 2.1. Orientation of microfibrils in the S2 layer of the cell wall (adapted from Dickson and Walker (1997).

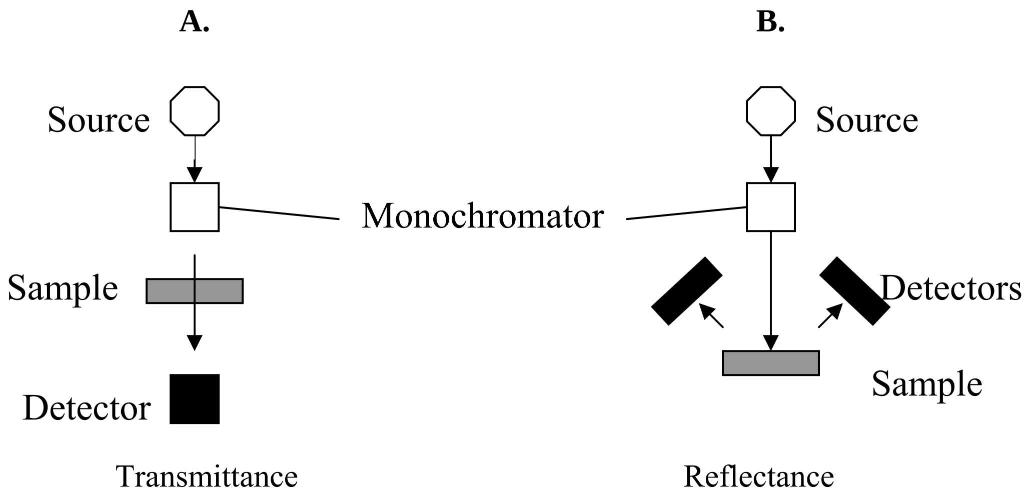

Fig. 2.2. Two types of near infrared spectroscopy commonly utilized for estimating wood properties. Transmittance (A.) through the sample and reflectance (B.) of near infrared energy from the surface of the sample.

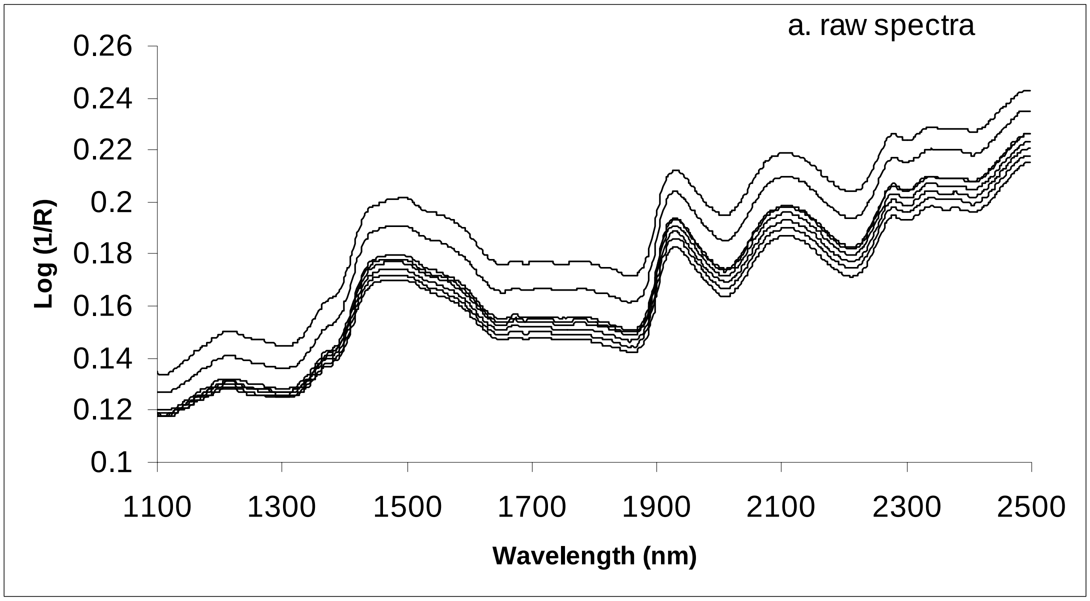

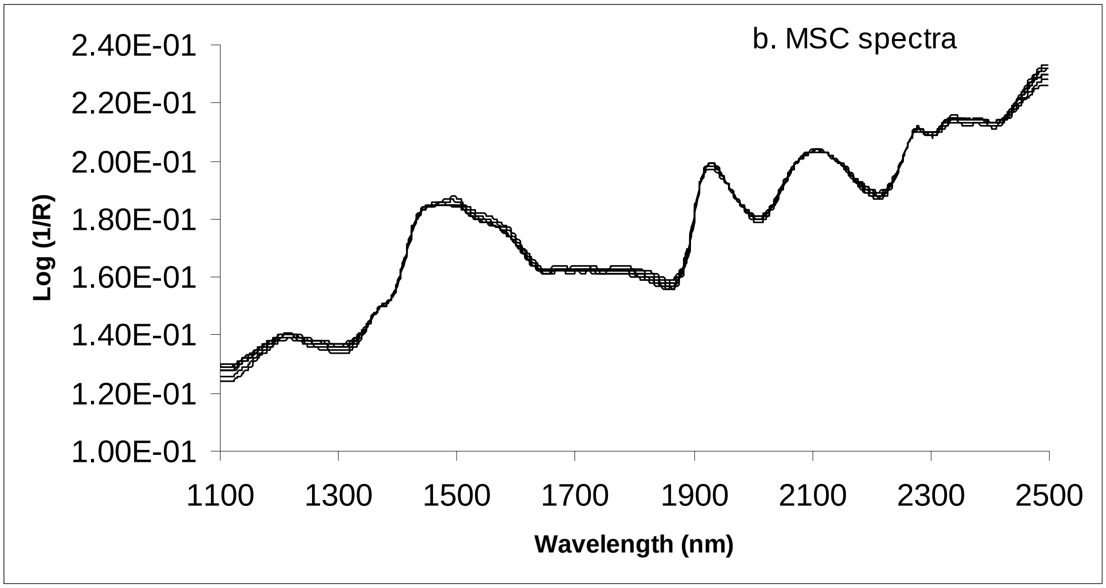

Fig. 2.3. Math treatments on spectra, with the raw spectra (a.), multiplicative scatter correction treated (b.), standard normal variate treated (c.), first derivative treated (d.), and second derivative treated spectra (e.).

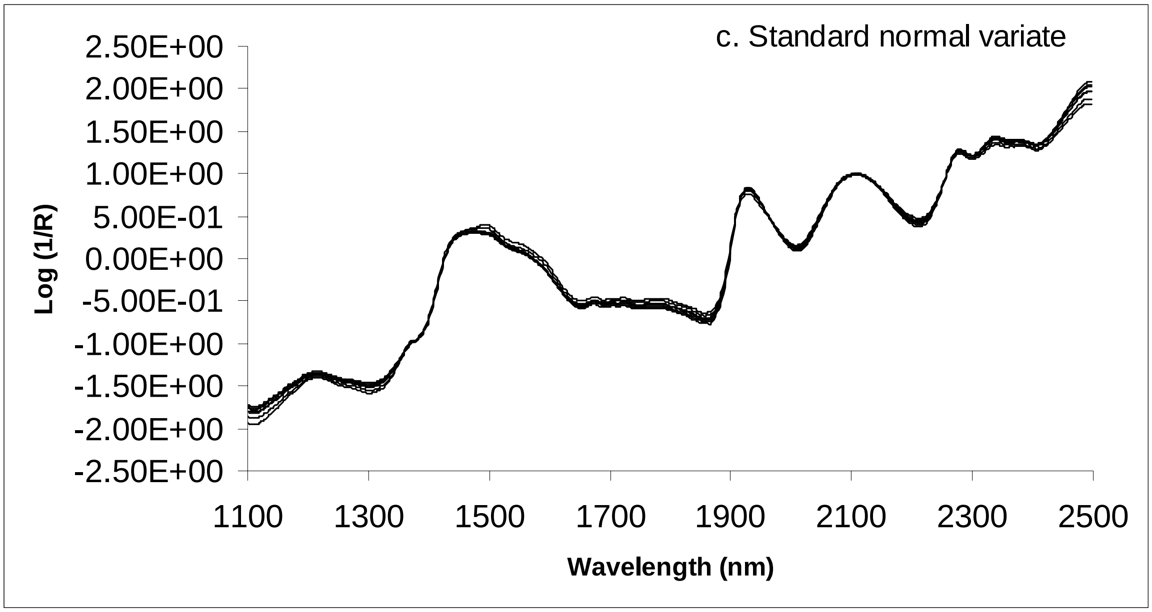

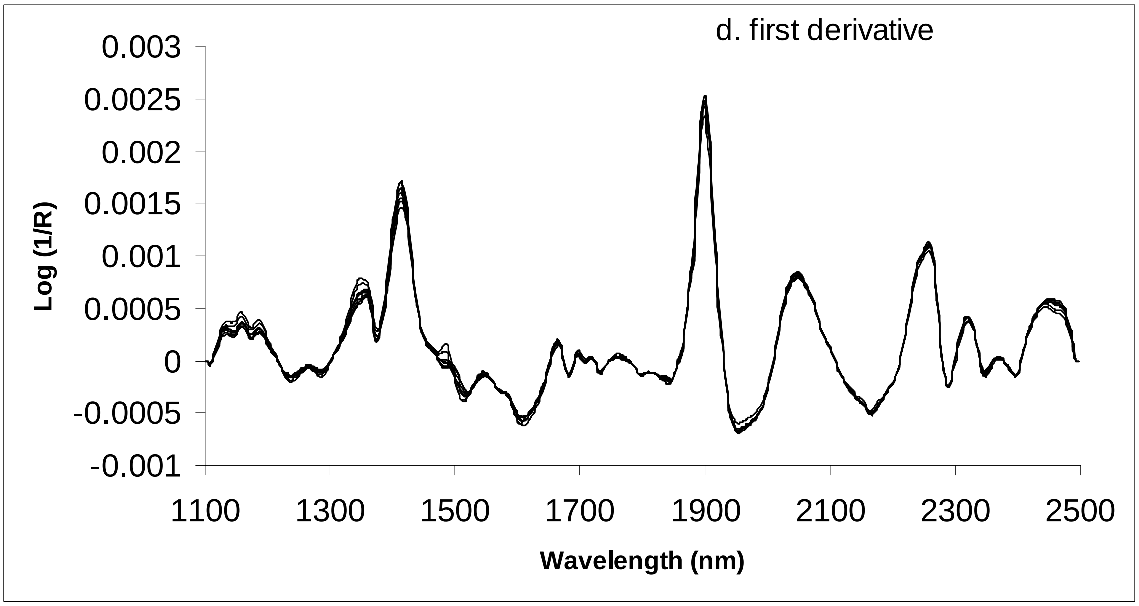

Fig. 2.3. Math treatments on spectra, with the raw spectra (a.), multiplicative scatter correction treated (b.), standard normal variate treated (c.), first derivative treated (d.), and second derivative treated spectra (e.).

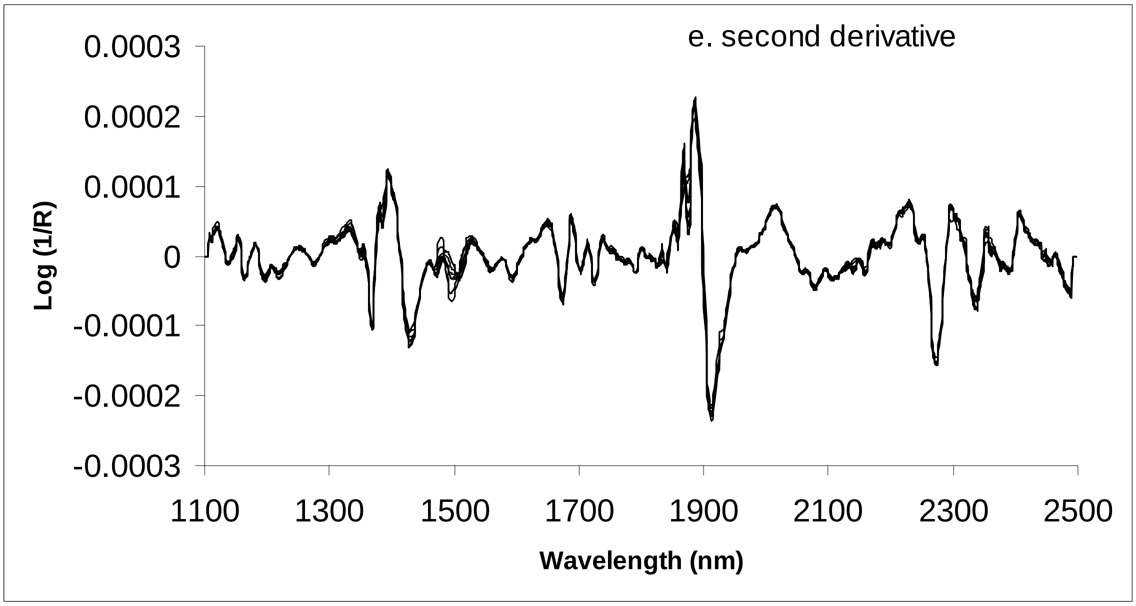

Fig. 2.3. Math treatments on spectra, with the raw spectra (a.), multiplicative scatter correction treated (b.), standard normal variate treated (c.), first derivative treated (d.), and second derivative treated spectra (e.).

Literature Cited

Alén, R., 2000. Structure and chemical composition of wood. In: P. Stenius (Editor), Papermaking science and technology Published in cooperation with the Finnish Paper Engineers' Association and TAPPI, Helsinki ; [Atlanta], pp. 12-57.

American Forest and Paper Association, 2000. Standard method of testing small clear specimens of timber. ASTM D 143.

Axrup, L., Markides, K. and Nilsson, T., 2000. Using miniature diode array NIR spectrometers for analysing wood chips and bark samples in motion. J. Chemometrics, 14(5-6): 561-572.

Bailey, I.W. and Vestal, M.R., 1937. The orientation of cellulose in the secodary wall. J. Arnold Arboretum, 18(3): 185-195.

Barton, F.E., 2002, Theory and principles of near infrared spectroscopy, Near Infrared Spectroscopy: Procceding of the 10th International Conference, Kyonjgu, Korea, A.M.C. Davies and R.K. Cho, NIR Publications, 1-6.

Birkett, M.D. and Gambino, M.J.T., 1988. Potential applications for near-infrared spectroscopy in the pulping industry. Pap. S. Afr., November/December: 34-38.

Booker, R.E., Harington, J. and Shiokura, T., 1997, Variation of Young's modulus with microfibril angle, density and spiral grain, Proceedings of the IAWA / IUFRO International Workshop on the Significance of Microfibril Angle to Wood, Westport, New Zealand, B.G. Butterfield, University of Canterbury Press, 116-139.

Bowyer, J.L., Shmulsky, R. and Haygreen, J.G., 2002. Forest products and wood science : an introduction. Iowa State Press, Ames Iowa, xiv, 554 pp.

Butterfield, B.G., 2003. Wood anatomy in realtion to wood quality. In: J.R. Barnett and G. Jeronimidis (Editors), Wood quality and its biological basis. Blackwell ; Published in the USA/Canada by CRC Press, Oxford Boca Raton, FL, pp. 53-86.

Cave, I.D., 1966. Theory of X-ray measurement of microfibril angle in wood. For. Prod. J., 16(10): 37-42.

Cave, I.D., 1968. The ansotropic elasticity of plant cell wall. Wood Sci.Technol., 2: 268-278.

Cousins, W.J., 1972. Measruement of mean microfibril angles of wood tracheids. Wood Sci. Technol., 6(1): 37-42.

Dickson, R.L. and Walker, J.C.F., 1997. Pines: growing comodities or designer trees. Commonwealth Forestry Review, 76(4): 273-279.

Downes, G.M., Beckers, E.P.J., Turvey, N.D. and Porada, H., 1993. Strength and Structure of Stems from Fast Grown *Pinus radiata*. Trees-Structure and Function. 7(3): 131-136.

Downes, G.M. and Turvey, N.D., 1993. Relationships between Stem Structure and Bending Strength in *Pinus radiata* Seedlings. Trees-Structure and Function, 7(2): 86-91.

Downes, G.M., Nyakuengama, J.G., Evans, R., Northway, R., Blakemore, P., Dickson, R.L. and Lausberg, M., 2002. Relationship between wood density, microfibril angle and stiffness in thinned and fertilized *Pinus radiata*. Iawa Journal, 23(3): 253-265.

Echols, R.M., 1970, Moving slit radiography of wood samples for incremental measurements, Coference on tree ring analysis, University of British Columbia, Vancouver.

Evans, R., 1994. Rapid Measurement of the Transverse Dimensions of Tracheids in Radial Wood Sections from *Pinus radiata*. Holzforschung, 48(2): 168-172.

Evans, R., 1997, Rapid scanning of microfibril angle in increment cores by x ray diffractometry. In Microfibril Angle in Wood, Proceedings of the IAWA / IUFRO International Workshop on the Significance of Microfibril Angle to Wood, Westport, New Zealand, B.G. Butterfield, University of Canterbury Press, 116-139.

Evans, R., Kibblewhite, R.P. and Stringer, S., 1997. Kraft pulp fibre property prediction from wood properties in eleven radiata pine clones. Appita J., 50(1): 25-33.

Evans, R., 1999. A variance approach to the X-ray diffractometric estimation of microfibril angle in wood. Appita J., 52(4): 283-289, 294.

Evans, R., Hughes, N. and Menz, D., 1999a. Microfibril angle variation by scanning X-ray diffractometry. Appita J., 52(5): 363-367.

Evans, R., Kibblewhite, R.P. and Lausberg, M., 1999b. Relationships between wood and pulp properties of twenty-five 13 year old radiata pine trees. Appita J., 52(2): 132-139.

Garbutt, D.C.F., 1989. The analysis of cellulose in wood using a hydrogen peroxide, acetic acid delignifying reagent moderated by sodium perobrate. Pap. S. Afr., 9: 27-30.

Garbutt, D.C.F., Donkin, M.J. and Meyer, J.H., 1992. Near-infrared reflectance analysis of cellulose and lignin in wood. Pap. S. Afr., April: 45-48.

Gindl, W., Teischinger, A., Schwanninger, M. and Hinterstoisser, B., 2001. The relationship between near infrared spectra of radial wood surfaces and wood mechanical properties. J. Near Infrared Spectrosc., 9(4): 255-261.

Hatfield, R. and Fukushima, R.S., 2005. Can Lignin Be Accurately Measured? Crop Sci., 45(3): 832-839.

Hauksson, J.B., Sjöstrom, M., Edlund, U., Bergqvist, G. and Bergsten, U., 2001. Prediction of basic wood properties for Norway spruce. Interpretation of near infrared spectroscopy data using partial least squares regression. Wood Sci. and Technol., 35(6): 475-485.

Hoffmeyer, P. and Pedersen, J.G., 1995. Evaluation of Density and Strength of Norway Spruce Wood by Near-Infrared Reflectance Spectroscopy. Holz Roh Werkst., 53(3): 165-170.

Huang, C.L., 1995. Revealing fibril angle in wood sections by ultrasonic treatment. Wood and Fiber Sci., 27(1): 49-54.

Huang, C.L., Lindström, H., Nakada, R. and Ralston, J., 2003. Cell wall structure and wood properties determined by acoustics a selective review. Holz als Roh- und Werkstoff, 61(5): 321-335.

Johnson, D.B., Moore, W.E. and Zank, L.C., 1961. The spectrophotometric determination of lignin in small samples. Tappi J., 44: 789-793.

Kelley, S.S., Rials, T.G., Snell, R., Groom, L.H. and Sluiter, A., 2004. Use of near infrared spectroscopy to measure the chemical and mechanical properties of solid wood. Wood. Sci. Technol., 38(4): 257-276.

Kibblewhite, R.P., Riddell, M.J.C. and Shelbourne, C.J.A., 1998. Kraft fibre and pulp qualities of 29 trees of New Zealand grown *Eucalyptus nitens*. Appita J., 51(2): 114-121.

Kumar, S., 2004. Genetic parameter estimates for wood stiffness, strength, internal checking, and resin bleeding for radiata pine. Can. J. For. Res., 34(12): 2601-2610.

Marten, G.C., Shenk, J.S. and Barton, F.E., 1989. Near infrared reflectance spectroscopy (NIRS) : analysis of forage quality. United States. Agricultural Research Service. U.S. Dept. of Agriculture Agricultural Research Service. Rev. Aug. 1989 (with supplements). Ag. Handbook No. 643 110 pp.

McKenzie, A.W., 1994. A Guide To Pulp Evaluation. CSIRO, Australia, 66 pp.

Meder, R., Thumm, A. and Marston, D., 2003. Sawmill trial of at-line prediction of recovered lumber stiffness by NIR spectroscopy of *Pinus radiata* cants. J. Near Infrared Spectrosc., 11(2): 137-143.

Megraw, R.A., 1985. Wood quality factors in loblolly pine: the influence of tree age, position in tree, and cultural practice on wood specific gravity, fiber length, and fibril angle. TAPPI Press, Atlanta, GA, 88 pp.

Michell, A.J., 1995. Pulpwood quality estimation by near-infrared spectroscopic measurements on eucalypt woods. Appita J., 48(6): 425-428.

Muneri, A. and Raymond, C.A., 2001. Nondestructive sampling of *Eucalyptus globulus* and *E. nitens* for wood properties. II. Fibre length and coarseness. Wood Sci. Technol., 35(1/2): 41-56.

Næs, T., Isaksson, T., Fearn, T. and Davies, T., 2002. A user-friendly guide to multivariate calibration and classification. NIR, Chichester, 344 pp.

Norris, K.H. and Butler, W.L., 1961. Techniques for Obtaining Absorption Spectra on Intact Biological Samples. Ire Transactions on Biomedical Electronics, 8(3): 153-155.

Olsson, R.J.O., Tomani, P., Karlsson, M., Joseffson, T., Sjoberg, K. and Bjorklund, C., 1995. Multivariate characterization of chemical and physical descriptors in pulp using NIRR. Tappi J., 78(10): 158-166.

Panshin, A.J. and De Zeeuw, C., 1980. Textbook of wood technology: structure, identification, properties, and uses of the commercial woods of the United States and Canada. McGraw-Hill, New York, 722 pp.

Pereira, H., 1988. Variability in the chemical composition of plantation eucalyptus (*Eucalyptus globulus* Labill.). Wood and Fiber Sci., 20: 82-90.

Pereira, H., Graça, J. and Rodrigues, J.C., 2003. Wood chemistry in relation to quality. In: J.R. Barnett and G. Jeronimidis (Editors), Wood quality and its biological basis. Blackwell ; Published in the USA/Canada by CRC Press, Oxford Boca Raton, FL, pp. 53-86.

Pillow, M.Y., Terrell, B.Z. and Hiller, C.H., 1953. Patterns of variation in fibril angles in loblolly pine. U.F.S.F.P. Laboratory. D1935.

Poke, F.S., Wright, J.K. and Raymond, C.A., 2004. Predicting Extractives and Lignin Contents in *Eucalyptus globulus* Using Near Infrared Reflectance Analysis. J. Wood Chem. Technol., 24(1): 55-67.

Poke, F.S. and Raymond, C.A., 2006. Predicting extractives, lignin and cellulose contents using near infrared spectroscopy on solid wood in *Eucalyptus globulus*. J. Wood Chem. Technol., (In Press).

Polge, H., 1978. Fifteen years of wood radiation densitometry. Wood Sci. Technol., 12(3): 187-196.

Preston, R.D., 1952. The molecular structure of plant cell walls. Chapman & Hall, [London], 211 pp.

Pronto, M.B., 1998, Carbohydrate Analysis of Pulp using High-Performance Anion-Exchange Chromatography with Pulsed Amperometric Detection: A Comparison of Two Detector Settings, Pulping conference, Montreal; Canada, TAPPI; 1998, 1477-1484.

Raymond, C.A., Schimleck, L.R., Muneri, A. and Michell, A.J., 2001. Nondestructive sampling of *Eucalyptus globulus* and *E. nitens* for wood properties. III. Predicted pulp yield using near infrared reflectance analysis. Wood. Sci. Technol., 35(3): 203-215.

Raymond, C.A. and Schimleck, L.R., 2002. Development of near infrared reflectance analysis calibrations for estimating genetic parameters for cellulose content in *Eucalyptus globulus*. Can. J. For. Res., 32(1): 170-176.

Risén, J., Hultén, A.H. and Paulsson, M., 2004. Influence of Fiber Properties on the Network Strength of Softwood and Hardwood Kraft Pulp Fibers from Different Stages of a Bleaching Sequence. J. Wood Chem. Technol., 24(4): 289-306.

Roberts, C.A., Workman, J., Reeves, J.B., American Society of Agronomy., Crop Science Society of America. and Soil Science Society of America., 2004. Near-infrared spectroscopy in agriculture. American Society of Agronomy : Crop Science Society of America : Soil Science Society of America, Madison, Wis., 822 pp.

Saranpää, P., 2003. Wood Density and growth. In: J.R. Barnett and G. Jeronimidis (Editors), Wood quality and its biological basis. Blackwell ; Published in the USA/Canada by CRC Press, Oxford Boca Raton, FL, pp. 87-117.

Schimleck, L., Evans, R. and Ilic, J., 2001a. Application of near infrared spectroscopy to a diverse range of species demonstrating wide density and stiffness variation. IAWA J., 22(4): 415-429.

Schimleck, L.R., Wright, P.J., Michell, A.J. and Wallis, A.F.A., 1997. Near-infrared spectra and chemical compositions of *E. globulus* and *E. nitens* plantation woods. Appita J., 50(1): 40-46.

Schimleck, L.R. and Michell, A.J., 1998. Determination of within-tree variation of kraft pulp yield using near-infrared spectroscopy. Tappi J., 81(5): 229-236.

Schimleck, L.R., Michell, A.J., Raymond, C.A. and Muneri, A., 1999. Estimation of basic density of *Eucalyptus globulus* using near-infrared spectroscopy. Can. J. For. Res., 29(2): 194-201.

Schimleck, L.R., Raymond, C.A., Beadle, C.L., Downes, G.M., Kube, P.D. and French, J., 2000. Applications of NIR spectroscopy to forest research. Appita J., 53(6): 458-464.

Schimleck, L.R., Evans, R. and Ilic, J., 2001b. Estimation of *Eucalyptus delegatensis* wood properties by near infrared spectroscopy. Can. J. For. Res., 31(10): 1671-1675.

Schimleck, L.R. and Evans, R., 2002a. Estimation of microfibril angle of increment cores by near infrared spectroscopy. IAWA J., 23(3): 225-234.

Schimleck, L.R. and Evans, R., 2002b. Estimation of wood stiffness of increment cores by near infrared spectroscopy: The development and application of calibrations based on selected cores. IAWA J., 23(3): 217-224.

Schimleck, L.R., Evans, R. and Matheson, A.C., 2002. Estimation of *Pinus radiata* D. Don clear wood properties by near-infrared spectroscopy. J. Wood Sci., 48(2): 132-137.

Schimleck, L.R. and Evans, R., 2003. Estimation of air-dry density of increment cores by near infrared spectroscopy. Appita J., 56(4): 312-317.

Schimleck, L.R., Mora, C. and Daniels, R.F., 2003. Estimation of the physical wood properties of green *Pinus taeda* radial samples by near infrared spectroscopy. Can. J. For. Res., 33(12): 2297-2305.

Schimleck, L.R. and Evans, R., 2004. Estimation of *Pinus radiata* D. Don tracheid morphological characteristics by near infrared spectroscopy. Holzforschung, 58(1): 66-73.

Schimleck, L.R., Jones, P.D., Peter, G.F., Daniels, R.F. and Clark, A., 2004. Nondestructive estimation of tracheid length from sections of radial wood strips by near infrared spectroscopy. Holzforschung, 58(4): 375-381.

Schultz, T.P. and Burns, D.A., 1990. Rapid secondary analysis of lignocellulose: comparison of near infrared (NIR) and fourier transform infrared (FTIR). Tappi J., 73(5): 209-212.

Seifert, K., 1960. Zur frage der Cellulose-Schnellbestimmung nach der Acetylaceton-Mthode. Papier, 14: 104-106.

Sjöström, E., 1993. Wood chemistry: fundamentals and applications. Academic Press, San Diego, 293 pp.

Stamm, A.J., 1964. Wood and cellulose science. Ronald Press Co., New York,, x, 549 pp.

Sykes, R., Li, B.L., Hodge, G., Goldfarb, B., Kadla, J. and Chang, H.-M., 2005. Prediction of loblolly pine wood properties using transmittance near-infrared spectroscopy. Can. J. For.Res., 35(10): 2423-2431.

Thumm, A. and Meder, R., 2001. Stiffness prediction of radiata pine clearwood test pieces using near infrared spectroscopy. J. Near Infrared Spectrosc., 9(2): 117-122.

Thygesen, L.G., 1994. Determination of dry matter content and basic density of Norway spruce by near-infrared reflectance and transmission spectroscopy. J. Near Infrared Sectrosc., (9)2: 127-135.

Via, B.K., So, C.L., Shupe, T.F., Stine, M. and Groom, L.H., 2005. Ability of near infrared spectroscopy to monitor air-dry density distribution and variation of wood. Wood and Fiber Sci., 37(3): 394-402.

Wallis, A.F.A., Wearne, R.H. and Wright, P.J., 1997, New approaches to rapid analysis of cellulose in wood, International Symposium on Wood and Pulping Chemistry, Montreal, Quebec, Canadian Pulp and Paper Association,

Wimmer, R., Downes, G.M. and Evans, R., 2002a. Temporal variation of microfibril angle in *Eucalyptus nitens* grown in different irrigation regimes Tree Phys., 22(11): 817-817.

Wimmer, R., Downes, G.M. and Evans, R., 2002b. High-resolution analysis of radial growth and wood density in *Eucalyptus nitens*, grown under different irrigation regimes. Annals of Forest Science 59(5-6): 519-524.

Wimmer, R., Downes, G.M., Evans, R., Rasmussen, G. and French, J., 2002c. Direct effects of wood characteristics on pulp and handsheet properties of *Eucalyptus globulus*. Holzforschung., 56(3): 244-252.

Wright, J.A., Birkett, M.D. and Gambino, M.J.T., 1990. Prediction of Pulp Yield and Cellulose Content from Wood Samples Using near-Infrared Reflectance Spectroscopy. Tappi J., 73(8): 164-166.

Wright, P.J. and Wallis, A.F.A., 1996. Rapid determination of carbohydrates in hardwoods by high performance anion exchange chromatography. Holzforschung, 50(6): 518-524.

Yeh, T.F., Chang, H.M. and Kadla, J.F., 2004. Rapid prediction of solid wood lignin content using transmittance near-infrared spectroscopy. J. Agric. Food Chem., 52(6): 1435-1439.

Yeh, T.F., Yamada, T., Capanema, E., Chang, H.M., Chiang, V. and Kadla, J.F., 2005. Rapid Screening of Wood Chemical Component Variations Using Transmittance Near-Infrared Spectroscopy. J. Agric. Food Chem., 53(9): 3328-3332.

Zink-Sharp, A., 2003. The mechanical properties of wood. In: J.R. Barnett and G. Jeronimidis (Editors), Wood quality and its biological basis. Blackwell ; Published in the USA/Canada by CRC Press, Oxford Boca Raton, FL, pp. 53-86.

Chapter 3

VARIATION IN *PINUS TAEDA* WOOD PROPERTIES

Introduction

The high variability of *P. taeda* wood properties presents problems in selecting trees for genetic improvement and for producing products such as lumber, veneer, pulp, and paper. Properties such as density, microfibril angle, stiffness, radial and tangential diameter, coarseness, and specific surface all vary from the pith of the tree to the bark. This chapter explores the high resolution data measured by SilviScan that was used for the studies presented in later chapters.

Wood properties

Physical properties

Density

Density varies from pith to bark by an increase in percentage of latewood in a growth ring and an increase in the density of the latewood (Panshin and De Zeeuw 1980). Figure 3.1 illustrates the density of a single SilviScan strip used in the studies presented here. The density was measured at a resolution of 50 μm (black line); this data was then averaged to create 10 mm sections (gray line) that are used in the research described in chapter 4. As noted latewood density increases as does the percentage of latewood hence average density increases. The density of the earlywood appears to remain constant regardless of tree age. Samples taken from the coastal plain have a higher percentage of latewood than samples of the same age taken from the piedmont, leading to a higher average density. It is theorized that late summer rainfall in the in the coastal plain leads to greater production of latewood.

Microfibril angle

Microfibril angle also varies from pith to bark, with angles closest to the pith being the highest 30º+ and decreasing to approximately 10 to 15º (Megraw 1985). Microfibril angle is lower in latewood cells than in earlywood cells, because of changes in the rate of cell formation, the slower the maturation period, the lower the microfibril angle (Megraw 1985). SilviScan measures microfibril angle in 0.2 mm to 10 mm increments. The data used in this study was measured at 1 mm resolution (Figure 3.2 black line), it was then averaged to 10 mm increments (gray line) for use in the work described in chapter 4. Even at 1 mm resolution the variation in microfibril angle within rings is apparent, especially for the wide rings near the pith.

Stiffness

As the distance from the pith increases, the stiffness of the wood formed increases, because of both the increase in density and the decrease in microfibril angle. Figure 3.3 illustrates this increase, with the stiffness in the latewood being much higher than the earlywood; the black line represents the SilviScan data, while the gray line is the data averaged for the research presented in chapter 4. The stiffness estimated by SilviScan is calculated from density and microfibril angle.

Morphological properties

Coarseness and specific surface

The average coarseness increases as the distance form the pith increases, this is caused primarily by the increased percentage of latewood. Figure 3.4 shows the SilviScan data at a resolution of 50 μm (black line) and for the data averaged at a resolution of 10 mm. Coarseness and specific surface vary between latewood and earlywood rapidly as latewood begins to form in the growth ring. Average specific surface decreases from pith to bark, because of the increase in coarseness. Figure 3.5 illustrates the SilviScan data (black line) and the average data (grey line).

Wall thickness

The greater the distance the formation of wood cells occurs from the pith, the thicker the cell walls of the latewood. This increase in wall thickness leads to a greater density of the wood. In Figure 3.6 the 10 mm average data for wall thickness (gray line) increases with increasing distance from the pith, this increase is less clear in the SilviScan data (black line).

Perimeter, radial and tangential diameter

Cell perimeter being calculated from 2 times the sum of radial and tangential diameter will increase with any increase in either cell dimension. Radial diameter illustrated in Figure 3.6a shows no steady increase or decrease in cell dimensions with an increase in distance from pith, but does decrease in the latewood when compared to the earlywood within a single growth ring, because of the slowing of growth in the later part of the growing season. Tangential diameter does increase with distance from the pith (Figure 3.6b). Because radial diameter stays relatively constant (based on 10 mm averaged data, gray line), and tangential diameter increases with the distance from the pith, perimeter also increases with an increase in the distance from the pith (Figure 3.6c).

Discussion

With the exception of radial diameter the variation from pith to bark of the above wood properties makes it challenging to select trees based on them. A method that could measure, all of the above properties quickly with a single step and non-destructively would be a great asset to selection of trees for breeding and specific forest products, such as lumber, veneer, and pulp and paper. The primary objectives of the studies presented here, are to examine the use of near infrared spectroscopy to determine a wide range of wood properties non-destructively, and how to improve the measurement of these properties by improved mathematical treatment of data, the enhancement of calibrations, and the integration and prediction of the wood properties of samples from new sites.

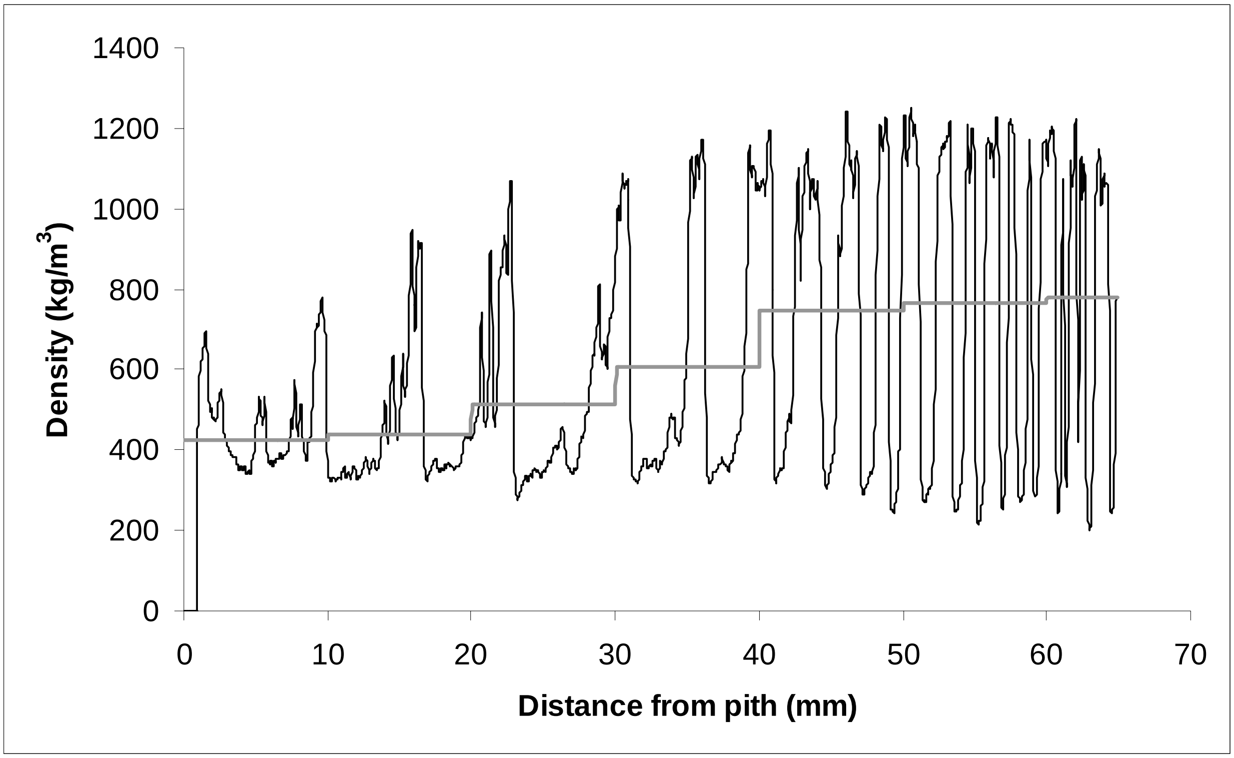

Fig. 3.1. Density of a single radial wooden strip measured by SilviScan, with the black line being the SilviScan data and the grey line being the data averaged into 10 mm sections.

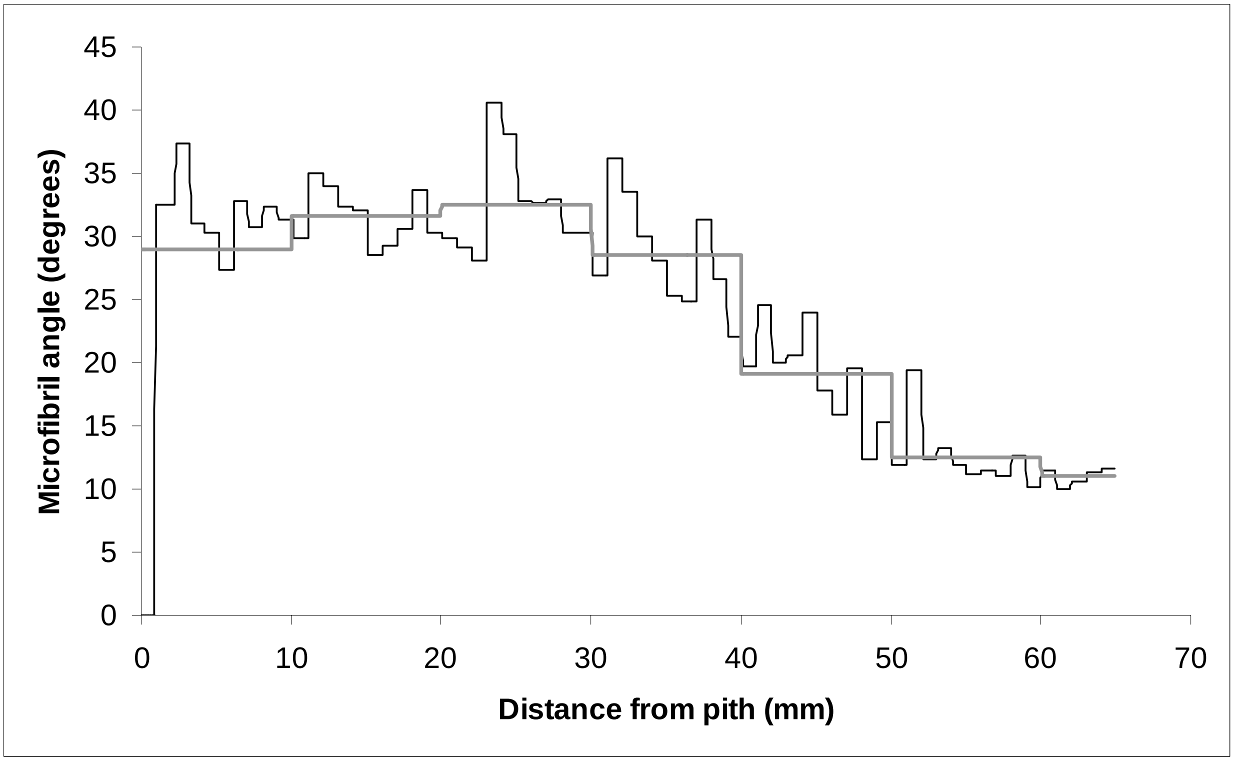

Fig. 3.2. Microfibril angle of a single radial wooden strip measured by SilviScan, with the black line being the SilviScan data and the grey line being the data averaged into 10 mm sections.

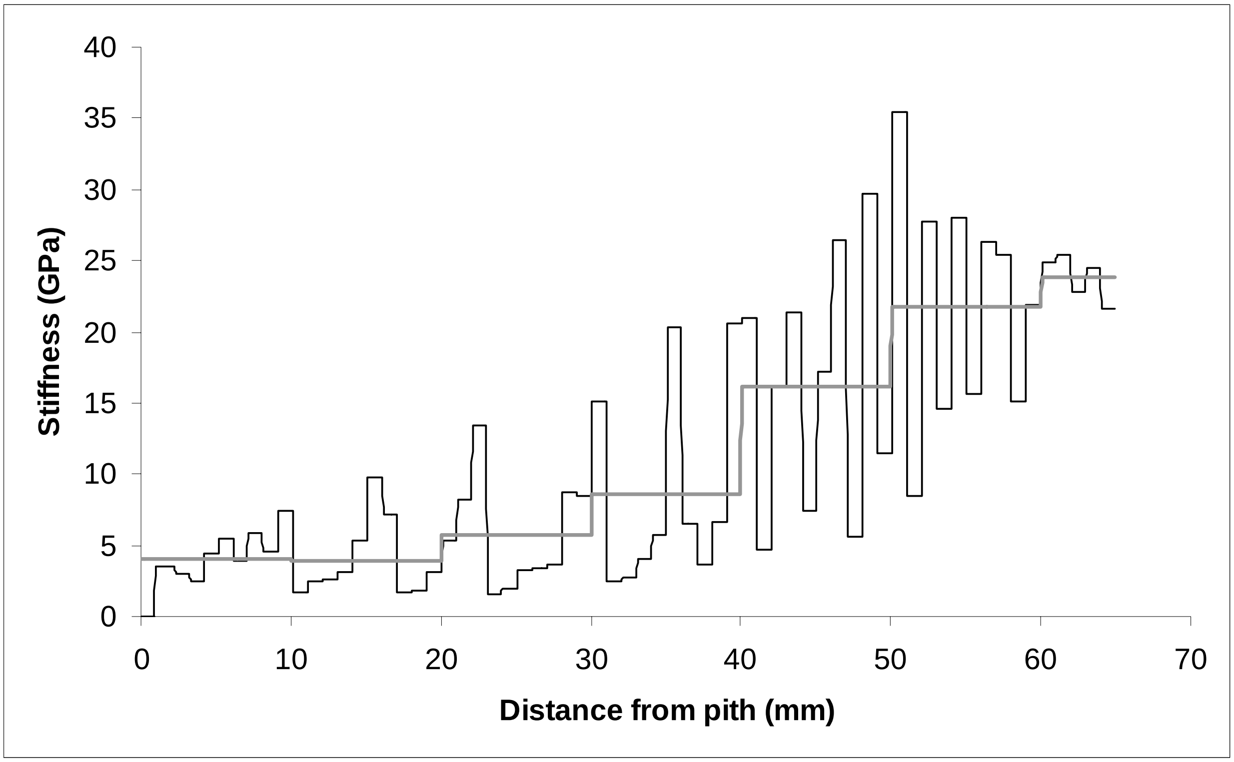

Fig. 3.3. Stiffness of a single radial wooden strip measured by SilviScan, with the black line being the SilviScan data and the grey line being the data averaged into 10 mm sections.

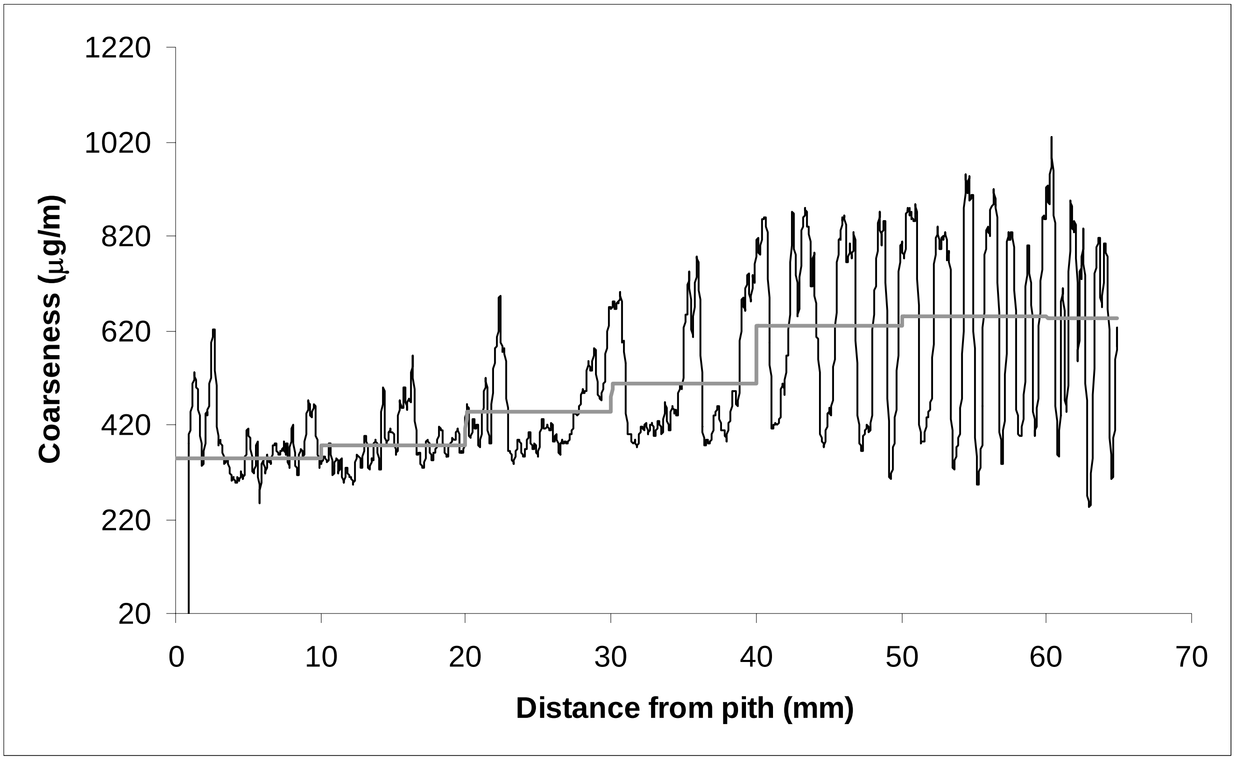

Fig. 3.4. Coarseness of a single radial wooden strip measured by SilviScan, with the black line being the SilviScan data and the grey line being the data averaged into 10 mm sections.

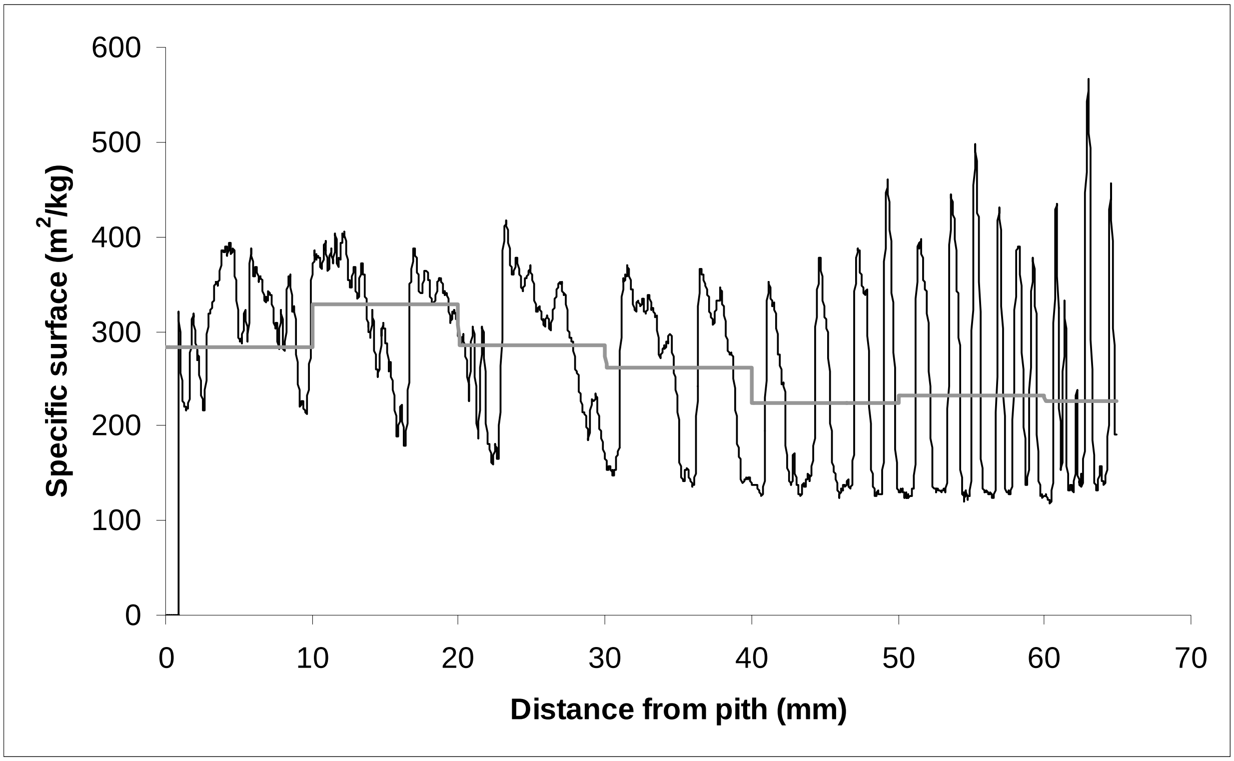

Fig. 3.5. Specific surface of a single radial wooden strip measured by SilviScan, with the black line being the SilviScan data and the grey line being the data averaged into 10 mm sections.

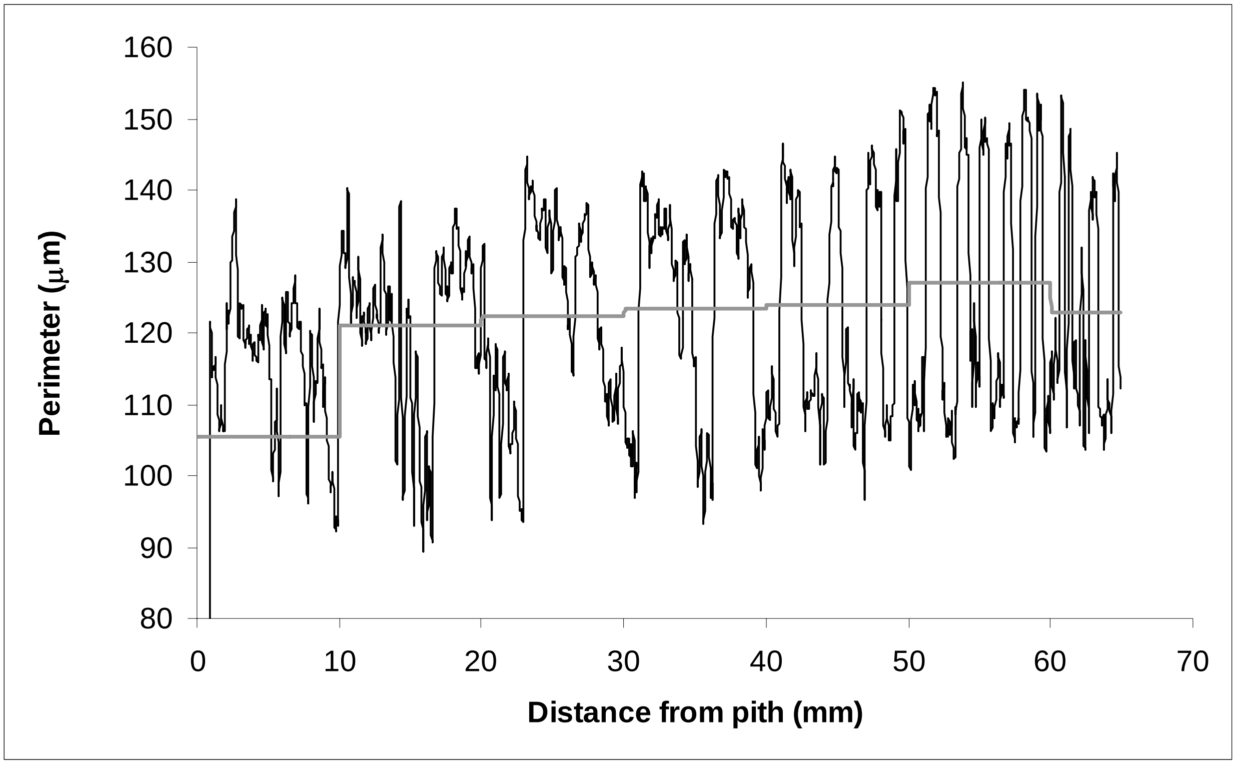

Fig. 3.6. Perimeter of a single radial wooden strip measured by SilviScan, with the black line being the SilviScan data and the grey line being the data averaged into 10 mm sections.

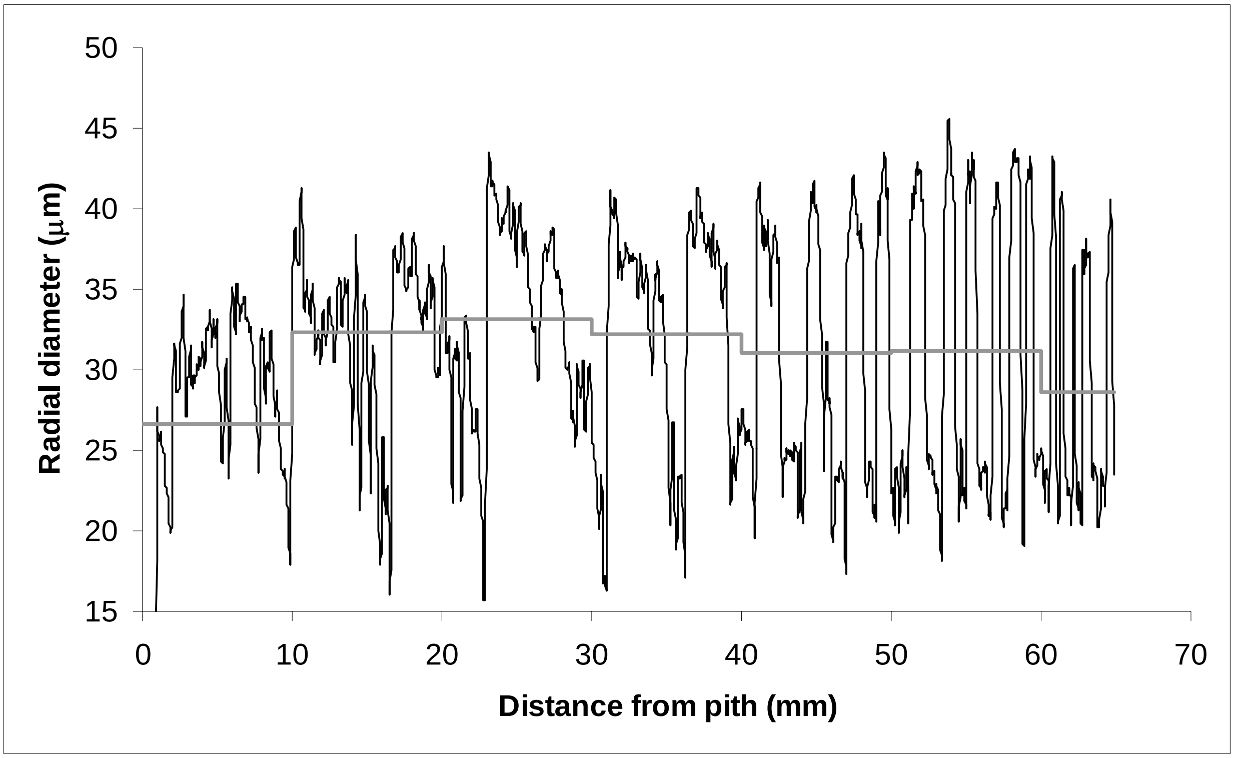

Fig. 3.7. Radial diameter of a single radial wooden strip measured by SilviScan, with the black line being the SilviScan data and the grey line being the data averaged into 10 mm sections.

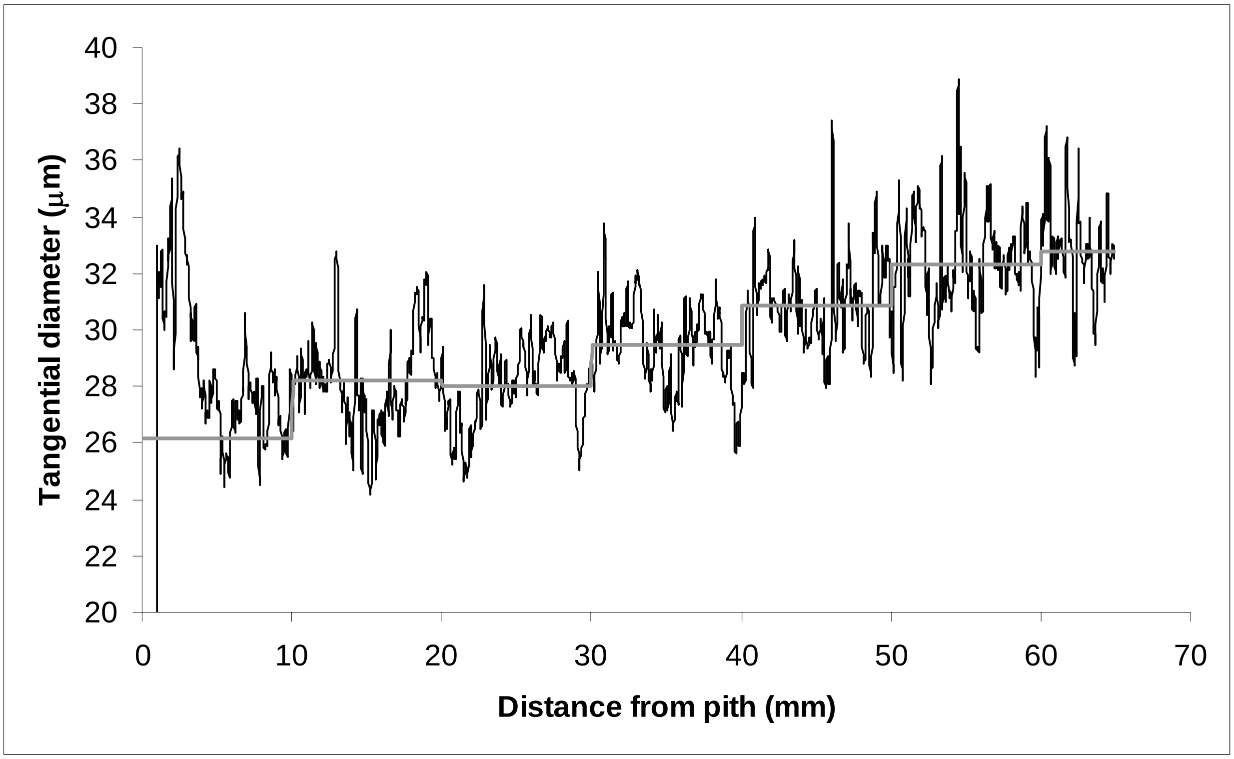

Fig. 3.8. Tangential diameter of a single radial wooden strip measured by SilviScan, with the black line being the SilviScan data and the grey line being the data averaged into 10 mm sections.

Literature cited

Megraw, R.A., 1985. Wood Quality Factors in Loblolly Pine: the Influence of Tree Age, Position in Tree, and Cultural Practice on Wood Specific Gravity, Fiber Length, and Fibril Angle. TAPPI Press, Atlanta, GA, 88 pp.

Panshin, A.J. and De Zeeuw, C., 1980. Textbook of Wood Technology: Structure, Identification, Properties, and Uses of the Commercial Woods of the United States and Canada. McGraw-Hill, New York, 722 pp.

Chapter 4

NONDESTRUCTIVE ESTIMATION OF PINUS TAEDA L. WOOD PROPERTIES FOR SAMPLES FROM A WIDE RANGE OF SITES IN GEORGIA[1]

---

[1] Jones, P. D., L. R. Schimleck, G. F. Peter, R. F. Daniels, and A. Clark III. 2005. Canadian Journal of Forest Research 35(1) 85-92.
Reprinted here with the permission of the publisher.

Abstract

Preliminary studies based on small sample sets show that near infrared (NIR) spectroscopy has the potential for rapidly estimating many important wood properties. However, if NIR is to be used operationally then calibrations using several hundred samples from a wide variety of growing conditions need to be developed and their performance tested on samples from new populations. In this study 120 *Pinus taeda* L. (loblolly pine) radial strips (cut from increment cores) representing 15 different sites from 3 physiographic regions in Georgia (USA) were characterized in terms of air-dry density, microfibril angle (MFA) and stiffness. NIR spectra were collected in 10 mm increments from the radial longitudinal surface of each strip and split into calibration (9 sites, 729 spectra) and prediction sets (6 sites, 225 spectra). Calibrations were developed using untreated and mathematically treated (first and second derivative and multiplicative scatter correction) spectra. Strong correlations were obtained for all properties, the strongest R^2 being 0.83 (density), 0.90 (MFA) and 0.93 (stiffness). When applied to the test set, good relationships were obtained (R_p^2 ranged from 0.80 to 0.90) but the accuracy of predictions varied depending on math treatment. The addition of a small number of cores from the prediction set (one core per new site) to the calibration set improved the accuracy of predictions and importantly minimized the differences obtained with the various math treatments. These results suggest that density, MFA and stiffness can be estimated by NIR with sufficient accuracy to be used in operational settings.

Keywords: air-dry density, microfibril angle, near infrared spectroscopy, *Pinus taeda*, SilviScan, stiffness.

Introduction

Plantation grown *Pinus taeda* L. (loblolly pine) is the major source of wood fiber and solid wood products in the Southern U.S. The deployment of genetically improved planting stock coupled with intensive silvicultural management has greatly improved the growth and yields of *P. taeda*. Li et al. (1999) report that *P. taeda* trees grown from seeds obtained from first-generation seed orchards have produced 7-12% more volume per acre at harvest than trees grown from wild seed, while for second-generation seed orchards it is estimated that gains in volume will be 13-21%. It is expected that the inclusion of quality traits such as stem straightness and wood quality in *P. taeda* breeding programs will greatly increase genetic gains and the value of the trees (Li et al. 1999). However, traditional methods of measuring wood properties are slow and cost prohibitive for measuring these properties in the large number of trees needed for improved breeding. Also the measurement of modulus of elasticity and modulus of rupture are destructive, so if a tree is determined to have traits that are desirable for inclusion in future generations; the tree has been destroyed and is therefore no longer available for crossing. Thus rapid, non-destructive methods for measuring wood properties must be developed.

Near infrared (NIR) spectroscopy has the potential to provide the forestry industry with a rapid tool for the nondestructive estimation of wood properties. Several studies (Birkett and Gambino 1988; Garbutt et al. 1992; Michell 1995; Raymond and Schimleck 2002; Schimleck et al. 2000; Wright et al. 1990) have used NIR spectroscopy to estimate chemical properties of wood. Studies have also shown that NIR spectroscopy can be used to estimate the physical-mechanical properties of wood, including density and stiffness (Gindl et al. 2001; Hoffmeyer and Pedersen 1995; Meder et al. 2003; Schimleck et al. 1999; Thumm and Meder 2001; Thygesen

1994). Recently, it has been shown that reasonable calibrations can be created for green *Pinus taeda* L. (loblolly pine) samples for air-dry density, microfibril angle (MFA) and stiffness (Schimleck et al. 2003b).

The successful application of NIR spectroscopy relies on the provision of accurate calibration data for large numbers of samples. Several recent NIR spectroscopic studies (Schimleck and Evans 2002b; 2002a; 2003; Schimleck et al. 2002; Schimleck et al. 2003b) have used data provided by the SilviScan instruments for calibration purposes. The SilviScan instruments, developed by CSIRO's Forestry and Forest Products Division, utilize x-ray densitometry, diffractometry and image analysis to accurately measure several wood properties at high spatial resolution.

Strong relationships between SilviScan and NIR-estimates for a range of wood properties including density, MFA, and stiffness have been obtained for *Eucalyptus delegatensis* R. T. Baker (alpine ash) and *Pinus radiata* D. Don (Radiata pine) samples (Schimleck et al. 2001b; Schimleck et al. 2002). Studies based on radial wooden strips cut from selected *P. radiata* increment cores have shown promising results for air-dry density, MFA, stiffness (determined using SilviScan-2 diffractometric data and measured density), and several tracheid morphological characteristics (Schimleck and Evans 2002b; 2002a; 2003; 2004). Calibrations performed well when applied to a separate test set of two cores that were from the same population as the calibration samples. However, in general these studies show the utility of NIR to estimate wood properties have been based on small sample sets with limited variation. It is expected, as with any statistical procedure that with a larger sample size that more of the population variation will be captured within the calibration, but the difficulty arises in determining if enough variation has been captured by the selected samples. The use of large sample sizes in agricultural applications indicates that calibrations based on large sample sets are more robust (Berzaghi et al. 2002).

P. taeda is grown on a wide variety of sites in the Southern U.S. and it has been shown that geographic regions within the Southern U.S. have differing wood properties (Talbert and Jett 1981; Zobel and McElwee 1958). In Georgia *P. taeda* is grown within three distinct regions (Upper and Lower Coastal Plain, and Piedmont). On-going research conducted by the Wood Quality Consortium (WQC) at the University of Georgia (Athens, GA, USA) is investigating how the wood properties of each geographic region differ. Thus, an important test of NIR for wood property estimation is how well general calibrations developed from wood samples obtained from trees growing in each geographic region predict wood properties from these regions. Therefore the objectives of this study are:

(*i*) To create wood property calibrations (air-dry density, MFA, stiffness) using samples drawn from a wide variety of sites chosen to represent the three physiographic regions where *P. taeda* is grown;

(*ii*) To examine the performance of the wood property calibrations when applied to samples from sites not included in the calibration;

(*iii*) To investigate methods for improving the applicability of wood property calibrations to samples from sites not initially included in the calibration set.

Materials and methods

Sample origin

Samples were collected from *P. taeda* plantations located in Georgia, USA. For each of the three physiographic regions in Georgia (Lower and Upper Atlantic Costal Plain, and

Piedmont) five plantations, ranging in age from 21 to 26 years, with a range of site indices were sampled, to represent trees presently being harvested as mature. The sites are summarized in Table 4.1. The calibration set was comprised of ninety breast height (1.37 m) increment cores sampled from three plantations within each region; ten increment cores per site were taken. One increment core developed blue stain and was unavailable for analysis because of discoloration, leaving eighty-nine cores for analysis. The prediction set was comprised of thirty breast height increment cores (5 cores per plantation, 2 plantations per region).

SilviScan analysis

One hundred and nineteen radial wooden strips were available for SilviScan analysis; these strips were cut from increment cores using a twin-blade saw. Strip dimensions were 2 mm tangentially, and 7 mm longitudinally; radial length was determined by the pith-to-bark length of the sample. The radial strips were extracted in warm acetone for 24 hours prior to SilviScan analysis.

Wood properties were measured using SilviScan-1 and -2 (Evans 1994; 1997; 1999). Air-dry density (referred to as density for the reminder of the text) was measured in 50-micron steps using x-ray densitometry. MFA was averaged over 1 mm intervals on SilviScan-2 using scanning x-ray diffractometry. An estimate of wood stiffness (same resolution as MFA) was obtained by combining x-ray densitometry and x-ray diffraction data. All measurements were made in a controlled environment of 40% relative humidity and a temperature of 20º C. The high resolution SilviScan data was averaged over 10 mm sections from pith-to-bark for correlation with the NIR spectra. The original 1 mm resolution SilviScan data and the 10 mm averaged data are illustrated in Figure 4.1 for a single radial strip used in the calibration. While the decrease in resolution from 1 mm to 10 mm does not show MFA variation within rings, the 10 mm data follows the pith-to-bark trend.

Near infrared spectroscopy

Diffuse reflectance NIR spectra were collected from the radial, longitudinal face of each strip using a NIRSystems Inc. Model 5000 scanning spectrometer. All measurements were made in a controlled environment of 40% relative humidity and a temperature of 20º C. Samples were conditioned in this environment for no less than one week prior to scanning. Samples were held in a custom made holder (Schimleck et al. 2001). A 5 mm x 10 mm mask was used to ensure an area of constant size was analyzed. The spectra were collected at 2 nm intervals over the wavelength range 1100-2500 nm. The instrument reference was a ceramic standard. Fifty scans were accumulated for each 10 mm section; these scans were averaged to give a single spectrum per section. A total of 729 spectra were collected from the 89 radial strips representing the calibration set, 225 spectra were collected from the 30 radial strips representing the prediction set. Table 4.2 contains the summary statistics for the two data sets**.**

Wood property calibrations

Wood property calibrations were developed using the Unscrambler (version 8.0) software package (Camo AS, Norway). Three math treatments, along with the raw spectral data were used to create the calibrations using Partial Least Square (PLS) regression. The math treatments were first and second derivatives (obtained from the untreated spectra using the Savtizky-Golay approach, with left and right gaps of eight nm) and Multiplicative Scatter Correction (MSC) (Næs et al. 2002). All three methods are known to reduce noise that occurs within spectral data (Næs et al. 2002). Calibrations were developed with four cross validation segments.

The Standard Error of Calibration (SEC) (determined from the residuals of the final calibration), the Standard Error of Cross Validation (SECV) (determined from the residuals of each cross validation phase), the coefficient of determination (R^2), and the ratio of performance to deviation (RPD_c) (Williams and Sobering 1993), calculated as the ratio of the standard deviation of the reference data to the SECV were used to assess calibration performance. Determination of RPD allows comparison of calibrations developed for different wood properties that have differing data ranges and units, the higher the RPD_c the more accurate the data is described by the calibration.

Prediction of wood properties

To examine the performance of the calibrations, they were used to predict the wood properties (air-dry density, MFA, stiffness) of the test set samples. The Standard Error of Prediction (SEP) (determined from the residuals of the predictions) was calculated and gives a measure of how well a calibration predicts parameters of interest for set of samples not included in the calibration set. The predictive ability of the calibrations was assessed by calculating the RPD_p (which is similar to the RPD_c) but uses the standard deviation of the prediction set reference data and the SEP.

Results

Wood Property Calibrations

Table 4.3 summarizes the calibration results for all math treatments. Density calibrations had coefficients of determination (R^2) that ranged from 0.78 (second derivative) to 0.83 (MSC), and RPD_c values that ranged from 2.11 (second derivative) to 2.30 (MSC). The number of factors varied between math treatments from 2 (second derivative) to 6 (raw data). Calibrations for MFA had R^2 between 0.89 (first derivative) and 0.90 (MSC). Based on RPD_c and R^2 values the MSC math treatment gave the strongest calibration statistics. Figure 4.2 shows the plots for both the MFA calibration (a) using the MSC math treatment and the standardized residual plot (b) for the same calibration. It is apparent that MFA variation increases at higher MFA's. Several transformations were examined, but did not reduce the variation observed for high MFA's. The stiffness calibration based on raw spectral data gave the highest R^2 value (0.93) and the highest RPD_c (3.65) however it was developed using 8 factors while stiffness calibrations developed using math treated spectra required fewer factors (5 or 6) and gave similar statistics. The MSC treatment gave the best calibration results overall for density, MFA and stiffness.

Wood property predictions

The true test of a calibration is to use it to predict values for a set of samples unrelated from those used to develop the calibration. Table 4.4 summarizes results for predictions made on the separate test set. A prediction R^2 (R_p^2) was calculated as the proportion of variation in the independent prediction set that was explained by the calibration. In general the wood property calibrations developed using different math treatments gave similar R_p^2 but the SEP and consequently the RPD_p varied greatly between math treatments. Predicted density had R_p^2 that ranged from 0.81 (second derivative) to 0.83 (MSC) while the RPD_p ranged from 0.88 (MSC) to 2.28 (first derivative), these extremes are shown in Figure 4.3. Predicted density had a strong relationship with measured density, as indicated by the strong R_p^2, but the predictions of density obtained using the MSC treated spectra were shifted upward from the line of equivalence, i.e. NIR underestimated density, causing a large error (SEP = 119.3 kg m^{-3}). The first derivative predictions were closer to the true values giving a smaller SEP (45.8 kg m^{-3}) and RPD_p (2.05). Predicted MFA also had little variation in R_p^2 ranging from 0.80 (second derivative) to 0.84

(MSC) while RPD_p varied from 1.01 (first derivative) to 2.34 (MSC). The RPD_p for stiffness had the lowest range between math treatments, ranging from 1.17 (first derivative) to 2.20 (second derivative), but the R_p^2 range was the same as for density only with slightly higher overall values, 0.87 (second derivative) to 0.90 (first derivative). None of the math treatments used, consistently provided the best predictive ability, while the first derivative worked well for density, it performed less efficiently for MFA and stiffness. Overall the second derivative treatment provided the best predictions, giving the best results for stiffness and reasonable results for density and MFA

Improvement of the wood property calibrations

Gutherie and Walsh (2002), while assessing soluble solids in mandarin fruit, found that their general calibration did not predict soluble solids well in samples from new sites owing to the specific variation of a particular site. Their solution was to add a single sample from each of the new sites which was sufficient to decrease the error associated with the predictions to acceptable levels. Based on the findings of Gutherie and Walsh (2002) we created a new calibration set by including NIR spectra collected from one randomly selected core from each new site in the prediction set for inclusion in the calibration set.

Table 4.5 summarizes the results for the wood property calibrations obtained after NIR spectra from a single core from each of the sites in the prediction set had been added to the calibration set. Each core was randomly selected and increased the number of spectra in the calibration set to 771 (95 increment cores). There were only slight increases in R^2 and RPD_c values but when applied to the prediction sets SEP and RPD_p values were improved for all wood properties (Table 4.6). In addition, the calibrations developed using the different math treatments all gave similar predictive results.

The RPD_p for density increased for all math treatments except for the second derivative, which was not altered. MFA had a range of increased values for RPD_p from 1.99 (raw data) to 2.40 (MSC), and R_p^2 values ranging from 0.80 (raw) to 0.85 (MSC). The largest overall improvement occurred for the MSC treated spectra for stiffness, RPD_p increased from 1.18 for the original predictions (Table 4.4) to 3.35 for the expanded predictions, an increase of 2.18. MSC treated spectra clearly gave the best results for MFA and stiffness; while for density the best results were obtained with first derivative spectra. In Figure 4.4, the data for density (a.), MFA (b.), and stiffness (c.) are shown for a single sample (selected at random) from the prediction set. The figure includes SilviScan data at the original resolution, the SilviScan data averaged at 10 mm, predicted wood properties at 10 mm using the original MSC calibrations, and predicted wood properties at 10 mm using the expanded MSC calibrations.

Discussion

The purpose of this study was to examine the use of NIR spectroscopy to estimate wood properties of increment cores that had been removed from standing trees non-destructively. Predicted wood properties of increment cores from sites not originally included in the calibration gave estimates that would be good for classification of wood properties, but had undesirable levels of error. The addition of a single core from each stand used in the prediction set decreased the error of the wood property predictions resulting in significantly more accurate estimates. Using a large and diverse population of wood cores increased the applicability of the calibrations for predicting *P. taeda* wood properties and increased the amount of work associated with creating the calibrations.

Development of calibrations using a large population size will give the best representation of the population of interest, in this study *P. taeda* grown in Georgia (USA). This study demonstrates that it is possible to create calibrations for density, MFA, and stiffness using a large population that represented a diverse range of sites. In a series of studies by Schimleck and Evans using similar techniques on a small *P. radiata* sample set (8 strips, 119 spectra) second derivative calibrations gave SEC values of 23.5 kg m^{-3} for density, 1.8 degrees for MFA, and 0.9 GPa for stiffness (Schimleck and Evans 2002a, 2002b, 2003). When these calibrations were used to predict the properties of 2 separate samples, the resulting SEP's were lower for one core and higher for the other than those reported here. While their work demonstrated that NIR spectroscopy could predict some wood properties of *P. radiata* (and possibly other *Pinus* species) they did not have sufficient samples to make the calibrations applicable to samples from new populations (or sites). The development of calibrations using large populations to create calibrations has been hindered by statistical software packages that could not cope with large numbers of spectra, and limited by computer processing power. Berzaghi et al. (2002) successfully created calibrations using a large sample size for the chemical analysis of forage crops, showing that with recent technological advancements large sample sets were manageable for use in creating calibrations. The only foreseeable problem with using large sample sets as used in the present study, is the matching of measured data (SilviScan) that has been averaged over a given distance, 10 mm in this study, with the spectral data that is associated with a given region of a strip, this can be overcome by having stringent data compiling techniques in place.

While the non-expanded calibrations resulted in higher prediction errors, the overall goodness of fit allows for the predicted values to be useful in classification of wood properties. The use of non-expanded calibrations would allow a researcher to identify when the transition from less desirable properties to more desirable properties occurs, for example when MFA starts to plateau. Non-expanded calibrations could be used to identify trees whose properties require additional research, for example a tree that has an extremely low juvenile wood MFA, which would reduce the cost of analysis. Samples from sites already in the calibration could be tested with a lower amount of associated error.

With the enhancement of calibrations by adding a single strip from the stand of interest the prediction error is lowered substantially, giving more accurate predictions. The associated SEP for predicted stiffness dropped from 4.58 GPa to 1.56 GPa using the expanded calibration created using the MSC math treatment. In all cases the addition of samples from the sites of interest decreased the associated prediction error. It is believed that this enhancement occurs not because of the increase in variability of the wood properties in the calibration, but because of slight variability in the spectra from each stand which could be expected owing to the unique growing conditions at each site. Each time a new site is sampled, a single sample must be added to the current calibration data set, and then the calibrations recalculated for the enhancement to occur.

Using a large population to create calibrations for the non-destructive estimation of wood properties is now possible with NIR spectroscopy. Handling of data for large sample sets requires protocols that allow for a minimum chance for errors when compiling calibration data and NIR spectra. Whether the research requires a calibration for classification (non-expanded) or accurate measurements (expanded) NIR spectroscopy is capable of providing both for selected wood properties. With an increase in resolution (i.e. spectra collected at 5 mm) the data sets will become larger and more complicated, but will allow for a greater understanding of wood properties, growth and age dependent transitions in these properties, and possibly within ring estimation of wood properties using NIR spectroscopy.

Conclusions

This study demonstrates that large data sets that include a wide range of environmental and genetic variation can establish good calibrations for density, MFA and stiffness based on NIR spectra obtained in 10 mm sections from the radial longitudinal face of *P. taeda* strips.

The calibrations gave strong relationships when used to predict the wood properties of a separate set of cores from sites not included in the calibration set but the accuracy of predictions varied depending on the math treatment employed.

The addition of a small number of cores from the prediction set (one core per site) to the calibration set greatly improved the accuracy of predictions and minimized the difference between mathematical processing treatments.

Acknowledgments

The authors thank the UGA Wood Quality Consortium for *P. taeda* sample collection and the Georgia TIP^3 program for funding the SilviScan analysis of the samples. The authors would also like to thank the UGA Wood Quality Consortium for sample preparation and the SilviScan team for the determination of wood properties. Florida Agricultural Experiment Station Journal Series R-10394.

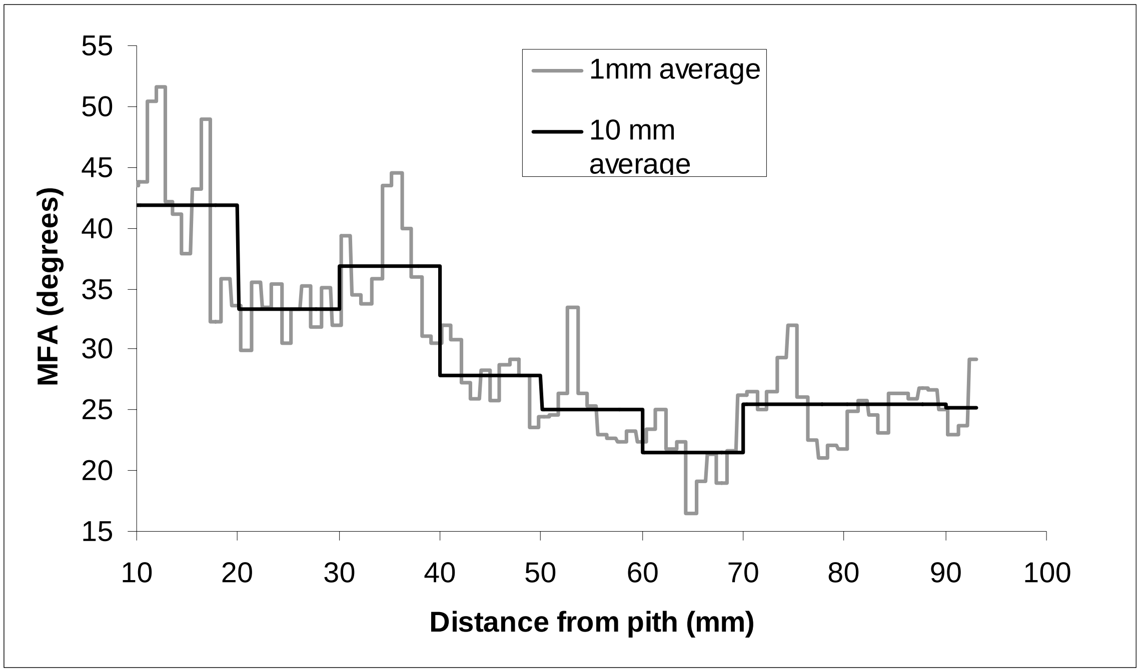

Fig. 4.1. SilviScan microfibril angle (MFA) data for a single sample from the calibration data set at both the original 1 mm resolution and 10 mm resolution (averaged).

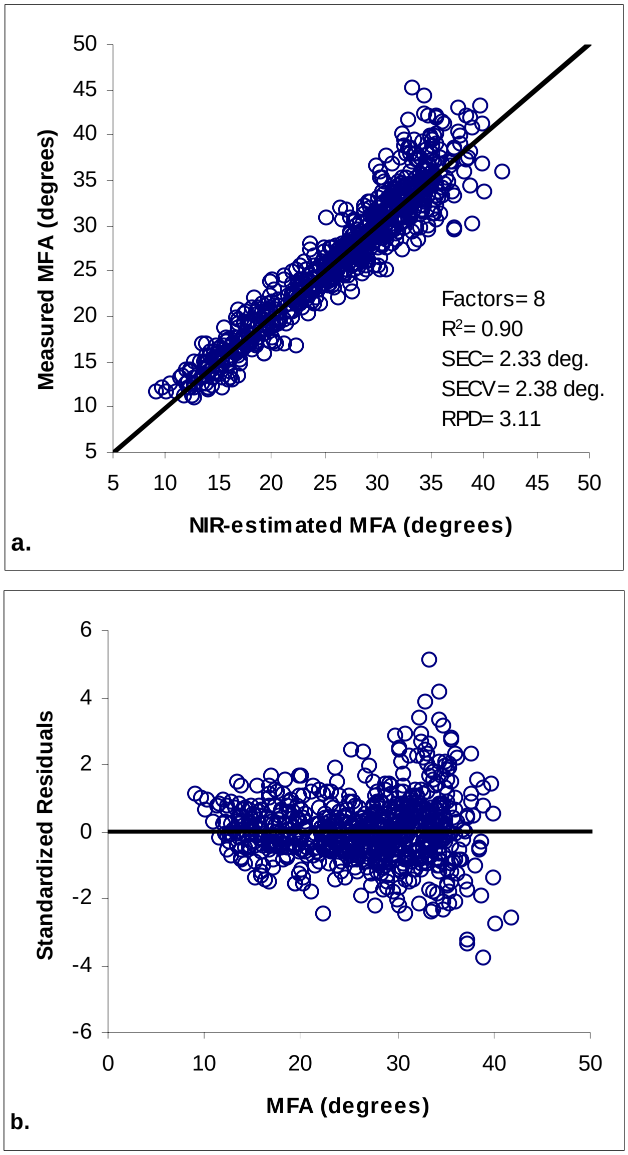

Fig. 4.2. Relationship between measured microfibril angle (MFA) and NIR-estimated MFA (a.) and standardized residuals (b.). MSC treated spectra were used for calibration.

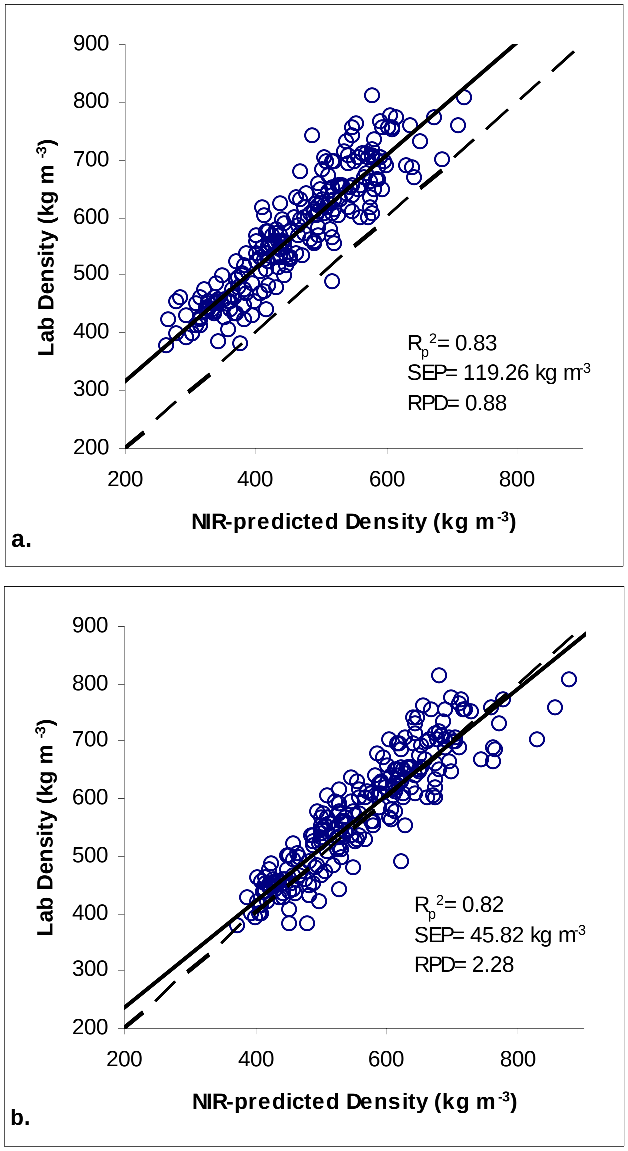

Fig. 4.3. Relationship between measured density and NIR-predicted density for (a.) MSC treated NIR spectra and (b.) first derivative treated NIR spectra. The regression line has been plotted (thick, dark line) in both figures, the thin broken line indicates a one-one relationship between measured and predicted density.

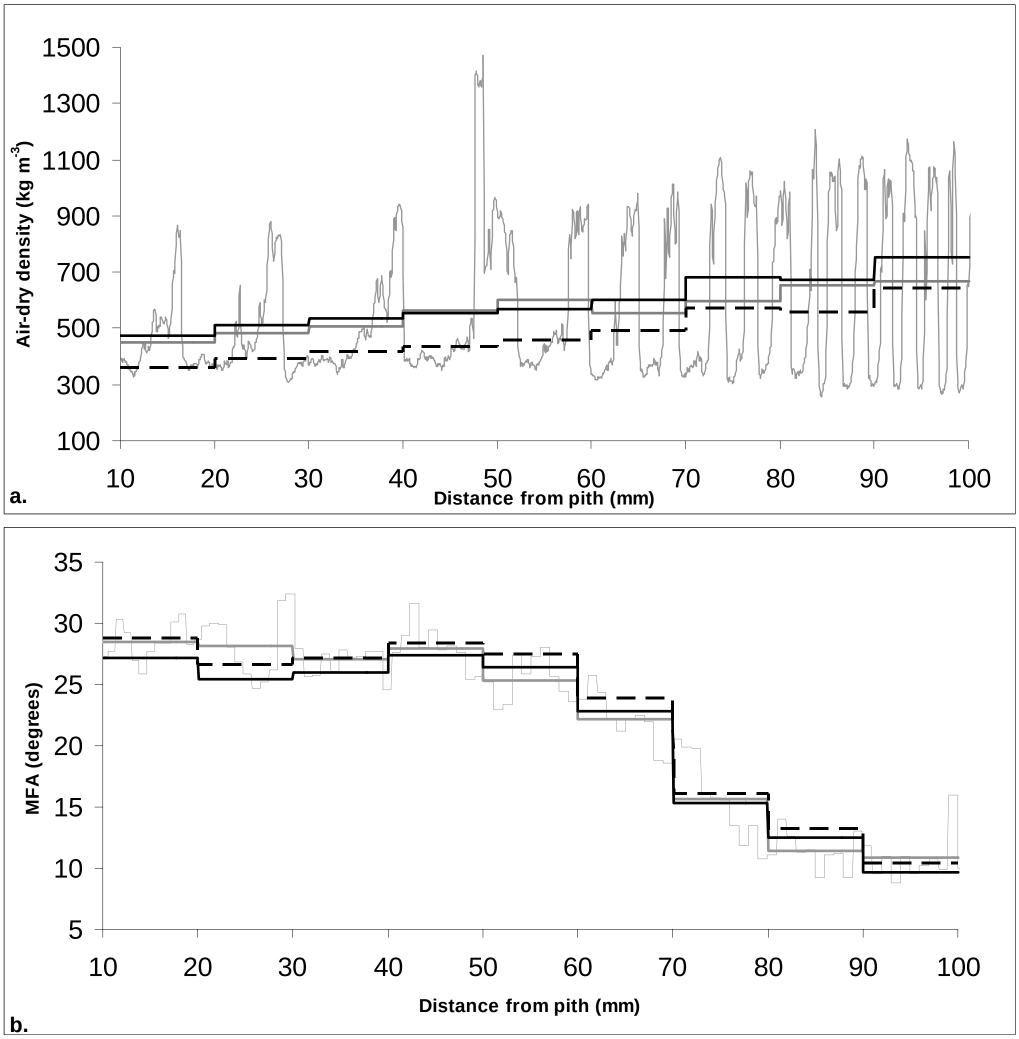

Fig. 4.4**.** Plot of pith-to-bark radial variation for (a.) density, (b.) microfibril angle (MFA), and (c.) stiffness for a randomly selected *P. taeda* radial strip. The solid thin gray line represents the original SilviScan data, the solid thick gray line represents SilviScan data averaged over 10 mm, the dashed black line represents values predicted by the original calibrations and the solid black line represents values predicted data using the expanded calibrations.

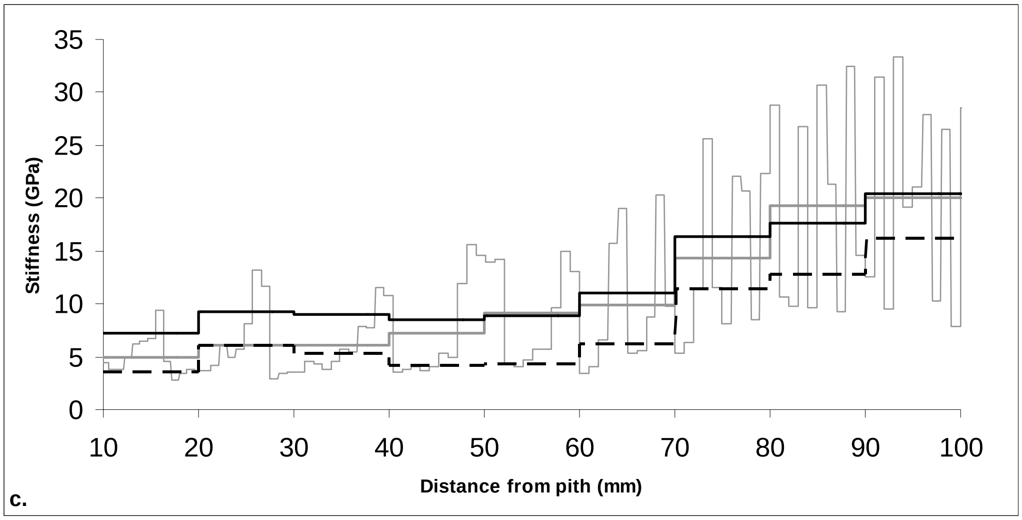

Fig. 4.4. Plot of pith-to-bark radial variation for (a.) density, (b.) microfibril angle (MFA), and (c.) stiffness for a randomly selected *P. taeda* radial strip. The solid thin gray line represents the original SilviScan data, the solid thick gray line represents SilviScan data averaged over 10 mm, the dashed black line represents values predicted by the original calibrations and the solid black line represents values predicted data using the expanded calibrations.

Table 4.1. Stand descriptions for samples used in the calibration and prediction sets including age, site index (SI$_{25}$), county, latitude (Lat.), longitude (Long.), and physiographic region.

Region	SI$_{25}$	Age	Lat.	Long.
Calibration Set				
Upper Atlantic Coastal Plain	67	24	32º 33’	-84º 60’
Upper Atlantic Coastal Plain	69	25	32º 78’	-82º 97’
Upper Atlantic Coastal Plain	78	22	31º 62’	-84º 99’
Lower Atlantic Coastal Plain	76	25	32º 26’	-81º 27’
Lower Atlantic Coastal Plain	79	25	31º 31’	-81º 60’
Lower Atlantic Coastal Plain	84	25	31º 11’	-81º 81’
Piedmont	54	25	33º 70’	-83º 22’
Piedmont	55	21	34º 09’	-85º 22’
Piedmont	61	26	32º 96’	-83º 62’
Prediction Set				
Upper Atlantic Coastal Plain	55	22	32º 13’	-84º 70’
Upper Atlantic Coastal Plain	67	24	32º 34’	-84º 60’
Lower Atlantic Coastal Plain	80	25	31º 42’	-81º 68’
Lower Atlantic Coastal Plain	81	24	31º 79’	-81º 57’
Piedmont	54	24	32º 77’	-84º 61’
Piedmont	66	26	33º 46’	-83º 10’

Table 4.2. Summary of wood of the variation in wood properties of the samples used for the calibration and prediction sets.

Wood	Calibration set (729 spectra)				Prediction set (225 samples)			
Property	Minimum	Maximum	Av.	Std. dev.	Minimum	Maximum	Av.	Std. dev.
Air-dry density (kg m^{-3})	337.47	832.55	577.16	98.73	378.02	811.21	575.95	104.39
MFA (degrees)	10.98	45.21	26.64	7.42	9.67	39.58	24.40	7.32
SilviScan stiffness (GPa)	2.35	23.04	9.60	4.89	2.70	23.21	10.14	5.38

Table 4.3. Summary of density, microfibril angle (MFA) and stiffness calibrations developed using untreated and math treated NIR spectra collected from the radial longitudinal face of radial wooden strips included in the calibration set. Calibration statistics include the coefficient of determination (R^2), the standard error of calibration (SEC), the standard error of cross validation (SECV), and the ratio of performance to standard deviation (RPD_c).

Math Treatment		Calibration				
		Factors	R^2	SEC	SECV	RPD_c
Density (kg m^{-3})	Raw	6	0.82	42.33	43.26	2.28
	MSC	5	0.83	41.22	42.94	2.30
	1st Derivative	5	0.82	42.05	43.26	2.28
	2nd Derivative	2	0.78	46.01	46.89	2.11
MFA (degrees)	Raw	8	0.89	2.43	2.51	2.95
	MSC	8	0.90	2.33	2.38	3.11
	1st Derivative	5	0.89	2.42	2.48	3.00
	2nd Derivative	6	0.89	2.42	2.63	2.83
Stiffness (GPa)	Raw	8	0.93	1.27	1.34	3.65
	MSC	5	0.91	1.48	1.53	3.19
	1st Derivative	5	0.92	1.36	1.40	3.50
	2nd Derivative	6	0.92	1.39	1.52	3.22

Table 4.4. Summary statistics for density, microfibril angle (MFA) and stiffness predicted using the original calibration set. Prediction statistics include the coefficient of determination (R_p^2), the standard error of prediction (SEP), and the ratio of performance to deviation (RPD_p).

Math Treatment		Prediction		
		R_p^2	SEP	RPD_p
Density ($kg\ m^{-3}$)	Raw	0.82	55.15	1.89
	MSC	0.83	119.26	0.88
	1st Derivative	0.82	45.82	2.28
	2nd Derivative	0.81	50.80	2.05
MFA (degrees)	Raw	0.81	4.54	1.61
	MSC	0.84	3.12	2.34
	1st Derivative	0.83	7.22	1.01
	2nd Derivative	0.80	5.27	1.39
Stiffness (GPa)	Raw	0.90	2.47	2.18
	MSC	0.89	4.58	1.18
	1st Derivative	0.90	4.61	1.17
	2nd Derivative	0.87	2.45	2.20

Table 4.5. Summary of density, microfibril angle (MFA) and stiffness calibrations developed using untreated and math treated NIR spectra collected from the radial longitudinal face of radial wooden strips included in the expanded calibration set. Calibration statistics include the coefficient of determination (R^2), the standard error of calibration (SEC), the standard error of cross validation (SECV), and the ratio of performance to standard deviation (RPD_c).

Math Treatment		Calibration				
		Factors	R^2	SEC	SECV	RPD_c
Density (kg m^{-3})	Raw	7	0.82	42.26	43.48	2.29
	MSC	6	0.82	41.67	42.49	2.34
	1st Derivative	6	0.83	41.19	42.67	2.33
	2nd Derivative	3	0.79	45.50	46.22	2.15
MFA (degrees)	Raw	9	0.89	2.50	2.55	2.93
	MSC	8	0.90	2.38	2.44	3.07
	1st Derivative	5	0.90	2.42	2.49	3.00
	2nd Derivative	7	0.90	2.39	2.58	2.90
Stiffness (GPa)	Raw	8	0.92	1.40	1.44	3.45
	MSC	8	0.93	1.31	1.34	3.70
	1st Derivative	5	0.92	1.40	1.45	3.43
	2nd Derivative	7	0.92	1.38	1.51	3.29

Table 4.6. Summary statistics for density, microfibril angle (MFA) and stiffness predicted using the expanded calibration set. Prediction statistics include the coefficient of determination (R_p^2), the standard error of prediction (SEP), and the ratio of performance to deviation (RPD_p).

	Math Treatment	Prediction		
		R_p^2	SEP	RPD_p
Density ($kg\ m^{-3}$)	Raw	0.85	41.65	2.47
	MSC	0.86	39.70	2.59
	1st Derivative	0.86	38.25	2.69
	2nd Derivative	0.81	49.99	2.05
MFA (degrees)	Raw	0.80	3.61	1.99
	MSC	0.85	2.99	2.40
	1st Derivative	0.82	3.25	2.21
	2nd Derivative	0.83	3.09	2.33
Stiffness (GPa)	Raw	0.90	1.84	2.85
	MSC	0.91	1.56	3.35
	1st Derivative	0.91	1.86	2.82
	2nd Derivative	0.88	1.84	2.85

Literature cited

Berzaghi, A.J.P., Flinn, P.C., Dardenne, P., Lagerholm, M., Shenk, J.S., Westerhaus, M.O. and Cowe, I.A., 2002, Comparison of linear and non-linear near infrared calibration methods using large forage databases, Near Infrared Spectroscopy: Proceedings of the 10th International Conference, NIR Publication, 107-111.

Birkett, M.D. and Gambino, M.J.T., 1988. Potential applications for near-infrared spectroscopy in the pulping industry. Pap. S. Afr., November/December: 34-38.

Evans, R., 1994. Rapid Measurement of the Transverse Dimensions of Tracheids in Radial Wood Sections from *Pinus radiata*. Holzforschung, 48(2): 168-172.

Evans, R., 1997, Rapid scanning of microfibril angle in increment cores by x ray diffractometry. In Microfibril Angle in Wood, Proceedings of the IAWA / IUFRO International Workshop on the Significance of Microfibril Angle to Wood, Westport, New Zealand, B.G. Butterfield, University of Canterbury Press, 116-139.

Evans, R., 1999. A variance approach to the X-ray diffractometric estimation of microfibril angle in wood. Appita J., 52(4): 283-289, 294.

Garbutt, D.C.F., Donkin, M.J. and Meyer, J.H., 1992. Near-infrared reflectance analysis of cellulose and lignin in wood. Pap. S. Afr., April: 45-48.

Gindl, W., Teischinger, A., Schwanninger, M. and Hinterstoisser, B., 2001. The relationship between near infrared spectra of radial wood surfaces and wood mechanical properties. J Near Infrared Spectrosc., 9(4): 255-261.

Guthrie, J.A. and Walsh, K.B., 2002, Assessing and enhancing near infrared calibration robustness for soluble solids content in mandarin fruit, Near Infrared Spectroscopy: Proceedings of the 10th International Conference, A.M.C. Davies and R.K. Cho, NIR Publications, 151-154.

Hoffmeyer, P. and Pedersen, J.G., 1995. Evaluation of Density and Strength of Norway Spruce Wood by Near-Infrared Reflectance Spectroscopy. Holz Roh Werkst., 53(3): 165-170.

Li, B., McKeand, S. and Weir, R., 1999. Tree improvement and sustainable forestry - impact of two cycles of loblolly pine breeding in the U.S.A. Forest Genetics, 6(4): 229-234.

Meder, R., Thumm, A. and Marston, D., 2003. Sawmill trial of at-line prediction of recovered lumber stiffness by NIR spectroscopy of *Pinus radiata* cants. J. Near Infrared Spectrosc., 11(2): 137-143.

Michell, A.J., 1995. Pulpwood quality estimation by near-infrared spectroscopic measurements on eucalypt woods. Appita J., 48(6): 425-428.

Næs, T., Isaksson, T., Fearn, T. and Davies, T., 2002. A user-friendly guide to multivariate calibration and classification. NIR, Chichester, 344 pp.

Raymond, C.A. and Schimleck, L.R., 2002. Development of near infrared reflectance analysis calibrations for estimating genetic parameters for cellulose content in *Eucalyptus globulus*. Can. J. For. Res., 32(1): 170-176.

Schimleck, L.R., Michell, A.J., Raymond, C.A. and Muneri, A., 1999. Estimation of basic density of *Eucalyptus globulus* using near-infrared spectroscopy. Can. J. For. Res., 29(2): 194-201.

Schimleck, L.R., Raymond, C.A., Beadle, C.L., Downes, G.M., Kube, P.D. and French, J., 2000. Applications of NIR spectroscopy to forest research. Appita J., 53(6): 458-464.

Schimleck, L.R., Evans, R. and Ilic, J., 2001. Estimation of *Eucalyptus delegatensis* wood properties by near infrared spectroscopy. Can. J. For. Res., 31(10): 1671-1675.

Schimleck, L.R. and Evans, R., 2002a. Estimation of microfibril angle of increment cores by near infrared spectroscopy. IAWA J., 23(3): 225-234.

Schimleck, L.R. and Evans, R., 2002b. Estimation of wood stiffness of increment cores by near infrared spectroscopy: The development and application of calibrations based on selected cores. IAWA J., 23(3): 217-224.

Schimleck, L.R., Evans, R. and Matheson, A.C., 2002. Estimation of *Pinus radiata* D. Don clear wood properties by near-infrared spectroscopy. J. Wood Sci., 48(2): 132-137.

Schimleck, L.R. and Evans, R., 2003. Estimation of air-dry density of increment cores by near infrared spectroscopy. Appita J., 56(4): 312-317.

Schimleck, L.R., Mora, C. and Daniels, R.F., 2003. Estimation of the physical wood properties of green *Pinus taeda* radial samples by near infrared spectroscopy. Can. J. For. Res., 33(12): 2297-2305.

Schimleck, L.R. and Evans, R., 2004. Estimation of *Pinus radiata* D. Don tracheid morphological characteristics by near infrared spectroscopy. Holzforschung, 58(1): 66-73.

Talbert, J.T. and Jett, J.B., 1981. Regional Specific-Gravity Values for Plantation Grown Loblolly-Pine in the Southeastern United-States. Forest Sci., 27(4): 801-807.

Thumm, A. and Meder, R., 2001. Stiffness prediction of radiata pine clearwood test pieces using near infrared spectroscopy. J. Near Infrared Spectrosc., 9(2): 117-122.

Thygesen, L.G., 1994. Determination of dry matter content and basic density of Norway spruce by near-infrared reflectance and transmission spectroscopy. J. Near Infrared Sectrosc., 2: 127-135.

Williams, P.C. and Sobering, D.C., 1993. Comparison of comercial near infrared transmittance and reflectance instruments for the analysis of whole grains and seeds. J Near Infrared Spectrosc., 1(1): 25-33.

Wright, J.A., Birkett, M.D. and Gambino, M.J.T., 1990. Prediction of Pulp Yield and Cellulose Content from Wood Samples Using near-Infrared Reflectance Spectroscopy. Tappi J., 73(8): 164-166.

Zobel, B.J. and McElwee, R.L., 1958. Natural variation in wood specific gravity of loblolly pine, and an analysis of contributing factors. Tappi J., 41(4): 158-161.

Chapter 5

NONDESTRUCTIVE ESTIMATION OF *PINUS TAEDA* L. TRACHEID MORPHOLOGICAL CHARACTERISTICS FOR SAMPLES FROM A WIDE RANGE OF SITES IN GEORGIA[2]

---

[2] Jones, P. D., L. R. Schimleck, G. F. Peter, R. F. Daniels, and A. Clark III. 2005. Wood Science and Technology 39(7) 529-545.

Reprinted here by permission of the publisher.

Abstract

Tracheid coarseness, specific surface, wall thickness, perimeter, and radial and tangential diameter from 120 radial strips of *Pinus taeda* L. (loblolly pine) trees grown on 14 sites in 3 physiographic regions of Georgia (USA) were measured by SilviScan. NIR spectra were also collected in 10 mm increments from the radial longitudinal surface of each strip and split into calibration (9 sites, 729 spectra) and prediction sets (6 sites, 225 spectra). NIR spectra were correlated using untreated and mathematically treated (first and second derivative and multiplicative scatter correction) with tracheid properties to develop calibrations for the estimation of these properties. Strong correlations were obtained for properties related to density, the strongest R^2 being 0.80 (coarseness), 0.78 (specific surface) and 0.84 (wall thickness). When applied to the test set, good relationships were obtained for the density related properties (R_p^2 ranged from 0.68 to 0.86) but the accuracy of predictions varied depending on math treatment. The addition of a small number of cores from the prediction set (one core per new site) to the calibration set improved the accuracy of predictions and, importantly, minimized the differences obtained with the various math treatments. These results suggest that density related properties can be estimated by NIR with sufficient accuracy to be used in operational settings.

Keywords: near infrared spectroscopy, *Pinus taeda*, SilviScan, tracheid morphological characteristics.

Introduction

In the Southeastern United States of America, *Pinus taeda* L. (loblolly pine) is the dominant plantation species owing to its ability to grow on a wide range of sites and the suitability of its wood for the manufacture of a wide range of forest products. Research directed at genetic improvement and the refinement of silvicultural practices has provided substantial improvements in the growth and yield of *P. taeda* (Li et al. 1999). The inclusion of quality traits such as stem straightness and wood quality in *P. taeda* breeding programs would greatly increase genetic gains and also the value of the trees (Li et al. 1999). Unfortunately, traditional methods for measuring wood properties are slow and cost prohibitive limiting their inclusion in tree breeding programs. Thus lower cost and more rapid methods for measuring wood properties are required.

Near infrared (NIR) spectroscopy has the potential to provide the forest industry with a low cost and rapid tool for the non-destructive estimation of the chemical (Birkett and Gambino 1988; Garbutt et al. 1992; Michell 1995; Raymond and Schimleck 2002; Schimleck et al. 2000; Wright et al. 1990) and physical-mechanical properties of wood (Gindl et al. 2001; Hoffmeyer and Pedersen 1995; Meder et al. 2003; Schimleck et al. 1999; Thumm and Meder 2001; Thygesen 1994). It has also been demonstrated that fundamental tracheid morphological characteristics such as wall thickness (Schimleck and Evans 2004) and length (Hauksson et al. 2001; Schimleck et al. 2004a) can be determined by NIR spectroscopy. Such properties are important in determining pulp fiber quality and paper performance but their consideration in tree breeding programs has been limited owing to the difficulties of routine measurement.

The study of Schimleck and Evans (2004) with *Pinus radiata* D. Don utilized data provided by the SilviScan instruments to develop calibrations for tracheid coarseness, perimeter, radial diameter, tangential diameter and wall thickness were based on a relatively small sample set (8 cores, 119 spectra). Coefficients of determination (R^2) ranged from 0.65 for tracheid radial diameter to 0.91 for coarseness. The calibrations, apart from tracheid perimeter and tracheid radial diameter, performed well when applied to a separate test set of two cores that were from the same population as the calibration samples. However, it is unknown if strong calibrations for these morphological traits can be obtained using wood cores from a larger and more diverse set of *P. taeda* trees.

If NIR spectroscopy is to be used in tree breeding or in other forestry operations robust calibrations based on large sample sets that encompass most of the variation in, genotypes and environments (sites and physiographic regions) will need to be developed. Recently Jones et al. (2005) developed robust calibrations for air-dry density, microfibril angle and stiffness using a large set of *P. taeda* wood cores obtained from 9 different sites representing three different physiographic regions (Upper and Lower Coastal Plain, and Piedmont) in Georgia (USA). The calibrations reported by Jones et al. (2005) had R^2 that ranged from 0.78 (air-dry density) to 0.93 (stiffness) and while having calibration errors larger than those reported by Schimleck and Evans (Schimleck and Evans 2002b; 2002a; 2003) demonstrated that calibrations for these properties could be obtained using a highly diverse population of trees. Hence it may also be possible to obtain good calibrations for tracheid morphological characteristics using large, diverse set of samples.

The objectives of this study were to:

(*i*) Create calibrations for tracheid morphological characteristics (coarseness, perimeter, radial diameter, specific surface, tangential diameter, and wall thickness) using samples drawn from a wide variety of sites chosen to represent the three physiographic regions where *P. taeda* is grown in Georgia, USA;

(*ii*) Examine the performance of the tracheid morphology calibrations when applied to samples from sites not included in the calibration; and

(*iii*) Improve the applicability of tracheid morphological trait calibrations to samples from sites not initially included in the calibration set.

Materials and methods

Sample Origin

Samples were collected from *P. taeda* plantations located in Georgia, USA. For each of the three physiographic regions in Georgia where *P. taeda* is grown (Lower and Upper Atlantic Costal Plain, and Piedmont) five plantations, ranging in age from 21 to 26 years, with different site indices were sampled. The characteristics of the sites are summarized in Table 5.1. The calibration set was comprised of ninety breast height (1.37 m) increment cores sampled from three plantations within each region; ten increment cores per site were taken. One increment core developed blue stain and was unavailable for analysis because of discoloration, leaving eighty-nine cores for analysis. The prediction set was comprised of thirty breast height increment cores (5 cores per plantation, 2 plantations per region).

SilviScan analysis

One hundred nineteen radial wooden strips were available for SilviScan analysis; these strips were cut from increment cores using a twin-blade saw. Strip dimensions were 2 mm tangentially, and 7 mm longitudinally; radial length was determined by the pith-to-bark length of the sample. The radial strips were extracted in 30º C acetone for 24 hours prior to SilviScan analysis.

The SilviScan-1 image analysis system (Evans 1994) was used to determine radial tracheid dimensions ($\boldsymbol{R}$) and tangential tracheid dimensions ($\boldsymbol{T}$). Tracheid coarseness ($\boldsymbol{C}$), perimeter (external perimeter of rectangular tracheid cross-section, $\boldsymbol{P}$), specific surface ($\boldsymbol{S}$) and tracheid wall thickness ($\boldsymbol{w}$), were determined from relationships that have been in use in various forms for several decades (Evans 1994):

$$\boldsymbol{P}=2(\boldsymbol{R}+\boldsymbol{T}) \tag{1}$$

$$\boldsymbol{C}=\mathbf{RTD} \tag{2}$$

$$\boldsymbol{w}=\boldsymbol{P}/8-1/2(\boldsymbol{P}/16-\boldsymbol{C}/\boldsymbol{d})^{1/2} \tag{3}$$

$$\mathbf{S}=\mathbf{P}/\mathbf{C} \tag{4}$$

Note: $\boldsymbol{D}$ = air-dry density and was determined using X-ray densitometry on SilviScan-1 (Evans 1994) and $\boldsymbol{d}$ is approximately equal to 1500 kg/m^3 for all softwoods (Kellogg et al. 1975).

All measurements were made in a conditioned atmosphere maintained at 40% RH and 20ºC (giving sample moisture content of approximately 8%). The image analysis data provided by Silviscan-1 were obtained in 50-micron steps. Averages were then determined for all tracheid morphological characteristics over 10-mm sections from pith to bark for correlation with the NIR data.

Near infrared spectroscopy

Diffuse reflectance NIR spectra were collected from the radial face of each strip using a NIRSystems Inc. Model 5000 scanning spectrometer. Samples were held in a custom made holder (Schimleck et al. 2001b). A 5 mm x 10 mm mask was used to ensure an area of constant size was analyzed. The spectra were collected at 2 nm intervals over the wavelength range 1100-

2500 nm. The instrument reference was a ceramic standard. Fifty scans were accumulated for each 10 mm section; these scans were averaged to give a single spectrum per section. All measurements were made in a controlled environment of 40% relative humidity and a temperature of 20ºC. A total of 729 spectra were collected from the 89 radial strips representing the calibration set, 225 spectra were collected from the 30 radial strips representing the prediction set. Table 5.2 shows the summary statistics for the two data sets.

Tracheid morphological characteristic calibrations

Calibrations for the tracheid morphological characteristics were developed using the Unscrambler (version 8.0) software package (Camo AS, Norway). Three math treatments; first and second derivatives (obtained from the untreated spectra using the Savtizky-Golay approach, with left and right gaps of eight nm) and Multiplicative Scatter Correction (MSC) (Næs et al. 2002), along with the raw spectral data were used to create the calibrations using Partial Least Square (PLS) regression. Figure 5.1 shows the effect of the different math treatments on an individual spectrum, a) raw (solid black line) and MSC transformation (dashed grey line), b) shows the first derivative, and c) illustrates the second derivative. All three methods are known to reduce noise that occurs within spectral data (Næs et al. 2002). Calibrations were developed with four cross validation segments.

The standard error of calibration (SEC) (determined from the residuals of the final calibration), the standard error of cross validation (SECV) (determined from the residuals of each cross validation phase), the coefficient of determination (R^2), and the ratio of performance to deviation (RPD_c) (Williams and Sobering 1993), calculated as the ratio of the standard deviation of the reference data to the SECV were used to assess calibration performance. Determination of RPD allows comparison of calibrations developed for different wood properties that have differing data ranges and units, the higher the RPD_c the more accurate the data is described by the calibration.

Prediction of wood properties

To examine the performance of the calibrations, they were used to predict the tracheid morphological characteristics (coarseness, perimeter, radial diameter, specific surface, tangential diameter, and wall thickness) of the test set samples. The standard error of prediction (SEP) (determined from the residuals of the predictions) was calculated and gives a measure of how well a calibration predicts parameters of interest for set of samples not included in the calibration set. The predictive ability of the calibrations was assessed by calculating the RPD_p (which is similar to the RPD_c) but uses the standard deviation of the prediction set reference data and the SEP.

Results

The tracheid morphological characteristics examined in this study can be classified into two distinct groups. The first group includes properties strongly related to density (coarseness, specific surface, and wall thickness), while the second group includes properties measured by image analysis (tracheid perimeter and radial and tangential diameter). Because of the interrelationships between the different morphological characteristics, we examined how each of the characteristics were related in a pair-wise manner (Table 5.3). Air-dry density has strong relationships with coarseness (R^2-value = 0.86), specific surface (-0.93) and wall thickness (0.97) as expected. Similarly coarseness, specific surface, and wall thickness are strongly correlated with each other. The relationships of coarseness and wall thickness with density were similar to those reported by Schimleck and Evans (2004) for *P. radiata*. The properties measured using image analysis also show strong relationships with each other, but not with any of the density related properties.

Calibrations and predictions

Density related properties

The density related properties all gave reasonable calibrations (Table 5.4). R^2 for the coarseness calibrations ranged from 0.76 (raw and MSC treated spectra) to 0.80 (second derivative treated spectra), while calibration errors were similar with RPD_c ranging from 2.00 (untreated spectra) to 2.04 (first derivative treated spectra). Specific surface calibrations yielded R^2 ranging from 0.73 (second derivative treated spectra) to 0.78 (first derivative treated spectra) and also had similar levels of calibration error despite the number of factors used varying from 3 to 7. The calibrations for wall thickness gave the strongest R^2 (0.84 for Raw, MSC, and first derivative treated spectra), and had RPD_c values ranging from 2.20 (second derivative treated spectra) to 2.46 (MSC treated spectra). Figure 5.2 illustrates the calibrations for coarseness (a) and wall thickness (b) using MSC treated spectra.

The principle test of a calibration is to use it in prediction with a set of samples unrelated to those used to develop the calibration. Table 5.4 summarizes results for predictions made on the separate test set (225 spectra collected from 30 cores representing 6 sites not included in the calibration). A prediction R^2 (R_p^2) was calculated as the proportion of variation in the independent prediction set that was explained by the calibration. In general the wood property calibrations developed using different math treated spectra gave similar R_p^2 but the SEP and consequently the RPD_p varied greatly between math treatments (Table 5.4).

Regardless of math treatment, the coarseness calibrations provided reasonable R_p^2 ranging from 0.71 to 0.83, however the RPD_p varied from 0.81 (untreated spectral data) to 2.10

(first derivative treated data). Figure 5.3 compares predictions of coarseness obtained using the untreated spectra (a) and the first derivative treated spectra (b). Figure 5.2 highlights the effect that the different math treatments have on the predictive accuracy of the coarseness calibrations. Predictions of coarseness based on the untreated spectra (a) have a large amount of error because they deviate from the line of equivalence (light gray dashed line); while predictions of coarseness based on the first derivative treated spectra (b) lie almost upon the line.

Predictions of specific surface using the first derivative treated spectra gave the highest R_p^2 (0.78) while predictions based on the untreated spectra had the lowest R_p^2 (0.68) (Table 5.4). Of the three density related properties, wall thickness predictions gave the highest R_p^2 (0.86, obtained using MSC and first derivative treated spectra). However RPD_p for the two math treatments were quite different, 1.02 (MSC treated spectra) and 2.66 (first derivative treated spectra) (Table 5.4).

Image analysis derived properties

The image analysis derived properties did not provide calibration statistics as strong as those obtained for the density related properties (Table 5.4). The strongest R^2 obtained for the perimeter and radial diameter calibrations were 0.50 (second derivative treated spectra) and 0.46 (first and second derivative treated spectra) respectively. Calibrations for tangential diameter faired better with R^2 ranging from 0.59 (untreated spectra) to 0.64 (second derivative treated spectra) while the best RPD_c was 1.57 for the MSC treated spectra.

When the calibrations were applied to the test set, the calibrations for tangential diameter provided the strongest predictions with R_p^2 ranging from 0.58 (MSC treated spectra) to 0.63 (first derivative treated spectra), while RPD_p values for the same math treatments ranged from 1.41 to 1.59. Predictions of perimeter and radial diameter were poor with the highest R_p^2 being 0.53 for perimeter (first derivative treated spectra) and 0.42 for radial diameter (first derivative treated spectra).

Table 5.5 shows the most important wavelength for each morphological property and respective math treatment. For each of the density related properties the most important wavelength was the same. Calibrations for image analysis derived properties used different wavelengths.

Improvement of tracheid morphological characteristic calibrations and predictions

The predictive performance of calibrations can be improved by including a small number of samples from the prediction set in the calibration set (Guthrie and Walsh 2002; Jones et al. 2005) Table 6 summarizes the results for these enhanced wood property calibrations and predictions obtained after NIR spectra from a single randomly selected core from each of the sites in the prediction set was added to the calibration set. The new cores increased the number of spectra in the calibration set to 771 (95 increment cores). In general the enhanced calibrations had statistics similar to those reported for the original calibrations (Table 5.4). However, prediction error was decreased and RPD_p's were improved for all but 3 of the enhanced calibrations.

Predictions of coarseness with the enhanced calibrations all had R_p^2 greater than 0.78 and RPD_p's greater than 2.0. With the exception of the coarseness calibration based on first derivative treated spectra, the other enhanced coarseness calibrations all provided considerable reductions in predictive errors. The coarseness calibration based on untreated spectra demonstrated the largest improvement with RPD_p increasing from 0.81 to 2.11. For specific surface the enhanced calibrations all provided decreases in prediction error. The largest improvement was for the MSC treated data with a 108% increase in RPD_p. Predictions of wall thickness generally improved when the enhanced calibrations were used, the exception being results for the first derivative treated spectra where the RPD_p fell from 2.66 to 2.57.

The image analysis derived properties did not show the large reduction in prediction errors observed for coarseness, specific surface and wall thickness. Tangential diameter continued to have the highest R_p^2 and RPD_p values, followed by perimeter and radial diameter.

In Figure 5.4, radial variation for coarseness (a), tangential diameter (b), and wall thickness (c) are shown for a single, randomly selected sample from the prediction set. The figure includes SilviScan data at the original resolution, the SilviScan data averaged at 10 mm, predicted data at 10 mm using the original calibrations (based on first derivative treated spectra), and predicted data at 10 mm using the expanded calibrations again based on first derivative treated spectra. Figures 4 a-c show that the data predicted by the respective calibrations corresponds closely to the SilviScan measured data, particularly for the enhanced calibrations.

Discussion

Three aspects important for the use of NIR spectroscopy for prediction of tracheid morphological characteristics have been examined: First, the use of a large sample size to create robust calibrations; second, the use of the calibrations to predict the properties of cores from sites not included in the calibration and third, the enhancement of calibrations to reduce predictive error.

Development of calibrations using a large number of samples that contain a wide range of variation in the traits will give the best representation of the species as a whole. Berzaghi et al. (2002) successfully created calibrations for the chemical analysis of forage crops using a large sample size, showing that with recent technological advancements large sample sets were manageable for creating calibrations. In the current study 729 spectral samples were used to create calibrations, and to predict the variation of *P. taeda* tracheid morphological characteristics in plantations. Working with such large sample sets presents a number of practical difficulties. The handling and matching of spectral data and SilviScan data takes a great deal of patience and vigilance to assure that the proper data is matched with the scanned area. This can only be achieved through stringent data handling protocols. With an increase in resolution (i.e. spectra collected at 5 mm) the data sets will become larger and more complicated, but will allow for a greater understanding of wood properties, growth and age dependent transitions in these properties, and possibly within ring estimation of wood properties using NIR spectroscopy. With previous work, calibrations had been performed using WinISI II (Infrasoft international, 2000), as the data sets became larger (n>500) the importation of constituents and the management of data became difficult because of the user interface; with Unscrambler the importation of data is very intuitive because its similarity to commonly used spreadsheet interfaces.

Calibrations for properties that are highly correlated with density gave promising results when applied to samples from sites other than those included in the calibrations. Wall thickness and coarseness are of particular importance for the pulp and paper industry as they help determine bonding potential of tracheids and individual fiber or tracheid strength (McKenzie 1994). Schimleck and Evans (2004) suggested that coarseness and wall thickness calibrations might decrease in accuracy using large data sets; this study demonstrates that with large data sets obtained from trees grown on a wide range of sites strong calibrations can be developed for coarseness, specific surface, and wall thickness. Schimleck and Evans (2004) examined the use of NIR to predict coarseness, wall thickness, perimeter, radial diameter, and tangential diameter for *P. radiata* for a limited sample set (8 radial strips, 119 spectra). Calibrations based on second derivative spectra gave SEC values of 31.0 μg/m, and 0.2 μm for coarseness and wall thickness respectively. When these calibrations are used to predict the properties of 2 different cores, from the same site, the resulting $\mathrm{RPD_p}$'s of the individual cores were 1.9 and 1.6 for coarseness and 2.7 and 1.4 for wall thickness (Schimleck and Evans 2004). This work demonstrated that NIR spectroscopy could predict some wood properties of *P. radiata;* however, their sample size was probably too small to develop calibrations robust enough to predict properties of samples from new populations (or sites). Here we report that calibrations developed with a much larger and more diverse set of *P. taeda* wood cores resulted in SEC values of 37.55 μg/m for coarseness (non-enhanced calibration) and 0.28 μm for wall thickness (non-enhanced calibration) using the second derivative data. The $\mathrm{RPD_p}$ values for the same two properties were 1.44 (coarseness) and 2.20 (wall thickness).

In this study the properties measured by image analysis did not produce calibrations adequate for predicting these properties, with the exception of tangential diameter. In contrast, Schimleck and Evans (2004) were able to obtain reasonable calibrations for radial and tangential diameter as well as perimeter. Radial diameter and tangential diameter were strongly related to each other (Table 5.3) hence similar calibration statistics could be expected for both properties, but this was not observed. It is possible that a stronger calibration was obtained for tangential diameter because of the orientation of the NIR beam to the sample. Owing to our sampling methodology NIR energy may have had a greater interaction with the tangential walls and consequently information relating to tangential diameter may be reflected in the spectra to a greater extent than radial diameter. The tangential diameter calibrations would only be useful for classification purposes or approximate estimations.

The predictive accuracy of the coarseness, specific surface and wall thickness calibrations can be enhanced by adding a single sample from new sites and creating a new calibration. While not all expanded calibrations produced lower prediction errors, the expansion decreased the variability between prediction errors for the same properties using the differing math treatments.

Conclusions

This study demonstrates that large data sets that include a wide range of environmental and genetic variation can establish good calibrations for density related tracheid morphological characteristics based on NIR spectra obtained in 10 mm sections from the radial face of *P. taeda* strips. Reasonable calibrations were obtained for tangential diameter, while the calibrations for perimeter and radial diameter were poor.

Calibrations for density related properties gave strong relationships when used to predict the tracheid morphologies of a separate set of cores from sites not included in the calibration set but the accuracy of predictions varied depending on the math treatment employed. Predictions of tangential diameter had moderate relationships, while predictions of perimeter and radial diameter were poor.

The addition of a small number of cores from the prediction set (one core per site) to the calibration set minimized the difference between mathematical treatments and improved the accuracy of predictions for density related properties.

Acknowledgements

The authors thank the UGA Wood Quality Consortium for *P. taeda* sample collection and the Georgia TIP^3 program for funding the SilviScan analysis of the samples. The authors would also like to thank the UGA Wood Quality Consortium for sample preparation and the SilviScan team for the determination of wood properties.

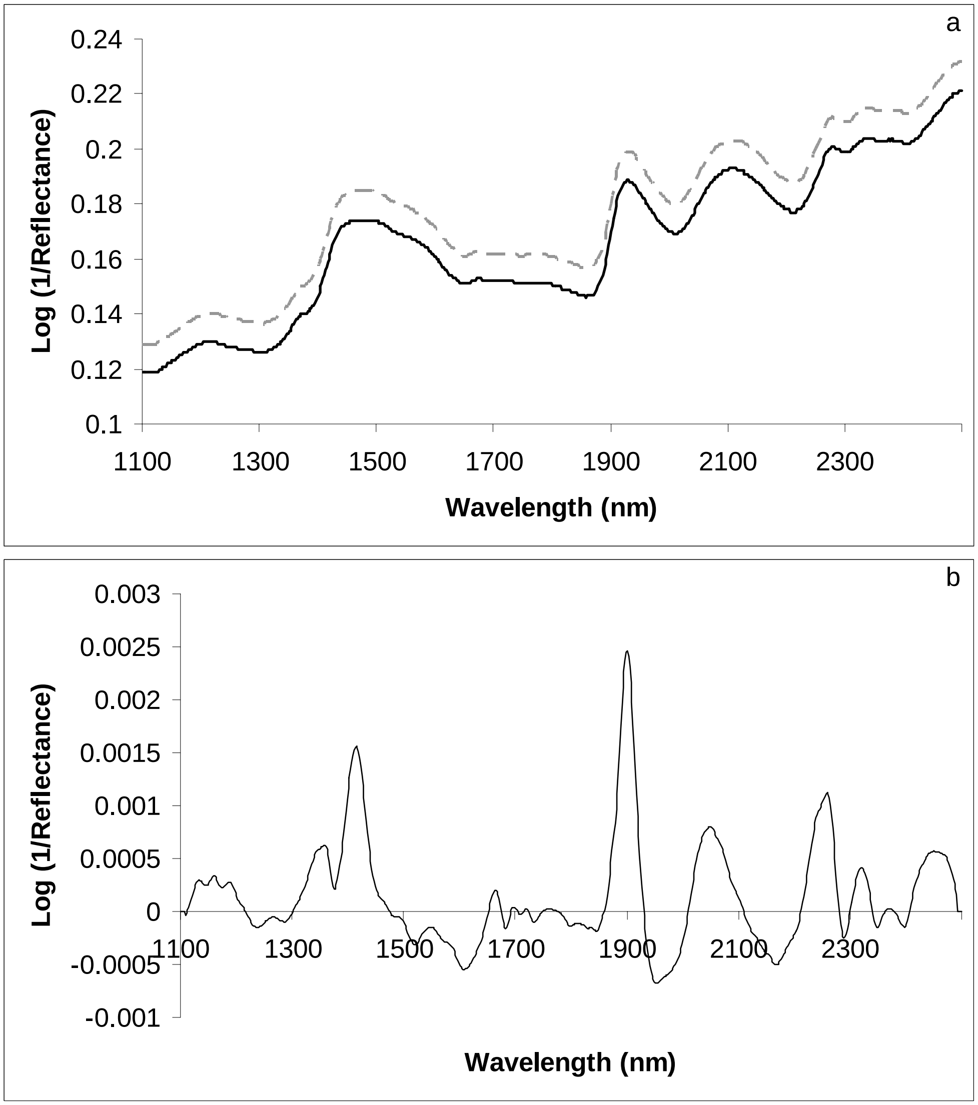

Fig. 5.1 Spectrum of an individual sample and the effect of each math treatment on the spectrum, raw (solid black line) and MSC (dashed grey line) (a), first derivative (b), and second derivative (c).

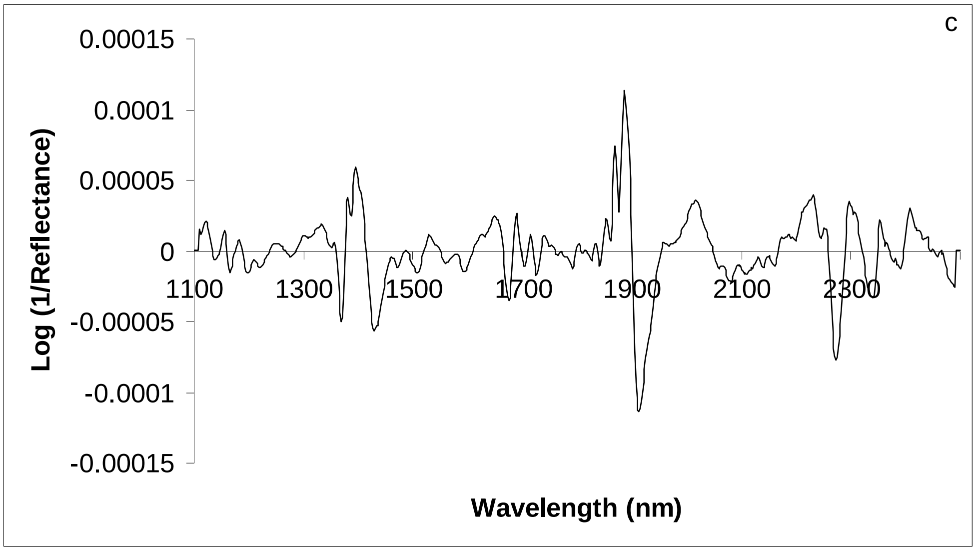

Fig. 5.1. Spectrum of an individual sample and the effect of each math treatment on the spectrum, raw (solid black line) and MSC (dashed grey line) (a), first derivative (b), and second derivative (c).

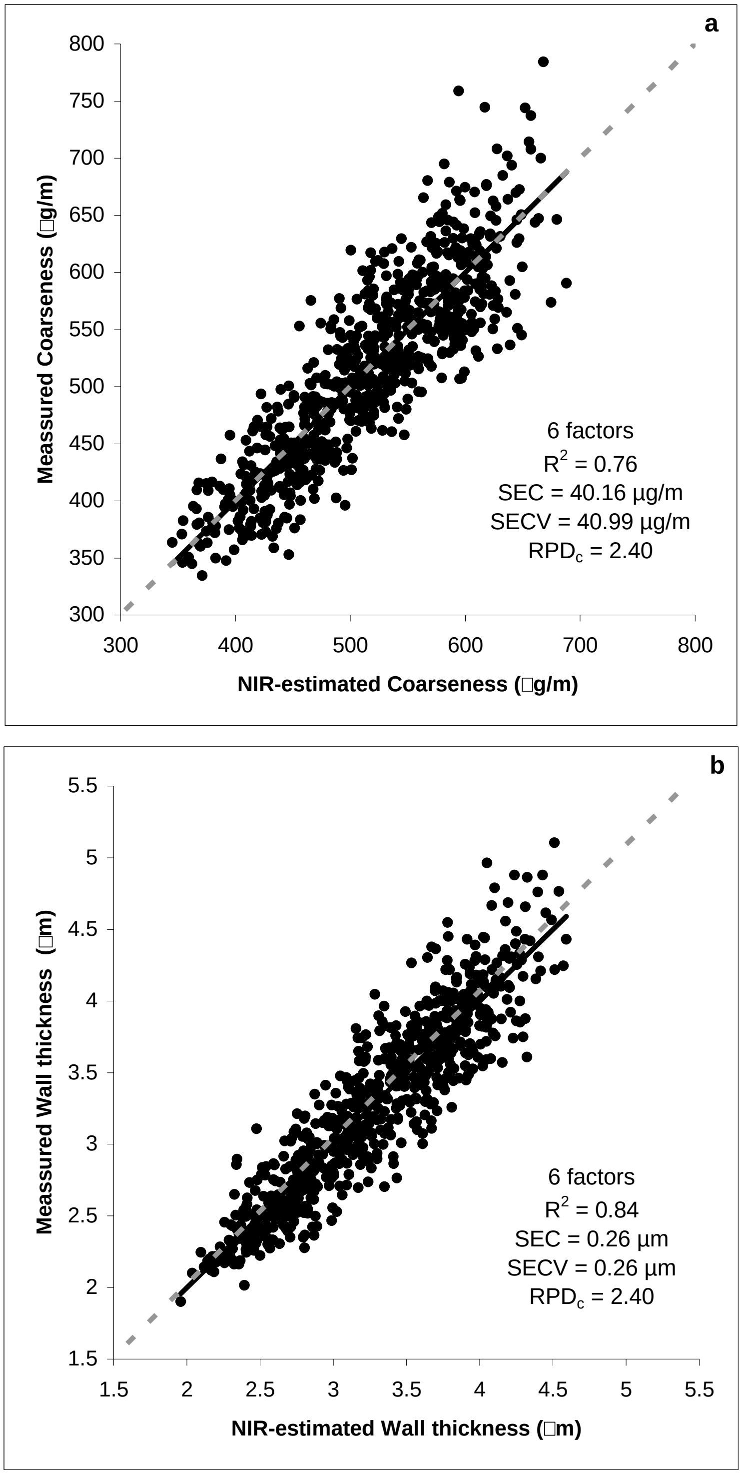

Fig. 5.2. Relationship between SilviScan measured coarseness and NIR-estimated coarseness (a) and measured wall thickness and NIR-estimated wall thickness (b). MSC treated spectra were used for both calibrations. The dashed gray line represents the line of equivalence.

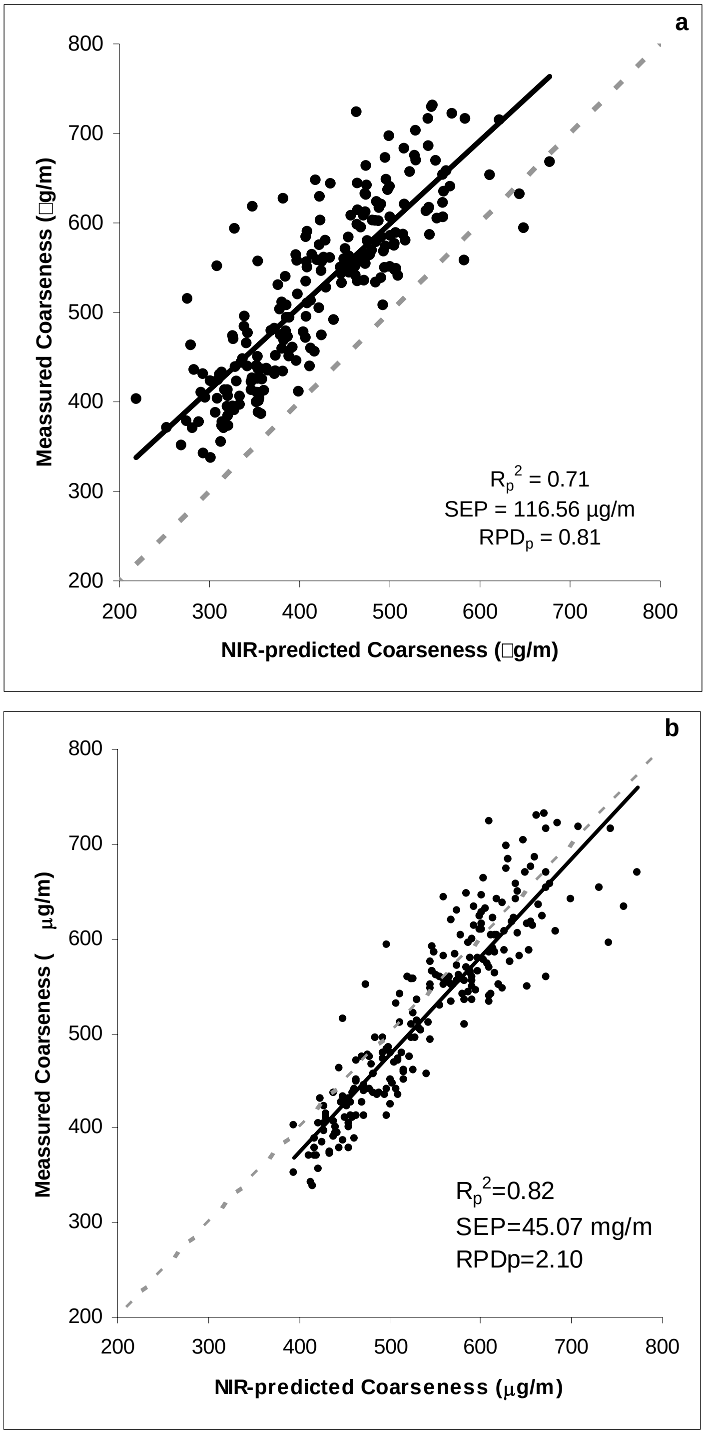

Fig. 5.3. Prediction results for coarseness using two different math treatments, untreated spectra (a) and first derivative treated spectra (b). The dashed gray line represents the line of equivalence.

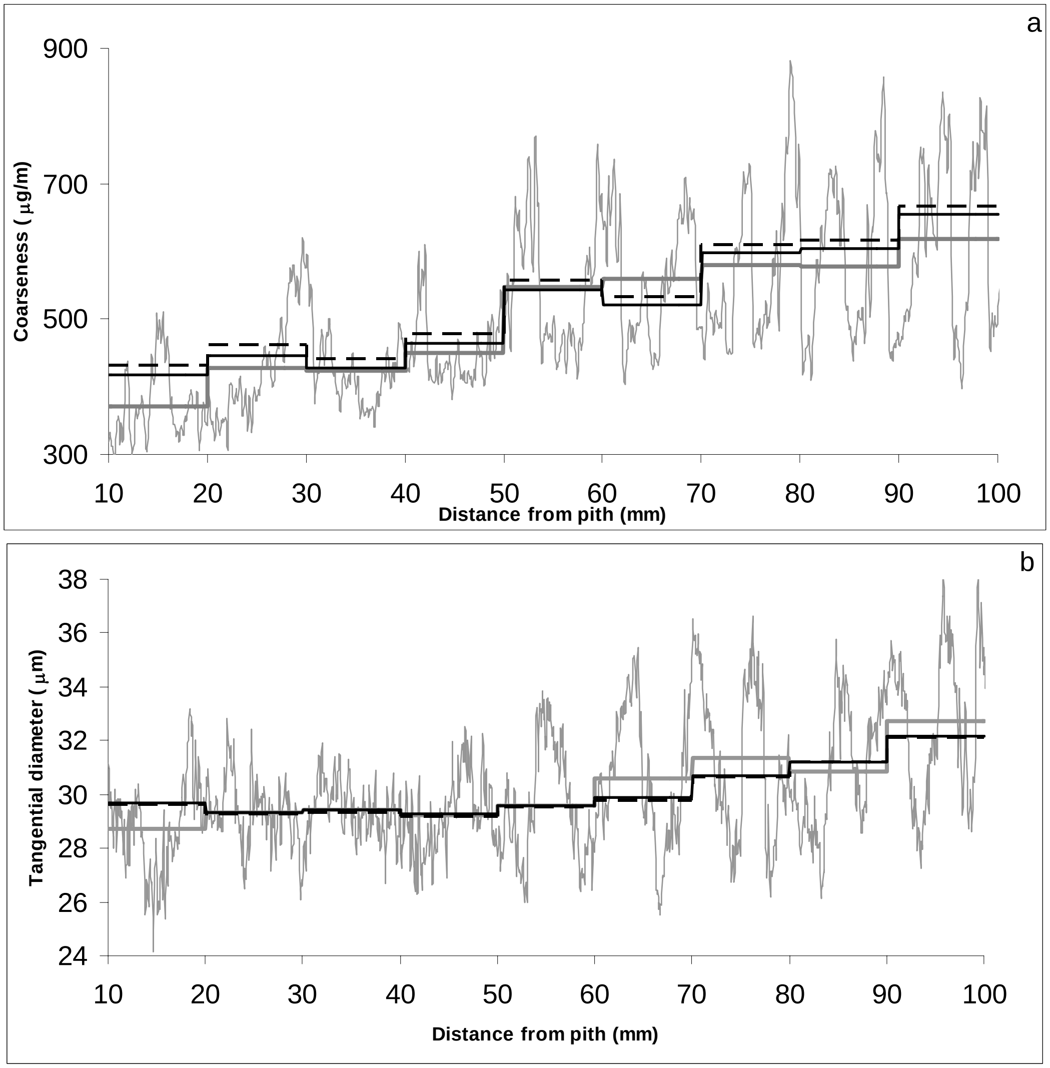

Fig. 5.4. Plot of pith-to-bark radial variation for (a) coarseness, (b) tangential diameter, and (c) wall thickness for a randomly selected *P. taeda* radial strip. The solid thin gray line represents the original SilviScan data, the solid thick gray line represents SilviScan data averaged over 10 mm, the dashed black line represents values predicted by the original calibrations and the solid black line represents values predicted using the expanded calibrations.

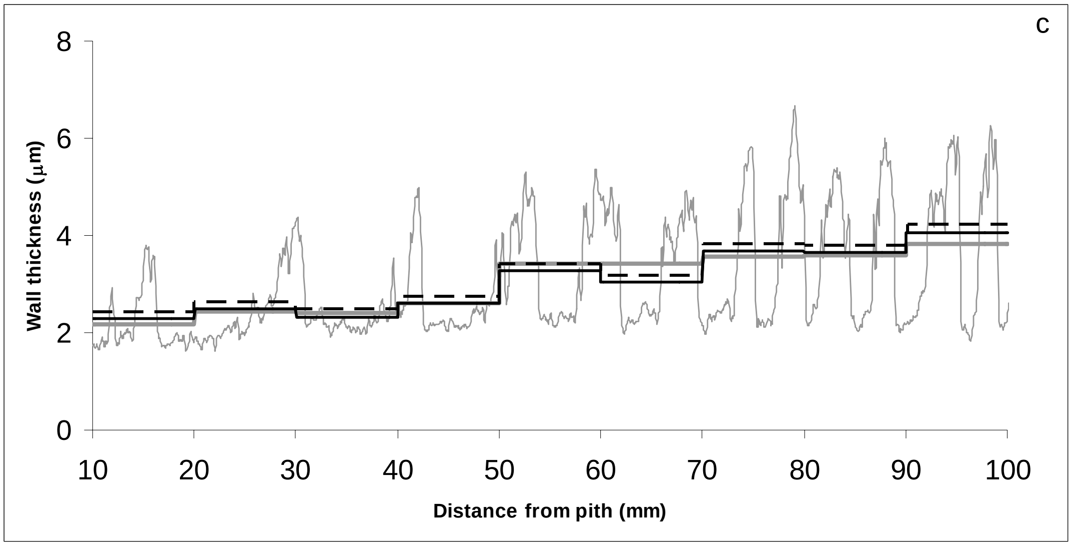

Fig. 5.4. Plot of pith-to-bark radial variation for (a) coarseness, (b) tangential diameter, and (c) wall thickness for a randomly selected *P. taeda* radial strip. The solid thin gray line represents the original SilviScan data, the solid thick gray line represents SilviScan data averaged over 10 mm, the dashed black line represents values predicted by the original calibrations and the solid black line represents values predicted using the expanded calibrations.

Table 5.1. Stand descriptions for samples used in the calibration and prediction sets including age, site index (SI_{25}), county, latitude (Lat.), longitude (Long.), and physiographic region.

Region	SI_{25}	Age	County	Lat.	Long.
Calibration Set					
Upper Atlantic Coastal Plain	67	24	Marion	32º 33’	-84º 60’
Upper Atlantic Coastal Plain	69	25	Wilkinson	32º 78’	-82º 97’
Upper Atlantic Coastal Plain	78	22	Clay	31º 62’	-84º 99’
Lower Atlantic Coastal Plain	76	25	Effingham	32º 26’	-81º 27’
Lower Atlantic Coastal Plain	79	25	Glynn	31º 31’	-81º 60’
Lower Atlantic Coastal Plain	84	25	Camden	31º 11’	-81º 81’
Piedmont	54	25	Greene	33º 70’	-83º 22’
Piedmont	55	21	Polk	34º 09’	-85º 22’
Piedmont	61	26	Jones	32º 96’	-83º 62’
Prediction Set					
Upper Atlantic Coastal Plain	55	22	Stewart	32º 13’	-84º 70’
Upper Atlantic Coastal Plain	67	24	Marion	32º 34’	-84º 60’
Lower Atlantic Coastal Plain	80	25	Wayne	31º 42’	-81º 68’
Lower Atlantic Coastal Plain	81	24	Liberty	31º 79’	-81º 57’
Piedmont	54	24	Talbot	32º 77’	-84º 61’
Piedmont	66	26	Greene	33º 46’	-83º 10’

Table 5.2. Summary of variation in tracheid morphological traits of samples used for the calibration and prediction sets.

Tracheid morphological characteristic	Calibration set (729 spectra)				Prediction set (225 spectra)			
	Minimum	Maximum	Av.	Std. dev.	Minimum	Maximum	Av.	Std. dev.
Density related								
Coarseness (µg/m)	334.56	784.44	515.27	83.02	338.03	731.60	526.56	94.72
Specific surface (m^2/kg)	180.81	379.46	264.45	35.21	191.71	353.81	261.64	37.76
Wall thickness (µm)	1.90	5.10	3.28	0.63	2.09	5.00	3.31	0.69
Image analysis derived								
Perimeter (µm)	107.98	142.86	125.38	5.86	108.18	146.64	126.66	6.17
Radial diameter (µm)	26.52	39.20	32.68	2.15	26.94	40.46	32.89	2.11
Tangential diameter (µm)	26.65	35.42	30.01	1.59	26.80	35.30	30.43	1.73

Table 5.3. Coefficients of determination between SilviScan measured morphological traits.

	Density (kg/m^3)	Coarseness (µg/m)	Specific Surface (m^2/kg)	Wall Thickness (µm)	Perimeter (µm)	Radial Diameter (µm)	Tangential Diameter (µm)
Density (kg/m^3)	1						
Coarseness (µg/m)	0.86	1					
Specific Surface (m^2/kg)	-0.93	-0.92	1				
Wall Thickness (µm)	0.97	0.95	-0.95	1			
Perimeter (µm)	-0.11	0.37	-0.06	0.10	1		
Radial Diameter (µm)	0.01	0.01	0.25	-0.26	0.85	1	
Tangential Diameter (µm)	0.13	0.67	-0.44	0.53	0.70	0.98	1

Table 5.4. Summary of calibrations and predictions obtained using untreated and math treated NIR spectra collected in 10 mm sections from the radial longitudinal face of radial wooden strips coarseness, specific surface, wall thickness, perimeter, radial diameter and tangential diameter. Calibration statistics include the coefficient of determination (R^2, R_p^2), the standard error of calibration (SEC), the standard error of cross validation (SECV), the standard error of prediction (SEP), and the ratio of performance to standard deviation (RPD_c, RPD_p).

Math Treatment		Calibration					Prediction		
		Factors	R^2	SEC	SECV	RPD_c	R_p^2	SEP	RPD_p
Coarseness (µg/m)	Raw	7	0.76	40.70	41.47	2.00	0.71	116.56	0.81
	MSC	6	0.76	40.40	41.13	2.02	0.81	75.51	1.25
	1st Derivative	5	0.77	39.64	40.60	2.04	0.82	45.07	2.10
	2nd Derivative	6	0.80	37.55	40.97	2.03	0.83	65.80	1.44
Specific Surface (m^2/kg)	Raw	7	0.77	16.81	17.22	2.04	0.68	37.62	1.00
	MSC	5	0.76	17.28	17.59	2.00	0.77	35.35	1.07
	1st Derivative	5	0.78	16.60	17.11	2.06	0.78	26.48	1.43
	2nd Derivative	3	0.73	18.33	18.63	1.89	0.77	20.47	1.84
Wall Thickness (µm)	Raw	7	0.84	0.25	0.26	2.44	0.81	0.78	0.88
	MSC	6	0.84	0.25	0.26	2.46	0.86	0.68	1.02
	1st Derivative	5	0.84	0.25	0.26	2.41	0.86	0.26	2.66
	2nd Derivative	3	0.80	0.28	0.29	2.20	0.80	0.32	2.15
Perimeter (µm)	Raw	10	0.42	4.47	4.56	1.29	0.37	7.36	0.84
	MSC	9	0.42	4.45	4.54	1.29	0.33	9.12	0.68
	1st Derivative	10	0.49	4.18	4.45	1.32	0.53	4.62	1.33
	2nd Derivative	7	0.50	4.14	4.64	1.26	0.41	8.31	0.74
Radial Diameter (µm)	Raw	10	0.39	1.68	1.72	1.25	0.25	2.83	0.75
	MSC	10	0.39	1.68	1.73	1.25	0.28	3.66	0.58
	1st Derivative	10	0.46	1.58	1.70	1.27	0.42	1.77	1.20
	2nd Derivative	7	0.46	1.58	1.78	1.21	0.29	1.79	1.18
Tangential Diameter (µm)	Raw	10	0.59	1.01	1.04	1.53	0.58	1.21	1.43
	MSC	10	0.62	0.98	1.01	1.57	0.58	1.22	1.41
	1st Derivative	6	0.60	1.00	1.01	1.56	0.63	1.09	1.59
	2nd Derivative	6	0.64	0.95	1.02	1.56	0.59	1.17	1.47

Table 5.5. Summary of the most important wavelength for each morphological property and respective math treatment.

	Math Treatment			
Property	**Raw**	**MSC**	**1^{st} Derivative**	**2^{nd} Derivative**
Coarseness	2086 nm	2498 nm	1412 nm	1876 nm
Specific Surface	2086 nm	2498 nm	1412 nm	1876 nm
Wall Thickness	2086 nm	2498 nm	1412 nm	1876 nm
Perimeter	1102 nm	1974 nm	1902 nm	1868 nm
Radial Diameter	2126 nm	2496 nm	1412 nm	1876 nm
Tangential Diameter	1492 nm	2498 nm	1906 nm	1492 nm

Table 5.6. Summary of enhanced calibrations and predictions obtained using untreated and math treated NIR spectra collected in 10 mm sections from the radial longitudinal face of radial wooden strips for coarseness, specific surface, wall thickness, perimeter, radial diameter and tangential diameter. Calibration statistics include the coefficient of determination (R^2, R_p^2), the standard error of calibration (SEC), the standard error of cross validation (SECV), the standard error of prediction (SEP), and the ratio of performance to standard deviation (RPD_c, RPD_p).

Math Treatment		Calibration					Prediction		
		Factors	R^2	SEC	SECV	RPD_c	R_p^2	SEP	RPD_p
Coarseness (μg/m)	Raw	8	0.76	40.66	41.50	2.02	0.78	44.99	2.11
	MSC	7	0.77	40.16	40.99	2.04	0.58	40.80	2.32
	1st Derivative	5	0.77	40.08	41.14	2.03	0.83	46.65	2.03
	2nd Derivative	6	0.80	37.84	41.31	2.02	0.84	38.48	2.46
Specific Surface (m^2/kg)	Raw	8	0.77	17.00	17.52	2.02	0.79	18.21	2.07
	MSC	6	0.77	17.04	17.50	2.02	0.80	16.91	2.23
	1st Derivative	5	0.77	16.77	17.36	2.03	0.78	17.88	2.11
	2nd Derivative	3	0.73	18.31	18.68	1.89	0.79	17.57	2.15
Wall Thickness (μm)	Raw	8	0.84	0.25	0.26	2.45	0.86	0.27	2.59
	MSC	6	0.83	0.26	0.26	2.40	0.86	0.25	2.74
	1st Derivative	5	0.84	0.26	0.26	2.40	0.87	0.27	2.57
	2nd Derivative	3	0.80	0.28	0.29	2.19	0.80	0.31	2.24
Perimeter (μm)	Raw	10	0.40	4.56	4.66	1.27	0.36	5.24	1.17
	MSC	8	0.40	4.56	4.64	1.27	0.33	5.39	1.14
	1st Derivative	10	0.48	4.25	4.51	1.31	0.53	4.49	1.37
	2nd Derivative	6	0.46	4.35	4.72	1.25	0.45	5.60	1.10
Radial Diameter (μm)	Raw	10	0.38	1.69	1.73	1.24	0.33	1.86	1.14
	MSC	8	0.35	1.73	1.76	1.22	0.27	1.98	1.07
	1st Derivative	10	0.45	1.59	1.71	1.26	0.46	1.60	1.32
	2nd Derivative	4	0.33	1.76	1.83	1.17	0.24	2.35	0.90
Tangential Diameter (μm)	Raw	10	0.59	1.04	1.06	1.52	0.58	1.18	1.46
	MSC	10	0.62	1.00	1.04	1.56	0.58	1.11	1.56
	1st Derivative	6	0.60	1.02	1.04	1.55	0.62	1.04	1.65
	2nd Derivative	6	0.63	0.98	1.04	1.55	0.36	1.03	1.68

Literature cited

Birkett, M.D. and Gambino, M.J.T., 1988. Potential applications for near-infrared spectroscopy in the pulping industry. Pap. S. Afr., November/December: 34-38.

Evans, R., 1994. Rapid Measurement of the Transverse Dimensions of Tracheids in Radial Wood Sections from *Pinus radiata*. Holzforschung, 48(2): 168-172.

Garbutt, D.C.F., Donkin, M.J. and Meyer, J.H., 1992. Near-infrared reflectance analysis of cellulose and lignin in wood. Pap. S. Afr., April: 45-48.

Gindl, W., Teischinger, A., Schwanninger, M. and Hinterstoisser, B., 2001. The relationship between near infrared spectra of radial wood surfaces and wood mechanical properties. J. Near Infrared. Spectrosc., 9(4): 255-261.

Guthrie, J.A. and Walsh, K.B., 2002, Assessing and enhancing near infrared calibration robustness for soluble solids content in mandarin fruit, Near Infrared Spectroscopy: Proceedings of the 10th International Conference, A.M.C. Davies and R.K. Cho, NIR Publications, 151-154.

Hauksson, J.B., Sjöstrom, M., Edlund, U., Bergqvist, G. and Bergsten, U., 2001. Prediction of basic wood properties for Norway spruce. Interpretation of near infrared spectroscopy data using partial least squares regression. Wood Sci. and Technol., 35(6): 475-485.

Hoffmeyer, P. and Pedersen, J.G., 1995. Evaluation of Density and Strength of Norway Spruce Wood by Near-Infrared Reflectance Spectroscopy. Holz Roh Werkst., 53(3): 165-170.

Jones , P.D., Schimleck, L.R., Peter, G.F., Daniels, R.F. and Clark III, A., 2005. Nondestructive estimation of *Pinus taeda* L. wood properties for samples from a wide range of sites in Georgia. Can. J. For. Res., 35(1): 85-92.

Kellogg, R.M., Wellwood, R.W. and Sastry, C.B.R., 1975. Relationships between cell wall composition and cell wall density. Wood and Fibre, 7(3): 170-177.

Li, B., McKeand, S. and Weir, R., 1999. Tree improvement and sustainable forestry - impact of two cycles of loblolly pine breeding in the U.S.A. Forest Genetics, 6(4): 229-234.

McKenzie, A.W., 1994. A Guide To Pulp Evaluation. CSIRO, Australia, 66 pp.

Meder, R., Thumm, A. and Marston, D., 2003. Sawmill trial of at-line prediction of recovered lumber stiffness by NIR spectroscopy of *Pinus radiata* cants. J. Near Infrared Spectrosc., 11(2): 137-143.

Michell, A.J., 1995. Pulpwood quality estimation by near-infrared spectroscopic measurements on eucalypt woods. Appita J., 48(6): 425-428.

Næs, T., Isaksson, T., Fearn, T. and Davies, T., 2002. A user-friendly guide to multivariate calibration and classification. NIR, Chichester, 344 pp.

Raymond, C.A. and Schimleck, L.R., 2002. Development of near infrared reflectance analysis calibrations for estimating genetic parameters for cellulose content in *Eucalyptus globulus*. Can. J. For. Res., 32(1): 170-176.

Schimleck, L.R., Michell, A.J., Raymond, C.A. and Muneri, A., 1999. Estimation of basic density of *Eucalyptus globulus* using near-infrared spectroscopy. Can. J. For. Res., 29(2): 194-201.

Schimleck, L.R., Raymond, C.A., Beadle, C.L., Downes, G.M., Kube, P.D. and French, J., 2000. Applications of NIR spectroscopy to forest research. Appita J., 53(6): 458-464.

Schimleck, L.R., Evans, R. and Ilic, J., 2001. Estimation of *Eucalyptus delegatensis* wood properties by near infrared spectroscopy. Can. J. For. Res., 31(10): 1671-1675.

Schimleck, L.R. and Evans, R., 2002a. Estimation of microfibril angle of increment cores by near infrared spectroscopy. IAWA J., 23(3): 225-234.

Schimleck, L.R. and Evans, R., 2002b. Estimation of wood stiffness of increment cores by near infrared spectroscopy: The development and application of calibrations based on selected cores. IAWA J., 23(3): 217-224.

Schimleck, L.R. and Evans, R., 2003. Estimation of air-dry density of increment cores by near infrared spectroscopy. Appita J., 56(4): 312-317.

Schimleck, L.R. and Evans, R., 2004. Estimation of *Pinus radiata* D. Don tracheid morphological characteristics by near infrared spectroscopy. Holzforschung, 58(1): 66-73.

Schimleck, L.R., Jones, P.D., Peter, G.F., Daniels, R.F. and Clark, A., 2004. Nondestructive estimation of tracheid length from sections of radial wood strips by near infrared spectroscopy. Holzforschung, 58(4): 375-381.

Thumm, A. and Meder, R., 2001. Stiffness prediction of radiata pine clearwood test pieces using near infrared spectroscopy. J. Near Infrared Spectrosc., 9(2): 117-122.

Thygesen, L.G., 1994. Determination of dry matter content and basic density of Norway spruce by near-infrared reflectance and transmission spectroscopy. J. Near Infrared Sectrosc., 2: 127-135.

Williams, P.C. and Sobering, D.C., 1993. Comparison of comercial near infrared transmittance and reflectance instruments for the analysis of whole grains and seeds. J Near Infrared Spectrosc., 1(1): 25-33.

Wright, J.A., Birkett, M.D. and Gambino, M.J.T., 1990. Prediction of Pulp Yield and Cellulose Content from Wood Samples Using near-Infrared Reflectance Spectroscopy. Tappi J., 73(8): 164-166.

Chapter 6

NONDESTRUCTIVE ESTIMATION OF WOOD CHEMICAL COMPOSITION OF SECTIONS OF RADIAL WOOD STRIPS BY DIFFUSE REFLECTANCE NEAR INFRARED SPECTROSCOPY[3]

---

[3] Jones, P. D., L. R. Schimleck, G. F. Peter, R. F. Daniels, and A. Clark III. 2005. Submitted to Wood Science and Technology, 11/28/2005

Abstract

The use of calibrated near infrared (NIR) spectroscopy for predicting the chemical composition of *Pinus taeda* L. (loblolly pine) wood samples is investigated. Seventeen *P. taeda* radial strips, representing seven different sites were selected and NIR spectra were obtained from the radial longitudinal face of each strip. The spectra were obtained in 12.5 mm sections from predetermined positions that represented juvenile wood (close to pith), transition wood (zone between juvenile and mature wood) and mature wood (close to bark). For these sections, cellulose, hemicellulose, lignin (acid soluble and insoluble), arabinan, galactan, glucan, mannan, and xylan contents were determined by standard analytical chemistry methods. Calibrations were developed for each chemical consituent using the NIR spectra, wood chemistry data and partial least squares (PLS) regression. Relationships were variable with the best results being obtained for cellulose, glucan, xylan, mannan and lignin. Prediction errors were high and may be a consequence of the relatively small number of samples available for NIR analysis and the diverse origins of the samples in the test set.

Keywords: Near infrared spectroscopy; *Pinus taeda*; cellulose, hemicellulose, lignin.

Introduction

Pinus taeda L. (loblolly pine) is the dominant plantation species in the Southeastern United States of America. The forest products industry has widely accepted the use of *P. taeda* because of its ability to grow on a wide range of sites and its suitability to produce desirable products. The deployment of genetically improved planting stock coupled with intensive silvicultural management has greatly improved growth and yields of *P. taeda* (Li et al. 1999). It is expected that the inclusion of quality traits such as stem straightness and wood quality in *P. taeda* breeding programs will greatly increase genetic gains and the value of the trees (Li et al. 1999). Unfortunately, traditional methods for measuring wood properties are generally slow, costly, and destructive, limiting their application to tree breeding programs. Thus less expensive, rapid and nondestructive methods for measuring wood properties are required. Recently it has been demonstrated that near infrared (NIR) spectroscopy can successfully estimate several *Pinus radiata* D. Don and *P. taeda* wood properties (Jones et al. 2005a; 2005b; Schimleck and Evans 2002b; 2002a; 2003; 2004). In these studies NIR spectra were collected in 10 mm sections from the radial longitudinal face of intact radial wooden strips analyzed by the SilviScan instruments (Evans 1994; 1997; 1999). The NIR spectra and SilviScan data were used to develop calibrations for air-dry density, microfibril angle (MFA), stiffness (determined using SilviScan-2 diffraction data and measured density) and a number of tracheid morphological characteristics including; coarseness, perimeter, radial diameter, tangential diameter and wall thickness. Relationships were good for most properties, however Jones et al. (2005a) found that the relationships for perimeter, radial diameter and tangential diameter (both in calibration and prediction) were low when a population of *P. taeda* samples with diverse origins were examined.

While the SilviScan instruments measure many wood properties at high spatial resolution, they cannot measure wood chemical composition or tracheid (or fiber) length. We have shown (Schimleck et al. 2004a) that NIR spectroscopy can be used to estimate the tracheid length of sections of *P. taeda* radial strips, but we have not attempted to use NIR spectroscopy to estimate the chemical composition of radial sections.

Several studies (Birkett and Gambino 1988; Garbutt et al. 1992; Michell 1995; Poke et al. 2004; Raymond and Schimleck 2002; Schimleck et al. 1997; Wright et al. 1990) have used NIR spectroscopy to estimate the chemical composition of wood but these studies did not use intact wood, rather they used milled wood generally representing a composite whole tree sample or milled increment cores. Recently Kelley et al. (2004) estimated the chemical composition of three *P. taeda* trees grown in Arkansas (USA) using a reduced spectral range (650 nm-1150 nm) and NIR spectra collected from the surface of static bending samples**.** Poke and Raymond (2006) also estimated chemical composition of intact wood using NIR spectra collected in 20 mm increments from the transverse surface of *Eucalyptus globulus* Labill. (Tasmanian blue gum) pith-to-bark strips. An advantage of working with solid wood is that it eliminates milling samples prior to NIR analysis (Poke and Raymond 2006). In other recent studies Yeh et al. (2004; 2005) and Sykes et al. (2005) used transmittance NIR spectroscopy to estimate the lignin and α-cellulose content of wood wafers sliced from the tangential surface of increment cores. The utilization of thin wafers removed from the transverse face allows the analysis of within ring variation of wood properties at much higher spatial resolution than is presently possible using NIR reflectance spectra collected from the radial face. However, sample preparation is still time consuming relative to NIR reflectance spectroscopy with wood strips. Clearly if NIR spectroscopy can be used to estimate the chemical composition of radial wood sections, in addition to tracheid length, coarseness, density, MFA, stiffness and tracheid wall thickness, then its value as a nondestructive tool for the rapid estimation of wood properties will be greatly enhanced. Therefore the objectives of this study were to:

(i) Develop calibrations for wood chemical components including cellulose, hemicellulose, lignin (including acid insoluble, soluble and total) and individual monosaccharides (arabinan, galactan, glucan, mannan and xylan) using NIR spectra obtained in 12.5 mm sections from the radial - longitudinal surface of *P. taeda* radial wooden strips; and

(ii) Evaluate these calibrations by estimating the wood chemical composition of sections of radial wooden strips in a separate test set based on NIR spectra obtained from the radial longitudinal face of each strip.

Materials and methods

Sample origin

Seventeen breast height discs (approximately 40 mm thick) were collected from *Pinus taeda* L. (loblolly pine) trees growing on seven sites of variable age and site index in Georgia, (USA). A summary of the sites is given in Table 6.1. All samples were frozen and stored until processing.

While the discs were still frozen pith-to-bark radial strips (12.5 mm x 12.5 mm) were cut with a bandsaw from each disc for NIR and chemical analysis. The radial strips were defrosted and dried overnight in an oven set at 50 ºC to reduce the moisture content of the samples to approximately 7%.

Near infrared spectroscopy

Two or three 12.5 mm sections were selected on each radial strip and their positions recorded on the surface of each strip. The width of the section (12.5 mm) was used to ensure sufficient wood was available for wood chemical analysis. Sections were selected to be representative of wood close to the pith (juvenile wood), close to bark (mature wood) and the transition zone between and juvenile and mature wood. Some strips were short and insufficient wood was available to provide a section in the transition zone. NIR diffuse reflectance spectra were obtained from the radial longitudinal face of each 12.5 mm section using a NIRSystems Inc. Model 5000 scanning spectrophotometer (Silver Spring, Maryland, U.S.A.). Samples were held in a custom made holder similar to that illustrated in Schimleck et al. (2001a) with modifications to hold thicker samples. A 5 mm x 12.5 mm mask was used to ensure that a constant area was tested. Several samples were slightly twisted and a small gap between the spectrometer window and sample was occasionally observed permitting stray light to interfere with the NIR measurements. To minimize stray light the samples were tested in a light proof environment. The spectra were collected at 2 nm intervals over the wavelength range 1100-2500 nm. Fifty scans were accumulated for each 12.5 mm section and the results averaged to produce one spectrum per section for analysis. The instrument reference was a ceramic standard. All measurements were made in a conditioned atmosphere maintained at 40% RH and 20°C.

Wood chemical analysis

The selected 12.5 mm sections were extracted by soaking the blocks in acetone overnight. The sections were extracted three times with the acetone being drained between extractions. Following extraction the blocks were cut into small pieces using a utility knife and ground to a powder using a small stainless steel ball mill and a Wig-L-Bug.

The extracted and ground samples were prepared for carbohydrate analysis using a methodology based upon methods described in TAPPI test method T-249 cm-00 and Pronto et al. (1998).

The weighed samples were hydrolyzed with 72% sulfuric acid according to TAPPI T-249 cm-85, which was modified by changing the sample size and volumes. 0.175 g of air-dry sample was weighed in a digestion tube and at the same time a separate aliquot was removed for moisture analysis. After addition of 1.5 ml of 72% sulfuric acid, primary hydrolysis was carried out at 30ºC for 2 hrs. At the end of this period the acid concentration was adjusted to 3% with the addition of water and the secondary hydrolysis carried out in an autoclave set at 121°C for 1 hr. The hydrolyzed samples were cooled and filtered through tared glass fiber filters. The filtrate was collected and the volume adjusted to 50 ml. The filtrate was diluted 1 ml into 25 ml with an internal standard added to each flask.

From the diluted solution, the monosaccharide concentration was determined using High Performance Anion Exchange Chromatography with Pulsed Amperometric Detection (HPAEC-PAD). The system consisted of a Dionex HPLC system equipped with a GP50 gradient pump, and ED40 electrochemical detector, an AS40 auto sampler and a pneumatic controller for the 500mM NaOH post – column addition solution. The column was a Dionex CarboPac PA10 (4 x 250mm) and a CarboPac PA10 guard column (4 x 50mm). Elution of the monosaccharides was achieved with a weakly basic eluent followed by a stronger base column cleanup between injections. A post column addition of base was used to enhance detection of the monosaccharides. A chromatogram obtained for one of the *P. taeda* samples analyzed is shown in Figure 6.1. Peak areas were used to quantify the amount of each monosaccharide in the sample which were converted to % of the dry weight. Samples were run in duplicate.

The cellulose content (%) was determined based on the formula given by Easty and Malcolm (1982).

Cellulose = Glucan – (1/3*Mannan) [1]

The hemicellulose content (%) was determined as the difference between the total sugars and total cellulose, i.e.

Hemicellulose = (Arabinan + Galactan + Glucan + Mannan + Xylan) – cellulose [2]

Acid insoluble lignin was determined from insoluble material collected on the filter after the hydrolysis procedure used for carbohydrates. The hydrolysis procedure is essentially the same as the method described in TAPPI test method T-222 om-02. Acid soluble lignin was determined using TAPPI test method, UM250. Total lignin was determined by summing acid-insoluble and acid-soluble lignin.

Calibration development

A total of 46 diffuse reflectance NIR spectra, measured from the 17 radial strips, were available for NIR analysis. In the development of preliminary calibrations it was observed that four samples had large leverage and two samples had large residual X-variance (Figure 6.2). The NIR spectra and wet chemical data of these samples was investigated. It was found that 2 samples had abnormal NIR spectra (those with the large residual X-variance), another 2 had abnormal chromatograms (the 2 samples having the largest leverage,) while another sample had high moisture content when analyzed and suggested a weighing error. The sixth sample was excluded because of its proximity to a knot previously undetected prior to having the samples analyzed.

Owing to the small number of samples (40) preliminary calibrations were developed using all samples. Following the development of calibrations using all samples the spectra were split at random into calibration (28 spectra, representing 12 radial strips) and prediction (12 spectra, representing 5 radial strips each from a different site) sets. A statistical summary of the calibration and prediction sets is given in Table 6.2.

Calibrations were developed using Partial Least Squares (PLS) regression with four cross validation segments and a maximum of 10 factors (Unscrambler, version 8.0, Camo AS, Norway). The final numbers of factors used for each calibration were those recommended by the Unscrambler software. Calibrations were developed using second derivative spectra, left and right gap widths of 8 nm were used for the conversion, limiting the wavelength range available for calibration development to 1108 - 2492 nm. The Standard Error of Cross Validation (SECV) (determined from the residuals of each cross validation phase), the Standard Error of Calibration (SEC) (determined from the residuals of the final calibration) and the co-efficient of determination (R^2) were used to assess calibration performance.

The Standard Error of Prediction (SEP) was used to give a measure of how well a calibration predicts the parameter of interest for a set of unknown samples that are different from the calibration set. The predictive ability of calibrations was assessed by calculating the ratio of performance to deviation (RPD) (ratio of the standard deviation of the reference data to the SEP) (Williams and Sobering 1993). An RPD of greater than 2.5 is considered satisfactory for screening (Williams and Sobering 1993) however, it has been shown that calibrations with an RPD of approximately 1.5 can be useful for initial sample screening (Schimleck et al. 2003a).

Results

Variation in NIR spectra

Second derivative diffuse reflectance NIR spectra of two *P. taeda* wood samples (one juvenile wood the other mature wood) that show wide variation in their chemical composition are shown in Figure 6.3. For the 2 spectra shown glucan content varied from 34.53 to 44.03 % and total lignin varied from 26.25 to 31.18 %.

As discussed by Schimleck et al. (2004) NIR spectra show differences in wood chemistry and physical properties. When the juvenile and mature wood NIR spectra are compared large differences between the two types of wood can be observed. The juvenile wood spectrum has a lower overall absorbance relative to the mature wood spectrum because the mature wood sample has greater density giving higher absorbance. Many bands in the NIR spectrum from 1100-2500 nm have been assigned to cellulose (1490, 1780, 1820, 1900, 1930, 2100, 2276, 2336, 2352 and 2488 nm) while others (1143, 1417, 1446,1668, 1685 and 2132 nm) have aromatic origins (Osborne et al. 1993; Schimleck et al. 1996; Shenk et al. 1992). For the samples utilized in this study Table 6.3 lists the three wavelengths that have the strongest relationship with each property.

PLS calibrations – full set

Forty NIR diffuse reflectance spectra, obtained from the radial longitudinal face of *P. taeda* radial strips, were available for calibration development. Calibrations obtained for each chemical component are summarized in Table 6.4.

Cellulose, glucan, mannan, xylan, insoluble and total lignin displayed strong calibration coefficients with R^2 greater than 0.80. Of these many are strongly related to each other, such as glucan and cellulose (R-value = 0.99) and total lignin and insoluble lignin (R-value = 0.99). The calibration for arabinan had an R^2 of 0.72 while the relationships for acid-soluble lignin (0.57), hemicellulose (0.54) and galactan (0.18) were weak to poor. Only one factor was recommended for the galactan calibration, if four factors were used, for example, the R^2 improved to 0.69, but based on the residual Y-variance plot only one factor should be used. Figure 6.4 shows the relationships between measured values and NIR-estimated values for arabinan (a), cellulose (b), mannan (c), and total lignin (d).

For almost all calibrations the SECV, which is considered to be a better measure of calibration error than the SEC, was considerably larger than the SEC. A high SECV indicates that the sample excluded in each cross validation phase was not well predicted by the corresponding calibration and that the SEC is overly optimistic. For example the xylan calibration, which was developed, using 6 factors had a SEC of 0.11 and a SECV of 0.44. It is possible that the calibration has over fitted the data but reducing the number of factors used actually increased the SECV (0.49 for 5 factors, 0.55 for 4 factors, 0.54 for 3 factors). The large difference between the SEC and the SECV may be a consequence of the small number of trees included for each site and the large number of sites represented (7). It is probable that if a larger calibration set was used then the SEC and SECV would be more similar.

Prediction of wood chemical composition

The set of 40 spectra were split into a calibration (28 samples) and prediction set (12 samples). No samples from the 5 trees in the prediction set were present in the calibration set but the sites the trees were from were represented. Table 6.5 provides a summary of the calibrations and their performance on the prediction set. A prediction R^2 (R_p^2) was calculated as the proportion of variation in the independent prediction set that was explained by the calibration.

The calibrations statistics were similar to those reported in Table 6.3 with cellulose, insoluble and total lignin, glucan, mannan and xylan all having strong relationships, but with each having a SECV much larger than the SEC. The calibration for xylan again gave a very high R^2 (0.98, 6 factors) and the predictive performance of 4 and 5 factor calibrations was investigated but it was found that the 6-factor calibration gave the strongest predictive performance, indicating that the number of factors recommended by the software was appropriate.

When the calibrations were applied to the prediction set, R_p^2 were noticeably lower than the corresponding R^2, while SEP and SECV were similar. Figure 6.5 shows the relationships between measured values and NIR-predicted values for arabinan (a), cellulose (b), mannan (c), and total lignin (d). The strongest R_p^2 (0.68 and 0.66) were obtained for the predictions of arabinan and mannan. The remaining constituents noted for their good calibration statistics gave R_p^2 ranging from 0.11 to 0.61.

Discussion

Forty-six diffuse reflectance NIR spectra were collected in 12.5 mm sections from the radial longitudinal surface of 17 radial wooden strips. The sections were selected to represent juvenile, transition, and mature wood, and were analyzed using traditional chemical analysis methods to determine lignin and monosaccharide contents. Six of the spectra were eliminated, as outliers prior to calibration development owing to large residual X-variance and/or leverage, leaving forty to create calibrations for the measured properties. Coefficient of determination (R^2) ranged from 0.18 to 0.95, SEC's were low, but SECV's were noticeably higher than SEC's. Further calibrations for the same properties were obtained using a subset of 28 samples. When applied to a separate test set of 12 samples (representing 5 radial strips, each from a different site) the calibrations provided similar calibration statistics to those obtained using 40 samples, but with weaker R_p^2, and SEP values that were similar to the SECV's reported for the calibrations.

The calibration statistics obtained using both sets (40 and 28 samples) suggest that NIR spectroscopy may provide a useful tool for the rapid assessment of lignin and monosaccharide contents of intact sections of radial longitudinal strips though predictive statistics must be improved for the properties examined in this study to be estimated on a routine basis. The predictive performance of the calibrations, based on the subset of 28 samples, may have suffered because of the diverse origins of the samples in the test set. Other research based on *P. taeda* and using NIR spectroscopy has been successful in predicting the morphological and physical properties of samples from different sites in this work a large number of samples from various sites in Georgia were included in the calibration set and the predictive success of the calibrations was attributed to the diversity represented (Jones et al. 2005a; 2005b). Hence if a larger calibration set was utilized in this study stronger prediction may have been obtained. Further research with larger sample sets is required to develop calibrations and apply them to estimate wood chemical composition. However, the high cost associated with standard analytical chemical analyses limits the number of samples that can be examined. The time and cost of analytical chemical methods emphasizes the importance of developing a rapid alternative to routinely measure cellulose, glucan, and lignin contents on a large-scale.

The current cost of wet chemistry is both an argument for using NIR spectroscopy and the limiting factor in creating calibrations with a large enough population. This highlights the importance of identifying suitable samples prior to wood chemical content analysis. Win ISI, a software that uses a neighborhood concept to identify spectrally unique samples that best represent the population, was successfully used with *Eucalyptus nitens,* where estimated genetic gains in cellulose content based on NIR estimates from a subset of samples were similar to those obtained when the full sample set was analyzed using wet chemistry (Schimleck et al., 2004b). Perhaps a similar approach could work with pine species.

The results reported in this study demonstrate that it is possible to calibrate reflectance NIR spectroscopy for the estimation of glucan, xylan, cellulose, and lignin contents with intact radial strips of wood. Several studies exist in the literature that have used NIR spectroscopy to estimate the chemical composition of wood (Birkett and Gambino 1988; Garbutt et al. 1992; Michell 1995; Poke et al. 2004; Raymond and Schimleck 2002; Schimleck et al. 1997; Wright et al. 1990), however, these studies were based on NIR on spectra collected from milled chips (usually representing a whole-tree composite). Studies based on intact wood samples are rare, Kelley et al. (2004) developed calibrations for various wood sugars and lignin content using NIR spectra collected from the surface of static bending samples while Poke and Raymond (2006) estimated extractives, cellulose, and lignin contents using NIR spectra collected in 20 mm increments from the transverse surface of *E. globulus* pith-to-bark strips.

The work presented in this study complements that of Jones et al. (2005a; 2005b) and Schimleck et al. (2004b) who established the utility of using NIR spectroscopy for estimating air-dry density, MFA, stiffness, and a number of tracheid characteristics; including coarseness, length, and wall thickness of radial strips. The ability of NIR spectroscopy to estimate a wide range of properties, including several not measured by SilviScan, makes NIR spectroscopy a valuable tool for wood property assessment.

Conclusions

This study demonstrates that calibrations can be created for lignin and monosaccharide content of intact *P. taeda* radial strips. Prediction errors were high and may be a consequence of the diverse origins of the samples in the test set and the relatively small number of samples available for NIR analysis.

Further studies with larger samples sets are required; if the lignin and monosaccharide content of intact *P. taeda* radial strips are going to be used on a routine basis for the selection of trees for genetic improvement.

The high cost of analytical chemical methods could be offset in future studies by using software to select samples with unique spectra and that best represent the population.

Acknowledgements

The authors thank the UGA Wood Quality Consortium for sample collection and preparation and the Georgia TIP^3 program for funding the wood chemistry analysis necessary for this study. The authors would also like to thank the UGA Wood Quality Consortium for sample preparation, Mike Murphy for collecting the NIR spectra, and Mike Buchanan, Rallming Yang, and Kathleen Poll at IPST for the chemical analysis.

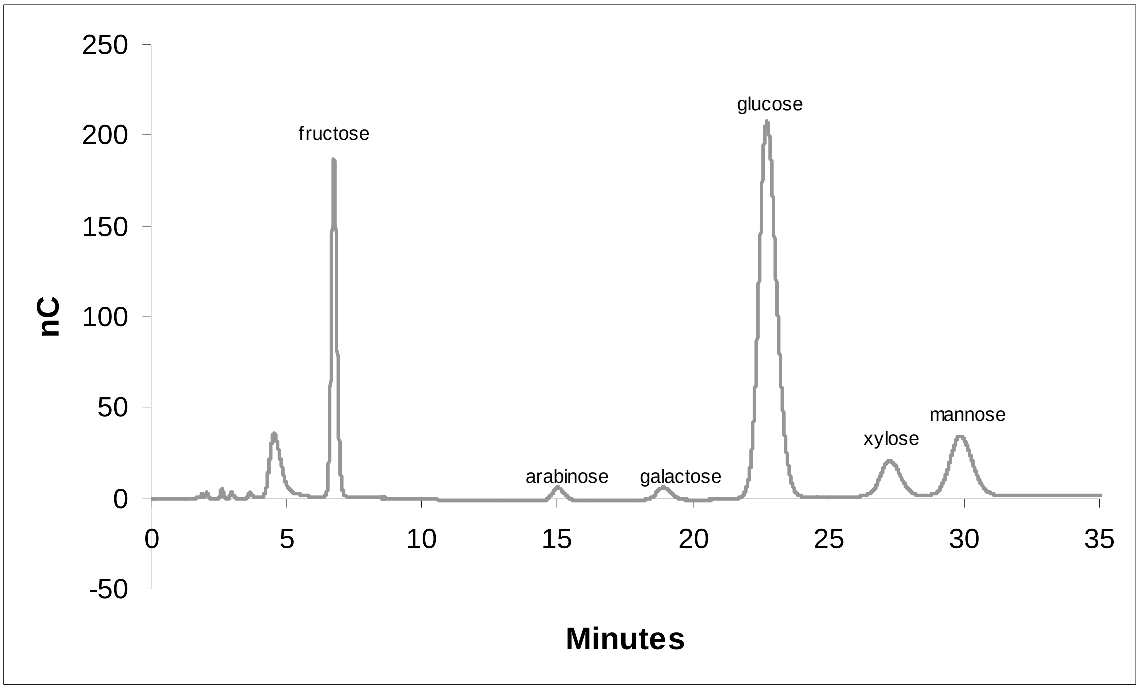

Fig. 6.1. Typical HPLC chromatogram of monosaccharides in *P. taeda* wood samples analyzed in this study.

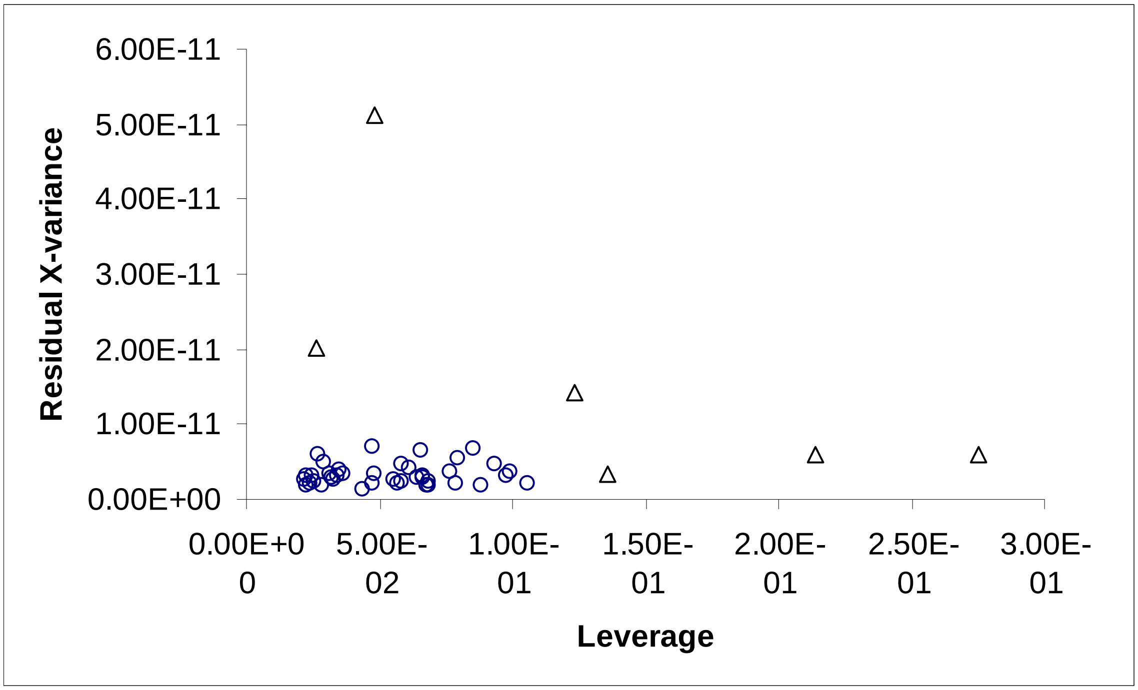

Fig. 6.2. Plot of residual X-variance vs. leverage for the *P. taeda* samples examined in this study. Samples with small leverage are shown by circles, while samples with larger leverage and/or large residual X-variance are indicated by triangles. Samples represented by triangles were identified as outliers (because of high influence and/or high residual X-variance) and omitted from the analysis.

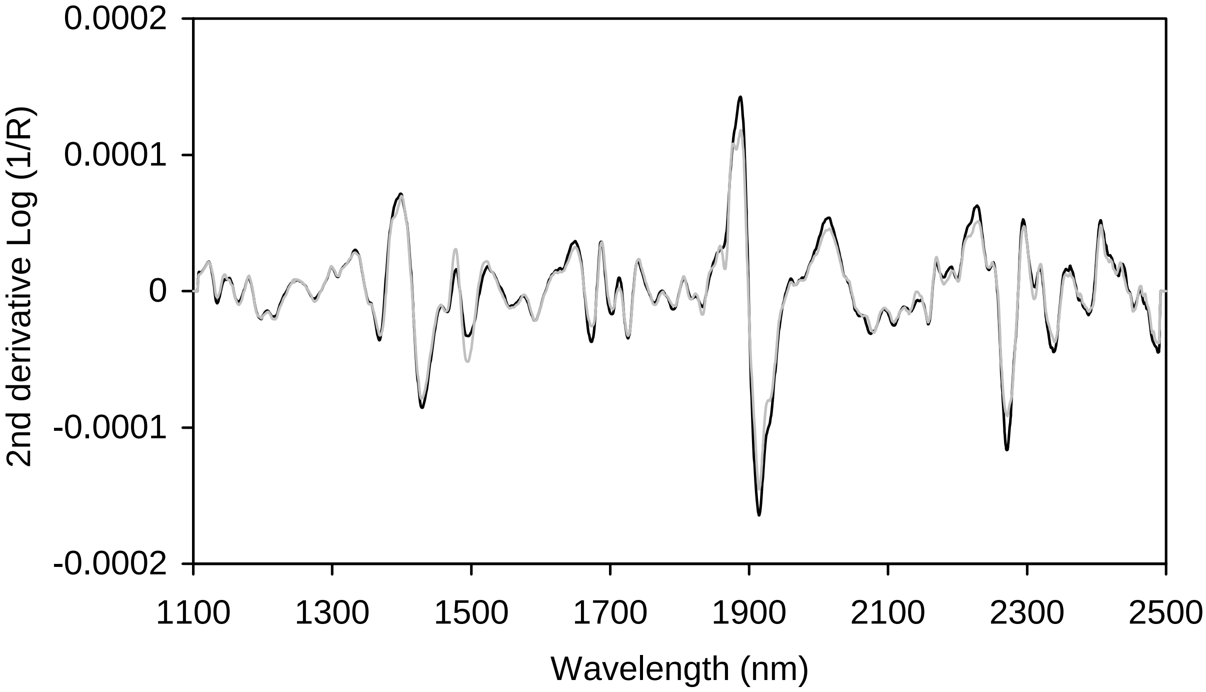

Fig. 6.3. Second derivative NIR spectra for juvenile wood (grey line) and mature wood (black line).

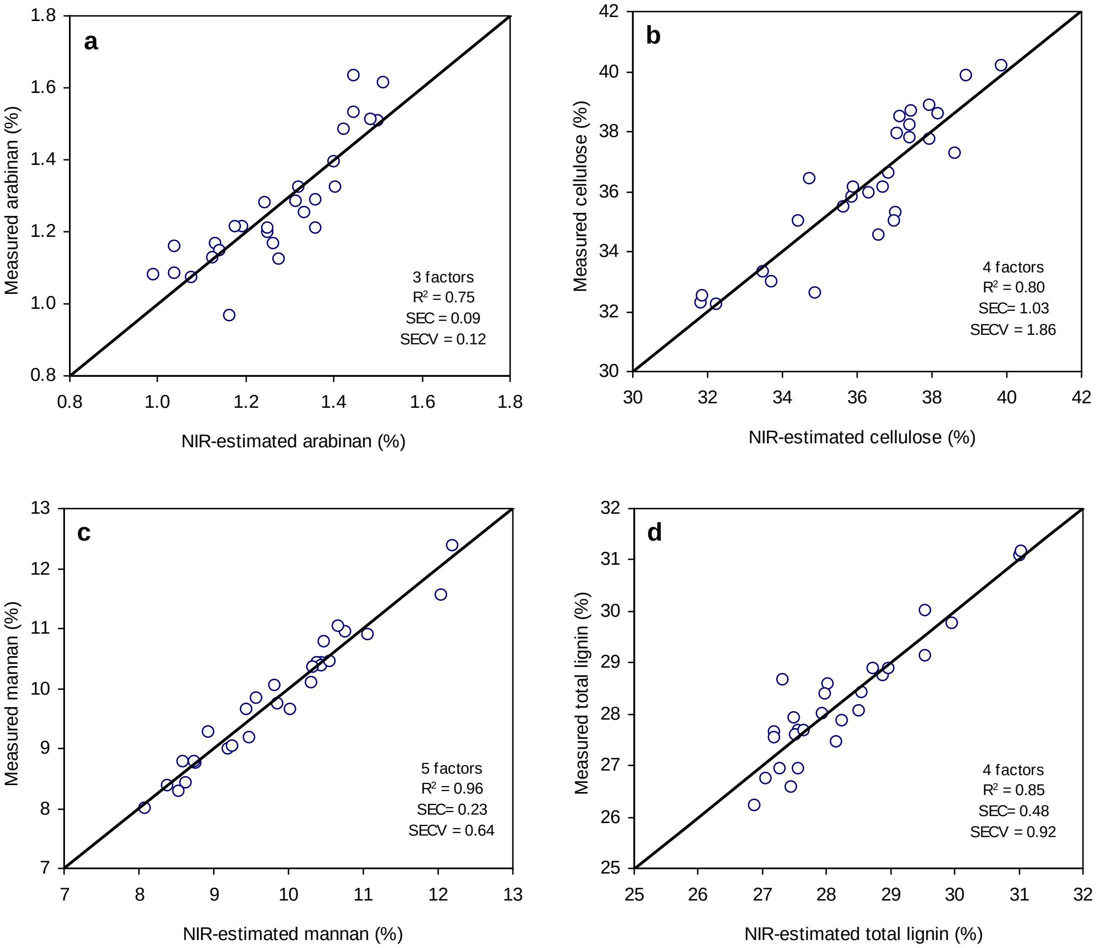

Fig. 6.4. Relationships between analytical chemistry and NIR-estimated values for arabinan (a), cellulose (b), mannan (c), and total lignin (d). Note that the regression line has been plotted in both figures.

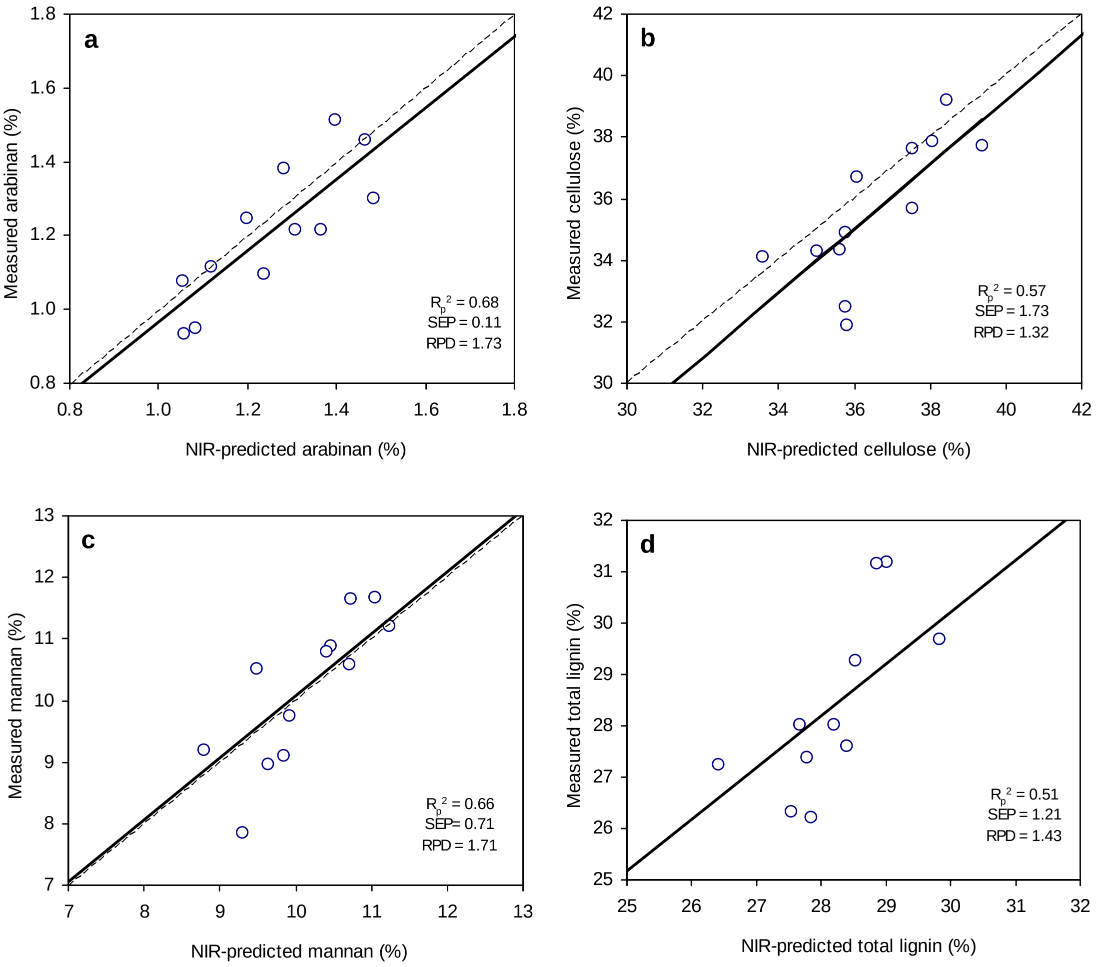

Fig. 6.5. Relationships between analytical chemistry and NIR-predicted values for arabinan (a), cellulose (b), mannan (c), and total lignin (d). Note that the regression line has been plotted (thick, dark line) in both figures and that the thin broken line indicates a one-one relationship between measured and predicted values.

Table 6.1. Stand descriptions for samples used in the calibration and prediction sets including physiographic region, site index (SI_{25}), age, latitude (Lat.), and longitude (Long.).

Region	SI_{25}	Age (yrs)	Lat. (N)	Long. (W)
Piedmont	55	21	34º09′	85º22′
Upper Atlantic Costal Plain	78	22	31º62′	84º99′
Lower Atlantic Costal Plain	76	25	32º26′	81º27′
Lower Atlantic Costal Plain	84	25	31º11′	81º81′
Lower Atlantic Costal Plain	79	25	31º31′	81º60′
Lower Atlantic Costal Plain	80	25	31º42′	81º68′
Lower Atlantic Costal Plain	81	24	31º79′	81º57′

Table 6.2. Summary of variation in measured wood chemical properties for the calibration and prediction sets.

Constituent	Calibration set (28 spectra)				Prediction set (12 spectra)			
	Minimum (%)	Maximum (%)	Avg. (%)	Std. dev.	Minimum (%)	Maximum (%)	Avg. (%)	Std. dev.
Arabinan	0.97	1.64	1.27	0.17	0.94	1.52	1.21	0.19
Cellulose	32.27	40.19	36.17	2.36	31.91	39.24	35.59	2.29
Galactan	1.20	6.29	2.21	1.29	1.48	3.73	2.39	0.80
Glucan	34.94	44.03	39.44	2.59	34.53	42.98	38.98	2.61
Hemicellulose	20.60	26.77	23.11	1.43	21.47	25.27	23.44	1.18
Mannan	8.01	12.40	9.81	1.08	7.85	11.68	10.19	1.20
Xylan	5.20	8.21	6.54	0.78	5.50	7.43	6.26	0.70
Insoluble	25.91	30.82	27.92	1.20	25.84	30.86	27.97	1.67
Soluble lignin	0.31	0.40	0.36	0.03	0.30	0.39	0.35	0.03
Total lignin	26.25	31.19	28.28	1.22	26.23	31.18	28.38	1.73

Table 6.3. Summary of the three wavelengths that give the strongest relationship per component, the R^2 value for each wavelength is presented below the wavelength in parentheses.

Constituent	1st wavelength (nm)	2nd wavelength (nm)	3rd wavelength (nm)
Arabinan	**1780** (0.60)	**1778** (0.56)	**1228** (0.56)
Cellulose	**1610** (0.49)	**1608** (0.41)	**1452** (0.39)
Galactan	**1130** (0.34)	**1156** (0.32)	**1606** (0.30)
Glucan	**1610** (0.53)	**1608** (0.44)	**2178** (0.42)
Hemicellulose	**2306** (0.40)	**1732** (0.38)	**2308** (0.37)
Mannan	**1130** (0.55)	**1696** (0.54)	**1698** (0.53)
Xylan	**1232** (0.66)	**1694** (0.65)	**1230** (0.65)
Insoluble Lignin	**1132** (0.51)	**1130** (0.50)	**1714** (0.48)
Soluble lignin	**1294** (0.51)	**1312** (0.52)	**1292** (0.51)
Total Lignin	**1130** (0.51)	**1132** (0.51)	**1704** (0.49)

Table 6.4. Summary of calibrations developed using all 40 samples. Note soluble lignin and therefore total lignin was not available for 1 sample.

Constituent (%)	No. of factors	R^2	SEC	SECV
Arabinan	3	0.72	0.09	0.12
Cellulose	5	0.84	0.92	1.68
Galactan	1	0.18	1.04	1.11
Glucan	4	0.80	1.12	1.78
Hemicellulose	3	0.54	0.91	1.13
Mannan	5	0.93	0.30	0.64
Xylan	6	0.95	0.16	0.41
Insoluble lignin	5	0.88	0.47	1.02
Soluble lignin	2	0.57	0.02	0.02
Total lignin	5	0.88	0.48	1.03

Table 6.5. Summary of calibrations developed using 28 samples and applied to the test set of 12 samples. Note 1 sample was omitted from the insoluble and total lignin calibrations.

Constituent (%)	Calibration set (28 samples)				Prediction set (12 samples)		
	No. of factors	R^2	SEC	SECV	R_p^2	SEP	RPD
Arabinan	3	0.75	0.09	0.12	0.68	0.11	1.73
Cellulose	4	0.80	1.03	1.86	0.57	1.73	1.32
Galactan	1	0.25	1.11	1.23	0.11	0.97	0.83
Glucan	4	0.82	1.09	1.96	0.57	1.88	1.39
Hemicellulose	3	0.59	0.92	1.24	0.30	1.04	1.14
Mannan	5	0.96	0.23	0.64	0.66	0.71	1.71
Xylan	6	0.98	0.11	0.44	0.61	0.46	1.52
*Insoluble lignin	4	0.85	0.47	0.91	0.51	1.26	1.33
Soluble lignin	2	0.66	0.02	0.02	0.36	0.02	1.50
*Total lignin	4	0.85	0.48	0.92	0..51	1.21	1.43

Literature cited

Birkett, M.D. and Gambino, M.J.T., 1988. Potential applications for near-infrared spectroscopy in the pulping industry. Pap. S. Afr., November/December: 34-38.

Easty, D.B. and Malcolm, E.W., 1982. Estimation of Pulping Yield in Continuous Digesters from Carbohydrate and Lignin Determinations. Tappi J., 65(12): 78-80.

Evans, R., 1994. Rapid Measurement of the Transverse Dimensions of Tracheids in Radial Wood Sections from *Pinus radiata*. Holzforschung, 48(2): 168-172.

Evans, R., 1999. A variance approach to the X-ray diffractometric estimation of microfibril angle in wood. Appita J., 52(4): 283-289, 294.

Evans, R., 1997, Rapid scanning of microfibril angle in increment cores by x ray diffractometry. In Microfibril Angle in Wood, Proceedings of the IAWA / IUFRO International Workshop on the Significance of Microfibril Angle to Wood, Westport, New Zealand, B.G. Butterfield, University of Canterbury Press, 116-139.

Garbutt, D.C.F., Donkin, M.J. and Meyer, J.H., 1992. Near-infrared reflectance analysis of cellulose and lignin in wood. Pap. S. Afr., April: 45-48.

Jones, P., Schimleck, L., Peter, G., Daniels, R. and Clark, A., 2005a. Non-destructive estimation of *Pinus taeda* L tracheid morphological characteristics for samples from a wide range of sites in Georgia. Wood Sci. Technol., 39(7): 529-545.

Jones, P.D., Schimleck, L.R., Peter, G.F., Daniels, R.F. and Clark III, A., 2005b. Nondestructive estimation of *Pinus taeda* L. wood properties for samples from a wide range of sites in Georgia. Can. J. For. Res., 35(1): 85-92.

Kelley, S.S., Rials, T.G., Snell, R., Groom, L.H. and Sluiter, A., 2004. Use of near infrared spectroscopy to measure the chemical and mechanical properties of solid wood. Wood. Sci. Technol., 38(4): 257-276.

Li, B., McKeand, S. and Weir, R., 1999. Tree improvement and sustainable forestry - impact of two cycles of loblolly pine breeding in the U.S.A. Forest Genetics, 6(4): 229-234.

Michell, A.J., 1995. Pulpwood quality estimation by near-infrared spectroscopic measurements on eucalypt woods. Appita J., 48(6): 425-428.

Osborne, B.G., Fearn, T. and Hindle, P.T., 1993. Practical NIR spectroscopy with applications in food and beverage analysis. Longman food technology. Longman Scientific & Technical ;Wiley, Harlow, Essex, England New York, 227 pp.

Poke, F.S., Wright, J.K. and Raymond, C.A., 2004. Predicting Extractives and Lignin Contents in *Eucalyptus globulus* Using Near Infrared Reflectance Analysis. J. Wood Chem. Technol., 24(1): 55-67.

Poke, F.S. and Raymond, C.A., 2006. Predicting extractives, lignin and cellulose contents using near infrared spectroscopy on solid wood in *Eucalyptus globulus*. J. Wood Chem. Technol., (In Press).

Pronto, M.B., 1998, Carbohydrate Analysis of Pulp using High-Performance Anion-Exchange Chromatography with Pulsed Amperometric Detection: A Comparison of Two Detector Settings, Pulping conference, Montreal; Canada, TAPPI; 1998, 1477-1484.

Raymond, C.A. and Schimleck, L.R., 2002. Development of near infrared reflectance analysis calibrations for estimating genetic parameters for cellulose content in *Eucalyptus globulus*. Can. J. For. Res., 32(1): 170-176.

Schimleck, L., Evans, R. and Ilic, J., 2001. Application of near infrared spectroscopy to a diverse range of species demonstrating wide density and stiffness variation. IAWA J., 22(4): 415-429.

Schimleck, L.R., Michell, A.J. and Vinden, P., 1996. Eucalypt wood classification by NIR spectroscopy and principal components analysis. Appita J., 49(5): 319-324.

Schimleck, L.R., Wright, P.J., Michell, A.J. and Wallis, A.F.A., 1997. Near-infrared spectra and chemical compositions of *E. globulus* and *E. nitens* plantation woods. Appita J., 50(1): 40-46.

Schimleck, L.R. and Evans, R., 2002a. Estimation of wood stiffness of increment cores by near infrared spectroscopy: The development and application of calibrations based on selected cores. IAWA J., 23(3): 217-224.

Schimleck, L.R. and Evans, R., 2002b. Estimation of microfibril angle of increment cores by near infrared spectroscopy. IAWA J., 23(3): 225-234.

Schimleck, L.R. and Evans, R., 2003. Estimation of air-dry density of increment cores by near infrared spectroscopy. Appita J., 56(4): 312-317.

Schimleck, L.R., Doran, J.C. and Rimbawanto, A., 2003. Near infrared spectroscopy for cost effective screening of foliar oil characteristics in a *Melaleuca cajuputi* breeding population. J. Agric. Food Chem., 51(9): 2433-2437.

Schimleck, L.R. and Evans, R., 2004. Estimation of *Pinus radiata* D. Don tracheid morphological characteristics by near infrared spectroscopy. Holzforschung, 58(1): 66-73.

Schimleck, L.R., Jones, P.D., Peter, G.F., Daniels, R.F. and Clark, A., 2004a. Nondestructive estimation of tracheid length from sections of radial wood strips by near infrared spectroscopy. Holzforschung, 58(4): 375-381.

Schimleck, L.R., Kube, P.D. and Raymond, C.A., 2004b. Genetic improvement of kraft pulp yield in *Eucalyptus nitens* using cellulose content determined by near infrared spectroscopy. Can. J. For. Res., 34(11): 2363-2370.

Shenk, J.S., Workman, J., J.J. and Westerhaus, M.O., 1992. Application of NIR spectroscopy to agricultural products, Handbook of Near-Infrared Analysis. Practical spectroscopy ; v. 13. M. Dekker, New York, pp. 385-386.

Sykes, R., Li, B.L., Hodge, G., Goldfarb, B., Kadla, J. and Chang, H.-M., 2005. Rapid prediction of wood properties of loblolly pine using transmittance near infrared spectroscopy. Can. J. For.Res., In press.

Williams, P.C. and Sobering, D.C., 1993. Comparison of comercial near infrared transmittance and reflectance instruments for the analysis of whole grains and seeds. J. Near Infrared Spectrosc., 1(1): 25-33.

Wright, J.A., Birkett, M.D. and Gambino, M.J.T., 1990. Prediction of Pulp Yield and Cellulose Content from Wood Samples Using near-Infrared Reflectance Spectroscopy. Tappi J., 73(8): 164-166.

Yeh, T.F., Chang, H.M. and Kadla, J.F., 2004. Rapid prediction of solid wood lignin content using transmittance near-infrared spectroscopy. J. Agric. Food Chem., 52(6): 1435-1439.

Yeh, T.F., Yamada, T., Capanema, E., Chang, H.M., Chiang, V. and Kadla, J.F., 2005. Rapid Screening of Wood Chemical Component Variations Using Transmittance Near-Infrared Spectroscopy. J. Agric. Food Chem., 53(9): 3328-3332.

Chapter 7

CONCLUSIONS

The studies described in this dissertation demonstrate the ability of near infrared spectroscopy to measure a wide range of physical, morphological, and chemical properties of *P. taeda* grown in Georgia. The non-destructive determination of density, microfibril angle, stiffness, coarseness, specific surface, wall thickness, cellulose, hemicellulose, and lignin content by near infrared spectroscopy in a rapid manner facilitates the estimation of the properties in large number of samples from standing trees greatly assisting tree breeding programs and also making it possible to examine within tree variation in great detail.

The studies of the physical and morphological properties demonstrate that large data sets that include a wide range of environmental (for each of the 3 physiographic regions in Georgia, 3 plantations ranging in age from 21 to 26 years, and with a range of site indices) and genetic variation can be used to establish good calibrations for density (R^2=0.83, RPD_c=2.30), microfibril angle (R^2=0.90, RPD_c=3.11), stiffness (R^2=0.93, RPD_c=3.65), and density-related tracheid morphological characteristics (coarseness R^2=0.80, RPD_c=2.03, specific surface R^2=0.78, RPD_c=2.06, and wall thickness R^2=0.84, RPD_c=2.46) based on near infrared spectra obtained in 10 mm sections from the radial face of wooden strips cut from increment cores. Reasonable calibrations were obtained for tangential diameter (R^2=0.64, RPD_c=1.56), while the calibrations for perimeter (R^2=0.50, RPD_c=1.26) and radial diameter (R^2=0.46, RPD_c=1.27) were poor. When the calibrations were applied to a separate test set (2 sites for each physiographic region) it was found that they generally performed well, however, the differing math treatments employed in the two studies (multiplicative scatter correction, first derivative, and second derivative) resulted in large variation in prediction error (i.e. density SEP ranged from 45.82 kg m^{-3} (first derivative) to 119.26 kg m^{-3} (multiplicative scatter correction)). The addition of a small number of cores from the prediction set (one core per site) to the calibration set greatly reduced the difference between the mathematical treatments. It is hoped that when an existing calibration is applied to samples from a new site it will perform well, but the actual performance of the calibration can not be assumed. Hence when applying an exiting calibration to samples from a new site it is recommended that a small number of samples from the new site be tested and added to the calibration, if required, to account for any new site or genetic variation.

Calibrations were also created to measure the lignin and monosaccharide content of intact *P. taeda* radial strips. Prediction errors were high and may be a consequence of the diverse origins of the samples in the test set (Piedmont, Lower and Upper Coastal Plains) and the relatively small number of samples available for near infrared analysis. Further studies with larger sample sets are required; if the lignin and monosaccharide content of intact *P. taeda* radial strips are going to be estimated on a routine basis. A problem with using large sample sets to obtain calibrations for properties such as cellulose and lignin content is the high cost of wet chemical analysis. The high cost of analytical chemical methods could be offset in future studies by using software to select samples with unique spectra that best represent the population.

Near infrared spectroscopy is a rapid, non-destructive technique that can be used to estimate the physical, morphological, and chemical properties of *P. taeda* on radial wooden strips from a wide range of sites in Georgia. With the addition of a small number of samples from new sites to the calibration, the prediction error for physical and morphological properties can be reduced. Further studies with larger sample sets are required, if the lignin and monosaccharide content of intact *P. taeda* radial strips is going to be estimated on a routine basis.

REFERENCES

Alén, R., 2000. Structure and chemical composition of wood. In: P. Stenius (Editor), Papermaking science and technology Published in cooperation with the Finnish Paper Engineers' Association and TAPPI, Helsinki pp. 12-57.

American Forest and Paper Association, 2000. Standard method of testing small clear specimens of timber. ASTM D 143

Axrup, L., Markides, K. and Nilsson, T., 2000. Using miniature diode array NIR spectrometers for analysing wood chips and bark samples in motion. J. Chemometrics, 14(5-6): 561-572.

Bailey, I.W. and Vestal, M.R., 1937. The orientation of cellulose in the secodary wall. J. Arnold Arboretum, 18(3): 185-195.

Barton, F.E., 2002, Theory and principles of near infrared spectroscopy, Near Infrared Spectroscopy: Procceding of the 10th International Conference, Kyonjgu, Korea, A.M.C. Davies and R.K. Cho, NIR Publications, 1-6.

Berzaghi, A.J.P., Flinn, P.C., Dardenne, P., Lagerholm, M., Shenk, J.S., Westerhaus, M.O. and Cowe, I.A., 2002, Comparison of linear and non-linear near infrared calibration methods using large forage databases, Near Infrared Spectroscopy: Proceedings of the 10th International Conference, NIR Publication, 107-111.

Birkett, M.D. and Gambino, M.J.T., 1988. Potential applications for near-infrared spectroscopy in the pulping industry. Pap. S. Afr., November/December: 34-38.

Booker, R.E., Harington, J. and Shiokura, T., 1997, Variation of Young's modulus with microfibril angle, density and spiral grain, Proceedings of the IAWA / IUFRO International Workshop on the Significance of Microfibril Angle to Wood, Westport, New Zealand, B.G. Butterfield, University of Canterbury Press, 116-139.

Bowyer, J.L., Shmulsky, R. and Haygreen, J.G., 2002. Forest products and wood science : an introduction. Iowa State Press, Ames Iowa, xiv, 554 pp.

Butterfield, B.G., 2003. Wood anatomy in realtion to wood quality. In: J.R. Barnett and G. Jeronimidis (Editors), Wood quality and its biological basis. Blackwell ; Published in the USA/Canada by CRC Press, Oxford Boca Raton, FL, pp. 53-86.

Cave, I.D., 1966. Theory of X-ray measurement of microfibril angle in wood. For. Prod. J., 16(10): 37-42.

Cave, I.D., 1968. The ansotropic elasticity of plant cell wall. Wood Sci.Technol., 2: 268-278.

Cousins, W.J., 1972. Measruement of mean microfibril angles of wood tracheids. Wood Sci. Technol., 6(1): 37-42.

Dickson, R.L. and Walker, J.C.F., 1997. Pines: growing comodities or designer trees. Commonwealth Forestry Review, 76(4): 273-279.

Downes, G.M., Beckers, E.P.J., Turvey, N.D. and Porada, H., 1993. Strength and Structure of Stems from Fast Grown *Pinus radiata*. 7(3): 131-136.

Downes, G.M. and Turvey, N.D., 1993. Relationships between Stem Structure and Bending Strength in *Pinus radiata* Seedlings. 7(2): 86-91.

Downes, G.M., Nyakuengama, J.G., Evans, R., Northway, R., Blakemore, P., Dickson, R.L. and Lausberg, M., 2002. Relationship between wood density, microfibril angle and stiffness in thinned and fertilized *Pinus radiata*. 23(3): 253-265.

Easty, D.B. and Malcolm, E.W., 1982. Estimation of Pulping Yield in Continuous Digesters from Carbohydrate and Lignin Determinations. Tappi J., 65(12): 78-80.

Echols, R.M., 1970, Moving slit radiography of wood samples for incremental measurements, Coference on tree ring analysis, University of British Columbia, Vancouver,

Evans, R., 1994. Rapid Measurement of the Transverse Dimensions of Tracheids in Radial Wood Sections from *Pinus radiata*. Holzforschung, 48(2): 168-172.

Evans, R., 1997, Rapid scanning of microfibril angle in increment cores by x ray diffractometry. In Microfibril Angle in Wood, Proceedings of the IAWA / IUFRO International Workshop on the Significance of Microfibril Angle to Wood, Westport, New Zealand, B.G. Butterfield, University of Canterbury Press, 116-139.

Evans, R., 1999. A variance approach to the X-ray diffractometric estimation of microfibril angle in wood. Appita J., 52(4): 283-289, 294.

Evans, R., Hughes, N. and Menz, D., 1999. Microfibril angle variation by scanning X-ray diffractometry. Appita J., 52(5): 363-367.

Garbutt, D.C.F., 1989. The analysis of cellulose in wood using a hydrogen peroxide, acetic acid delignifying reagent moderated by sodium perobrate. Pap. S. Afr., 9: 27-30.

Garbutt, D.C.F., Donkin, M.J. and Meyer, J.H., 1992. Near-infrared reflectance analysis of cellulose and lignin in wood. Pap. S. Afr., April: 45-48.

Gindl, W., Teischinger, A., Schwanninger, M. and Hinterstoisser, B., 2001. The relationship between near infrared spectra of radial wood surfaces and wood mechanical properties. J Near Infrared Spectrosc., 9(4): 255-261.

Guthrie, J.A. and Walsh, K.B., 2002, Assessing and enhancing near infrared calibration robustness for soluble solids content in mandarin fruit, Near Infrared Spectroscopy: Proceedings of the 10th International Conference, A.M.C. Davies and R.K. Cho, NIR Publications, 151-154.

Hatfield, R. and Fukushima, R.S., 2005. Can Lignin Be Accurately Measured? Crop Sci, 45(3): 832-839.

Hauksson, J.B., Sjöstrom, M., Edlund, U., Bergqvist, G. and Bergsten, U., 2001. Prediction of basic wood properties for Norway spruce. Interpretation of near infrared spectroscopy data using partial least squares regression. Wood Sci. and Technol., 35(6): 475-485.

Hoffmeyer, P. and Pedersen, J.G., 1995. Evaluation of Density and Strength of Norway Spruce Wood by Near-Infrared Reflectance Spectroscopy. Holz Roh Werkst., 53(3): 165-170.

Huang, C.L., 1995. Revealing fibril angle in wood sections by ultrasonic treatment. Wood and Fiber Sci., 27(1): 49-54.

Huang, C.L., Lindström, H., Nakada, R. and Ralston, J., 2003. Cell wall structure and wood properties determined by acoustics a selective review. 61(5): 321-335.

Johnson, D.B., Moore, W.E. and Zank, L.C., 1961. The spectrophotometric determination of lignin in small samples. Tappi, 44: 789-793.

Jones, P., Schimleck, L., Peter, G., Daniels, R. and Clark, A., 2005a. Non-destructive estimation of *Pinus taeda* L tracheid morphological characteristics for samples from a wide range of sites in Georgia. Wood Sci. Technol., 39(7): 529-545.

Jones , P.D., Schimleck, L.R., Peter, G.F., Daniels, R.F. and Clark III, A., 2005. Nondestructive estimation of *Pinus taeda* L. wood properties for samples from a wide range of sites in Georgia. Can. J. For. Res., 35(1): 85-92.

Jones, P.D., Schimleck, L.R., Peter, G.F., Daniels, R.F. and Clark III, A., 2005b. Nondestructive estimation of *Pinus taeda* L. wood properties for samples from a wide range of sites in Georgia. Can. J. For. Res., 35(1): 85-92.

Kelley, S.S., Rials, T.G., Snell, R., Groom, L.H. and Sluiter, A., 2004. Use of near infrared spectroscopy to measure the chemical and mechanical properties of solid wood. Wood. Sci. Technol., 38(4): 257-276.

Kellogg, R.M., Wellwood, R.W. and Sastry, C.B.R., 1975. Relationships between cell wall composition and cell wall density. Wood and Fibre, 7(3): 170-177.

Kibblewhite, R.P., Riddell, M.J.C. and Shelbourne, C.J.A., 1998. Kraft fibre and pulp qualities of 29 trees of New Zealand grown *Eucalyptus nitens*. 51(2): 114-121.

Kumar, S., 2004. Genetic parameter estimates for wood stiffness, strength, internal checking, and resin bleeding for radiata pine. Can. J. For. Res., 34(12): 2601-2610.

Li, B., McKeand, S. and Weir, R., 1999. Tree improvement and sustainable forestry - impact of two cycles of loblolly pine breeding in the U.S.A.. Forest Genetics, 6(4): 229-234.

Marten, G.C., Shenk, J.S. and Barton, F.E., 1989. Near infrared reflectance spectroscopy (NIRS) : analysis of forage quality. United States. Agricultural Research Service. U.S. Dept. of Agriculture Agricultural Research Service. Rev. Aug. 1989 (with supplements). Ag. Handbook No. 643 110 pp.

McKenzie, A.W., 1994. A Guide To Pulp Evaluation. CSIRO, Australia, 66 pp.

Meder, R., Thumm, A. and Marston, D., 2003. Sawmill trial of at-line prediction of recovered lumber stiffness by NIR spectroscopy of *Pinus radiata* cants. J. Near Infrared Spectrosc., 11(2): 137-143.

Megraw, R.A., 1985. Wood quality factors in loblolly pine: the influence of tree age, position in tree, and cultural practice on wood specific gravity, fiber length, and fibril angle. TAPPI Press, Atlanta, GA, 88 pp.

Michell, A.J., 1995. Pulpwood quality estimation by near-infrared spectroscopic measurements on eucalypt woods. Appita J., 48(6): 425-428.

Muneri, A. and Raymond, C.A., 2001. Nondestructive sampling of *Eucalyptus globulus* and *E. nitens* for wood properties. II. Fibre length and coarseness. Wood Sci. Technol., 35(1/2): 41-56.

Næs, T., Isaksson, T., Fearn, T. and Davies, T., 2002. A user-friendly guide to multivariate calibration and classification. NIR, Chichester, 344 pp.

Norris, K.H. and Butler, W.L., 1961. Techniques for Obtaining Absorption Spectra on Intact Biological Samples. Ire Transactions on Biomedical Electronics, 8(3): 153-&.

Olsson, R.J.O., Tomani, P., Karlsson, M., Joseffson, T., Sjoberg, K. and Bjorklund, C., 1995. Multivariate characterization of chemical and physical descriptors in pulp using NIRR. Tappi J., 78(10): 158-166.

Osborne, B.G., Fearn, T. and Hindle, P.T., 1993. Practical NIR spectroscopy with applications in food and beverage analysis. Longman food technology. Longman Scientific & Technical ;Wiley, Harlow, Essex, England New York, 227 pp.

Panshin, A.J. and De Zeeuw, C., 1980. Textbook of wood technology: structure, identification, properties, and uses of the commercial woods of the United States and Canada. McGraw-Hill, New York, 722 pp.

Pereira, H., 1988. Variability in the chemical composition of plantation eucalyptus (*Eucalyptus globulus* Labill.). Wood and Fiber Sci., 20: 82-90.

Pereira, H., Graça, J. and Rodrigues, J.C., 2003. Wood chemistry in relation to quality. In: J.R. Barnett and G. Jeronimidis (Editors), Wood quality and its biological basis. Blackwell ; Published in the USA/Canada by CRC Press, Oxford Boca Raton, FL, pp. 53-86.

Pillow, M.Y., Terrell, B.Z. and Hiller, C.H., 1953. Patterns of variation in fibril angles in loblolly pine. U.F.S.F.P. Laboratory. D1935.

Poke, F.S., Wright, J.K. and Raymond, C.A., 2004. Predicting Extractives and Lignin Contents in *Eucalyptus globulus* Using Near Infrared Reflectance Analysis. J. Wood Chem. Technol., 24(1): 55-67.

Poke, F.S. and Raymond, C.A., 2006. Predicting extractives, lignin and cellulose contents using near infrared spectroscopy on solid wood in *Eucalyptus globulus*. J. Wood Chem. Technol., (In Press).

Polge, H., 1978. Fifteen years of wood radiation densitometry. Wood Sci. Technol., 12(3): 187-196.

Preston, R.D., 1952. The molecular structure of plant cell walls. Chapman & Hall, London, 211 pp.

Pronto, M.B., 1998, Carbohydrate Analysis of Pulp using High-Performance Anion-Exchange Chromatography with Pulsed Amperometric Detection: A Comparison of Two Detector Settings, Pulping conference, Montreal; Canada, TAPPI; 1998, 1477-1484.

Raymond, C.A., Schimleck, L.R., Muneri, A. and Michell, A.J., 2001. Nondestructive sampling of *Eucalyptus globulus* and *E. nitens* for wood properties. III. Predicted pulp yield using near infrared reflectance analysis. Wood. Sci. Technol., 35(3): 203-215.

Raymond, C.A. and Schimleck, L.R., 2002. Development of near infrared reflectance analysis calibrations for estimating genetic parameters for cellulose content in *Eucalyptus globulus*. Can. J. For. Res., 32(1): 170-176.

Risén, J., Hultén, A.H. and Paulsson, M., 2004. Influence of Fiber Properties on the Network Strength of Softwood and Hardwood Kraft Pulp Fibers from Different Stages of a Bleaching Sequence. J. Wood Chem. Technol., 24(4): 289-306.

Roberts, C.A., Workman, J., Reeves, J.B., American Society of Agronomy., Crop Science Society of America. and Soil Science Society of America., 2004. Near-infrared spectroscopy in agriculture. American Society of Agronomy : Crop Science Society of America : Soil Science Society of America, Madison, Wis., 822 pp.

Saranpää, P., 2003. Wood Density and growth. In: J.R. Barnett and G. Jeronimidis (Editors), Wood quality and its biological basis. Blackwell ; Published in the USA/Canada by CRC Press, Oxford Boca Raton, FL, pp. 87-117.

Schimleck, L., Evans, R. and Ilic, J., 2001a. Application of near infrared spectroscopy to a diverse range of species demonstrating wide density and stiffness variation. IAWA J., 22(4): 415-429.

Schimleck, L.R., Michell, A.J. and Vinden, P., 1996. Eucalypt wood classification by NIR spectroscopy and principal components analysis. Appita J., 49(5): 319-324.

Schimleck, L.R., Wright, P.J., Michell, A.J. and Wallis, A.F.A., 1997. Near-infrared spectra and chemical compositions of *E. globulus* and *E. nitens* plantation woods. Appita J., 50(1): 40-46.

Schimleck, L.R. and Michell, A.J., 1998. Determination of within-tree variation of kraft pulp yield using near-infrared spectroscopy. Tappi J., 81(5): 229-236.

Schimleck, L.R., Michell, A.J., Raymond, C.A. and Muneri, A., 1999. Estimation of basic density of *Eucalyptus globulus* using near-infrared spectroscopy. Can. J. For. Res., 29(2): 194-201.

Schimleck, L.R., Raymond, C.A., Beadle, C.L., Downes, G.M., Kube, P.D. and French, J., 2000. Applications of NIR spectroscopy to forest research. Appita J., 53(6): 458-464.

Schimleck, L.R., Evans, R. and Ilic, J., 2001b. Estimation of *Eucalyptus delegatensis* wood properties by near infrared spectroscopy. Can. J. For. Res., 31(10): 1671-1675.

Schimleck, L.R. and Evans, R., 2002a. Estimation of wood stiffness of increment cores by near infrared spectroscopy: The development and application of calibrations based on selected cores. IAWA J., 23(3): 217-224.

Schimleck, L.R. and Evans, R., 2002b. Estimation of microfibril angle of increment cores by near infrared spectroscopy. IAWA J., 23(3): 225-234.

Schimleck, L.R., Evans, R. and Matheson, A.C., 2002. Estimation of *Pinus radiata* D. Don clear wood properties by near-infrared spectroscopy. J. Wood Sci., 48(2): 132-137.

Schimleck, L.R., Doran, J.C. and Rimbawanto, A., 2003a. Near infrared spectroscopy for cost effective screening of foliar oil characteristics in a *Melaleuca cajuputi* breeding population. J. Agric. Food Chem., 51(9): 2433-2437.

Schimleck, L.R. and Evans, R., 2003. Estimation of air-dry density of increment cores by near infrared spectroscopy. Appita J., 56(4): 312-317.

Schimleck, L.R., Mora, C. and Daniels, R.F., 2003b. Estimation of the physical wood properties of green *Pinus taeda* radial samples by near infrared spectroscopy. Can. J. For. Res., 33(12): 2297-2305.

Schimleck, L.R. and Evans, R., 2004. Estimation of *Pinus radiata* D. Don tracheid morphological characteristics by near infrared spectroscopy. Holzforschung, 58(1): 66-73.

Schimleck, L.R., Jones, P.D., Peter, G.F., Daniels, R.F. and Clark, A., 2004a. Nondestructive estimation of tracheid length from sections of radial wood strips by near infrared spectroscopy. Holzforschung, 58(4): 375-381.

Schimleck, L.R., Kube, P.D. and Raymond, C.A., 2004b. Genetic improvement of kraft pulp yield in Eucalyptus nitens using cellulose content determined by near infrared spectroscopy. Can. J. For. Res., 34(11): 2363-2370.

Schultz, T.P. and Burns, D.A., 1990. Rapid secondary analysis of lignocellulose: comparison of near infrared (NIR) and fourier transform infrared (FTIR). Tappi J., 73(5): 209-212.

Seifert, K., 1960. Zur frage der Cellulose-Schnellbestimmung nach der Acetylaceton-Mthode. Papier, 14: 104-106.

Shenk, J.S., Workman, J., J.J. and Westerhaus, M.O., 1992. Application of NIR spectroscopy to agricultural products, Handbook of Near-Infrared Analysis, Practical spectroscopy ; v. 13. M. Dekker, New York, pp. 385-386.

Sjöström, E., 1993. Wood chemistry : fundamentals and applications. Academic Press, San Diego, 293 pp.

Stamm, A.J., 1964. Wood and cellulose science. Ronald Press Co., New York,, 549 pp.

Sykes, R., Li, B.L., Hodge, G., Goldfarb, B., Kadla, J. and Chang, H.-M., 2005. Prediction of loblolly pine wood properties using transmittance near-infrared spectroscopy. Can. J. For. Res., 35(10): 2423-2431.

Talbert, J.T. and Jett, J.B., 1981. Regional Specific-Gravity Values for Plantation Grown Loblolly-Pine in the Southeastern United-States. Forest Sci., 27(4): 801-807.

Thumm, A. and Meder, R., 2001. Stiffness prediction of radiata pine clearwood test pieces using near infrared spectroscopy. J. Near Infrared Spectrosc., 9(2): 117-122.

Thygesen, L.G., 1994. Determination of dry matter content and basic density of Norway spruce by near-infrared reflectance and transmission spectroscopy. J. Near Infrared Spec., 2: 127-135.

Via, B.K., So, C.L., Shupe, T.F., Eckhardt, L.G., Stine, M. and Groom, L.H., 2005a. Prediction of wood mechanical and chemical properties in the presence and absence of blue stain using two near infrared instruments. J. Near Infrared Spec., 13(4): 201-212.

Via, B.K., So, C.L., Shupe, T.F., Stine, M. and Groom, L.H., 2005b. Ability of near infrared spectroscopy to monitor air-dry density distribution and variation of wood. Wood and Fiber Sci., 37(3): 394-402.

Wallis, A.F.A., Wearne, R.H. and Wright, P.J., 1997, New approaches to rapid analysis of cellulose in wood, International Symposium on Wood and Pulping Chemistry, Montreal, Quebec, Canadian Pulp and Paper Association,

Wear, D.N. and Greis, J.G., 2002. Southern forest resource assessment, General technical report SRS ; 53. Asheville, NC : Southern Research Station.

Williams, P.C. and Sobering, D.C., 1993. Comparison of comercial near infrared transmittance and reflectance instruments for the analysis of whole grains and seeds. J Near Infrared Spectrosc., 1(1): 25-33.

Wimmer, R., Downes, G.M. and Evans, R., 2002a. High-resolution analysis of radial growth and wood density in *Eucalyptus nitens*, grown under different irrigation regimes. 59(5-6): 519-524.

Wimmer, R., Downes, G.M. and Evans, R., 2002b. Temporal variation of microfibril angle in *Eucalyptus nitens* grown in different irrigation regimes Tree Phys., 22(11): 817-817.

Wimmer, R., Downes, G.M., Evans, R., Rasmussen, G. and French, J., 2002c. Direct effects of wood characteristics on pulp and handsheet properties of *Eucalyptus globulus*. 56(3): 244-252.

Wright, J.A., Birkett, M.D. and Gambino, M.J.T., 1990. Prediction of Pulp Yield and Cellulose Content from Wood Samples Using near-Infrared Reflectance Spectroscopy. Tappi J., 73(8): 164-166.

Wright, P.J. and Wallis, A.F.A., 1996. Rapid determination of carbohydrates in hardwoods by high performance anion exchange chromatography. Holzforschung, 50(6): 518-524.

Yeh, T.F., Chang, H.M. and Kadla, J.F., 2004. Rapid prediction of solid wood lignin content using transmittance near-infrared spectroscopy. J. Agric. Food Chem., 52(6): 1435-1439.

Yeh, T.F., Yamada, T., Capanema, E., Chang, H.M., Chiang, V. and Kadla, J.F., 2005. Rapid Screening of Wood Chemical Component Variations Using Transmittance Near-Infrared Spectroscopy. J. Agric. Food Chem., 53(9): 3328-3332.

Zink-Sharp, A., 2003. The mechanical properties of wood. In: J.R. Barnett and G. Jeronimidis (Editors), Wood quality and its biological basis. Blackwell ; Published in the USA/Canada by CRC Press, Oxford Boca Raton, FL, pp. 53-86.

Zobel, B.J. and McElwee, R.L., 1958. Natural variation in wood specific gravity of loblolly pine, and an analysis of contributing factors. Tappi J., 41(4): 158-161.

.